5-2000

Expression of vitronectin in eurkaryotic cells : evaluation of PAI-1 binding and implications for gene therapy

Christine Rene Schar

To the Graduate Council:

I am submitting herewith a dissertation written by Christine Rene Schar entitled "Expression of vitronectin in eurkaryotic cells : evaluation of PAI-1 binding and implications for gene therapy." I have examined the final electronic copy of this dissertation for form and content and recommend that it be accepted in partial fulfillment of the requirements for the degree of Doctor of Philosophy, with a major in Biochemistry and Cellular and Molecular Biology.

Cynthia B. Peterson, Major Professor

We have read this dissertation and recommend its acceptance:

Elizabeth Howell, Salil Niyogi, Barry Bruce
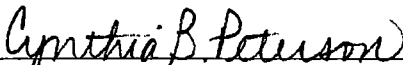
Accepted for the Council:

Carolyn R. Hodges

Vice Provost and Dean of the Graduate School
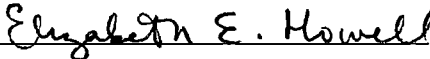
(Original signatures are on file with official student records.)
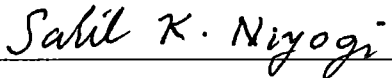
To the Graduate Council:
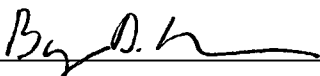
I am submitting herewith a dissertation written by Christine R. Schar entitled "Expression of Vitronectin in Eukaryotic Cells: Evaluation of PAI-1 Binding and Implications for Gene Therapy." I have examined the final copy of this dissertation for form and content and recommend that it be accepted in partial fulfillment of the requirements for the degree of Doctor of Philosophy, with a major in Biochemistry.

Cynthia B Peterson

Cynthia B. Peterson, Major Professor

We have read this dissertation
And recommend its acceptance:

Elizabeth E. Howell

Salil K. Niyogi

_By D. L_

Accepted for the Council:

Carw Minkel

Associate Vice Chancellor and
Dean of the Graduate School

Expression of Vitronectin in Eurkaryotic Cells: Evaluation of PAI-1 Binding and Implications for Gene Therapy

A Dissertation
Presented for the
Doctor of Philosophy
Degree
The University of Tennessee, Knoxville

Christine R. Schar
May, 2000

Dedication

Dedicated to my Mom and Dad, Marilyn and Ron Schar, who always told me I could do

anything I put my mind to.

Acknowledgements

Another thank you goes to Jeff Groah and Isaac. Thanks, Jeff, for either cooking or bringing me all those meals over the years. Thanks also for your adventurous spirit, which has taken us on many a road or plane trip. Finally, thanks for your support on those days when nothing seemed to work in the lab. I have to thank my dog, Isaac, who loves me unconditionally and does not complain when I tell him about the pitfalls of vitronectin research.

Finally, I want to say thanks to my family. Thank you, Brian and Michael, for helping me sharpen my wits over the years. Mom and Dad have always been supportive of me in whatever I do, and that did not change when I went to graduate school. My Dad always told me I could be anything I wanted to be. I doubt he foresaw this for me! Thanks for everything you two have done over the last 30 years!

Abstract

Vitronectin is a plasma protein involved in the maintenance of hemostasis, the balance between coagulation and fibrinolysis, as well as cellular adhesion. This multifunctional glycoprotein is present in the circulation as well as in the extracellular matrix. Vitronectin has a proposed domain structure that may explain why it is capable of binding s number of diverse ligands. The amino-terminal 44 amino acids are termed the somatomedin B domain. This domain is reported to be the primary high affinity binding site for two ligands, plasminogen activator inhibitor-1 (PAI-1) and the urokinase receptor (uPAR). However, ligand binding sites for these proteins have also been identified in the heparin binding domain near the carboxy-terminus.

The goal of this research was two fold: to determine if the high affinity binding site for PAI-1 was contained within the somatomedin B domain and to evaluate the potential for using gene transfer to confer an adhesive phenotype to endothelial cells. To achieve the first goal, the eukaryotic baculovirus expression system was utilized to express a somatomedin B deletion mutant. This recombinant protein was characterized funtionally for ligand binding abilities, with special attention focused on PAI-1 binding. The second goal was pursued using retroviral mediated gene transfer of PAI-1 and vitronectin into human umbilical vein endothelial cells. The cells were characterized in terms of protein expression levels, integrity of integrins and ability to withstand physiological shear stress.

Results of these studies indicate there are multiple PAI-1 binding sites, with the

high affinity site residing in the somatomedin B domain. In addition, over-expression of

PAI-1 or vitronectin by endothelial cells had no deleterious affects on cellular adhesion.

Table of Contents

List of Figures

Abbreviations Used

PAI-1	plasminogen activator inhibitor-1
uPAR	urokinase plasminogen activator receptor
uPA	urokinase-type plasminogen activator
tPA	tissue-type plasminogen activator
GPI	glycophosphatidylinsitol
TAT	thrombin/anti-thrombin complex
pro-uPA	non-cleaved, inactive urokinase-type plasminogen activator
PAI-2	plasminogen activator inhibitor-2
PN-1	protease nexin-1
CNBr	cyanogen bromide
ECM	extracellular matrix
BSA	bovine serum albumin
pVN	native, monomeric plasma vitronectin
mVN	multimeric vitronectin
mAB	monoclonal antibody
BSB	blue sepharose buffer
BBVN	Blue-bac vitronectin, expresses 72-kDa vitronectin
VN-his	recombinant 72-kDa vitronectin with a carboxy-terminal histidine tag
ssΔsBVN	recombinant vitronectin lacking the somatomedin B domain
ssΔsBVN-his	recombinant vitronectin lacking the somatomedin B domain with a carboxy- terminal histidine tag
pFB	pFASTBAC plasmid
mAB153	monoclonal antibody to the somatomedin B domain
PTFE	expanded polytetrafluoroethylene
HUVEC	human umbilical vein endothelial cells
pLXSN	retroviral plasmid containing the neomycin phosphotransferase gene
pLXSN/ssPAI-1	retroviral plasmid containing the PAI-1 gene with its signal sequence
pLXSN/ssVN	retroviral plasmid containing the vitronectin gene with its signal sequence
GP&E	NIH 3T3 cells transfected with gag, pol and env genes
neo	neomycin resistance gene
HUVEC/PAI-1	HUVEC cells transduced with PAI-1
HUVEC/VN	HUVEC cells transduced with vitronectin
HUVEC/pLXSN	HUVEC cells transduced with the vector pLXSN

Chapter 1

An Overview of Vitronectin Structure and Function

Biological Function and Relevance of Vitronectin

Proteins in the blood maintain hemostasis, the balance between coagulation and fibrinolysis. Vitronectin has emerged from the pool of blood proteins as an important factor regulating hemostasis. Vitronectin is a multifunctional glycoprotein present in a circulating form in the bloodstream as well as in a non-circulating form in the extracellular matrix. First identified as serum spreading factor, it was recognized as a factor in serum capable of promoting cellular adhesion and spreading (*1*). Also, vitronectin and the complement S-protein, the inhibitor of the membrane attack complex, are one and the same as determined by cDNA sequencing, functional and immunological studies (*2-4*).

Native vitronectin circulating in the bloodstream has an average molecular weight of 72,000. The amount of vitronectin present in serum ranges from 200 to 400 μg/ml, which comprises approximately 0.2 to 0.5% of the total protein in plasma. Vitronectin is mainly synthesized in the liver as a secreted glycoprotein. Other cells in the body, such as platelets, megakaryocytes and monocytes/macrophages, contain an immunologically identical protein to vitronectin, however, it is likely that vitronectin is endocytosed from plasma. Vitronectin is also released from activated platelets.

Vitronectin is a multidomain protein capable of binding a number of diverse ligands. A sampling of ligands known to interact with vitronectin encompasses receptors in cell membranes, constituents of the extracellular matrix, complement proteins and components involved in coagulation and fibrinolysis. Based on the ligands vitronectin is known to interact with, an additional role for vitronectin in wound healing, tissue remodeling, angiogenesis and tumor metastasis is predicted.

First, vitronectin functions in blood coagulation. The coagulation cascade is a complex one, with many checks and balances to ensure proper function. Within the vasculature and on the cell surface are heparin-like molecules that interact with vitronectin. Heparin, a glycosaminoglycan and a powerful anticoagulant, is commonly administered to prevent blood coagulation. It does so by helping inhibit the enzyme thrombin. Thrombin begins the formation of clots by cleaving the soluble protein fibrinogen into insoluble fibrin molecules, which then aggregate to form the framework of the clot. The action of thrombin is inhibited by antithrombin. Heparin accelerates the inhibitory activity of antithrombin by acting as a template on which thrombin and antithrombin can interact. Native vitronectin binds to heparin with a binding constant in the micromolar range (5). Vitronectin therefore competes with both thrombin and antithrombin for heparin binding, effectively reducing the anticoagulant ability of heparin. Vitronectin also regulates coagulation by binding to the thrombin/anti-thrombin complex (TAT). When vitronectin associates with TAT, these complexes are rapidly cleared from the circulation. It has been demonstrated that vitronectin-TAT complexes bind to human umbilical vein endothelial cells, which may be the first step in their

clearance from the circulation (*6*). They may also aid in cell adhesion and proliferation at the site of injury.

Vitronectin also has a role in fibrinolysis. For blood clots to dissolve, proteases must be present to degrade the fibrin mesh that has formed. A major protein involved in the dissolution of blood clots is plasmin. Active plasmin is generated from its precursor plasminogen by the action of plasminogen activators, which cleave plasminogen into plasmin. A potent inhibitor of plasminogen activators is plasminogen activator inhibitor-1 (PAI-1). PAI-1 binds to and inactivates the plasminogen activators, preventing plasmin formation and the ensuing degradation plasmin creates. However, PAI-1 is not a stable protein, converting readily to a latent state that is incapable of binding the plasminogen activators. PAI-1, upon binding to vitronectin, is stabilized in its active conformation. Therefore, vitronectin acts to prevent fibrinolysis by binding to prolonging the functional life span of the anti-fibrinolytic protein PAI-1.

The interaction of vitronectin and PAI-1 has other consequences as well. For example, the broad specificity protease plasmin has been implicated in the degradation of the extracellular matrix to allow cells to migrate (*7*). Proteases are important for processes such as tumor metastasis, tissue remodeling and wound healing. PAI-1 is a major inhibitor of plasmin formation, so the presence of PAI-1 may prevent plasmin formation and therefore proteolysis. Since PAI-1 is stabilized in its active conformation by vitronectin, the relative amounts of PAI-1 and vitronectin at a specific location could control whether a cell can free itself from its surroundings and migrate, which is important in tumor metastasis (*8*).

Angiogenesis, or the growth of new blood vessels, is critical for development and wound repair. For the growth of new blood vessels to occur, cells must migrate and proliferate. Therefore, it seems likely that vascular cell adhesion molecules must involved in the process of angiogenesis. Integrins are adhesive transmembrane proteins that help anchor the cell to one another and their surroundings. It has been shown that blood vessels involved in angiogenesis, in both the chicken and in humans, have increased expression of the integrin $\alpha_v\beta_3$ (9). Vitronectin is among the proteins recognized by the integrin $\alpha_v\beta_3$. But is vitronectin necessary for cell migration? A study by Stefansson suggests this is so. Smooth muscle cell migration was enhanced on vitronectin coated plates and the migration was shown to be $\alpha_v\beta_3$-dependant (10). When PAI-1 is present, it binds to vitronectin and disrupts smooth muscle cell migration (10). These studies only begin to demonstrate the complexity of integrin-mediated cell adhesion and migration.

Evidence is accumulating to support a role for vitronectin in microbial invasion. Vitronectin interacts with streptococci, staphylococci and *Escherichia coli*, providing an adhesive surface for these bacteria (11, 12). Specific attachment of *Pneumocystis carinii* to cultured lung epithelial cells occurs through its interaction with vitronectin (13). As for fungi, *Candida albicans* yeast cells specifically bind to soluble vitronectin and this interaction mediates adherence to a macrophage cell line (14). The ability of *C. albicans* to bind vitronectin in the extracellular matrix could be a factor in what makes this fungi so virulent (14).

Vitronectin has defined roles in diverse processes. It binds a wide variety of ligands. In binding its ligands, it regulates hemostasis, tissue remodeling, wound healing

4

and even tumor metastasis. A role is even emerging for vitronectin as being a sticky surface for bacterial and fungal adherence. How is it vitronectin can bind such a variety of ligands? Clues to address this question can be found through careful examination of the structural features of vitronectin.

Domain Structure and Post-translational Modifications

The human gene that encodes vitronectin is approximately 4.5 kilobases, consisting of 8 exons separated by 7 introns (*2*). There is no evidence for an alternately spliced gene product. Several genetic polymorphisms have been identified in the vitronectin DNA sequence, with one polymorphism (Thr➔Met-381) creating a protease cleavage site between amino acids arginine 379 and alanine 380 (*15*). Statistical analysis of the two forms of vitronectin found in the plasma of a number of subjects found the distribution compatible with a Hardy-Weinberg equilibrium distribution of two alleles (*16*). The protease responsible for cleavage at this site is unknown. The result of this limited proteolysis is the formation of a two-chain form of vitronectin (molecular weights of 62,000 and 10,000). The C-terminal fragment of vitronectin is not released, however. It is disulfide bonded to the remainder of the protein and released upon reduction of the disulfide.

Vitronectin contains 14 cysteine residues within its sequence. Eight of the fourteen cysteine residues are within the first 44 amino acids, the somatomedin B domain. These eight cysteine residues are believed to form a disulfide-bonded knot at the

amino-terminus of the protein. The other 6 cysteines are scattered throughout the remaining vitronectin sequence. Two disulfide bonds are formed between four of the cysteine residues. The two remaining cysteines are free, not disulfide-bonded.

Multi-domain Structure of Vitronectin

Vitronectin is often referred to as a multi-domain protein. It is believed to be folded into distinct modular domains, which separate its various functions within the molecule. Several lines of evidence suggest this may be true. Numerous regions of vitronectin share homology with other proteins, such as the somatomedin B domain and the hemopexin-like domains. Proteolytic digestion of vitronectin also implies vitronectin is a multi-domain protein. Proteases will digest the most accessible regions of proteins. In multi-domain proteins, the most accessible regions are the connecting regions between the domains and the surface exposed areas. Vitronectin contains many arginines and lysines (52 in its amino acid sequence) available for cleavage by trypsin-like proteases. However, trypsin has been shown to cleave native vitronectin only once, between R345 – G346, in the heparin binding domain (Figure 1-1) (*17*). Plasmin cleaves vitronectin near the endogenous cleavage site, at R361 – S362 (*18*) as well as near the amino-terminus at K88 - G89 (*19*). Two cleavage sites for thrombin are also present in vitronectin between R305 – T306 in the heparin binding domain and R370 – N371 within the second hemopexin-like domain (*19*). Forty-five alanine and leucine residues are available in the amino acid sequence of vitronectin for elastase cleavage. Once again, native vitronectin is surprisingly resistant to protease cleavage. Elastase cleavage of vitronectin only occurs twice within vitronectin, between amino acids A330 – M331 and L383 – S384, both in
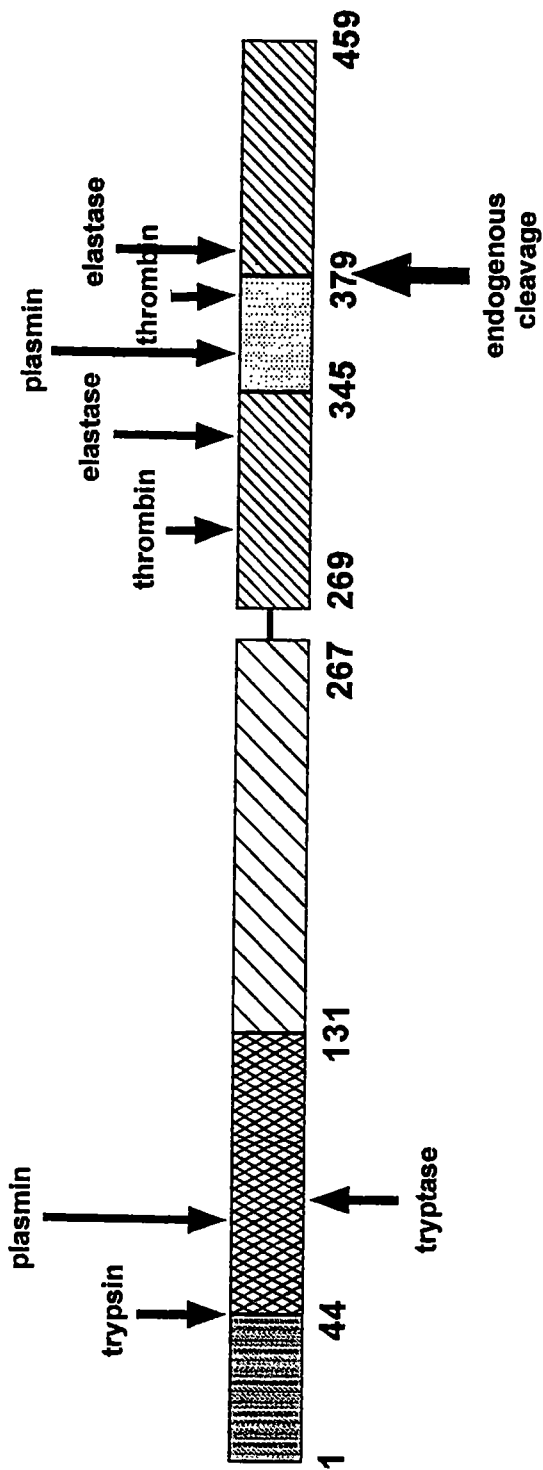
Figure 1-1: Protease Cleavage Sites Within the Proposed Domains of Vitronectin. The proposed domains of vitronectin are indicated by the boxes: the somatomedin B domain (▦), the connecting region (▨), the first hemopexin-like domain (☐), the second hemopexin-like domain (▧), and the heparin binding domain (▨). The protease cleavage sites for trypsin, plasmin, thrombin, tryptase and elastase are shown with arrows above the vitronectin schematic.

the second hemopexin-like domain (*19*). The clustering of protease susceptibility within

vitronectin suggests the presence of three domains.

Proteolytic digestion of vitronectin has also been used to determine the regions

responsible for ligand binding. Fragments isolated by proteolytic digestion often retain

their ligand binding specificity (see Figure 1-2 for domain structure and ligand binding

schematic). For example, vitronectin digested with trypsin (amino acids 1-45) still

retains PAI-1 binding ability (*17*). A plasmin digestion fragment encompassing amino

acids 1-361 has also been shown to retain PAI-1 binding ability (*18*). The following is a

description of each proposed domain, the post-translational modifications and ligand

binding abilities found therein.

Somatomedin B Domain

The amino-terminal portion of vitronectin contains several important features.

The first 44 amino acids form the somatomedin B domain of vitronectin. The

somatomedin B domain is believed to fold independently from the rest of the protein.

The protease resistance of this domain as well as its homology to other proteins supports

this hypothesis. Several proteins that contain somatomedin B-like domains have been

identified, such as the megakaryocyte-stimulating factor (*20*), the plasma cell membrane

glycoprotein PC-1 [Patthy, 1988 #94] and the tumor cell surface antigen gp130[RB13-6]

(*21*), all of which contain two tandem repeats of somatomedin B-like domains at their

amino-terminus. These proteins with somatomedin B-like domains also contain eight

cysteines. Eight cysteines are present within the amino acid sequence of the

somatomedin B domain. It is predicted that these eight cysteines form intramolecular

disulfide bonds, resulting in a disulfide-bonded knot.
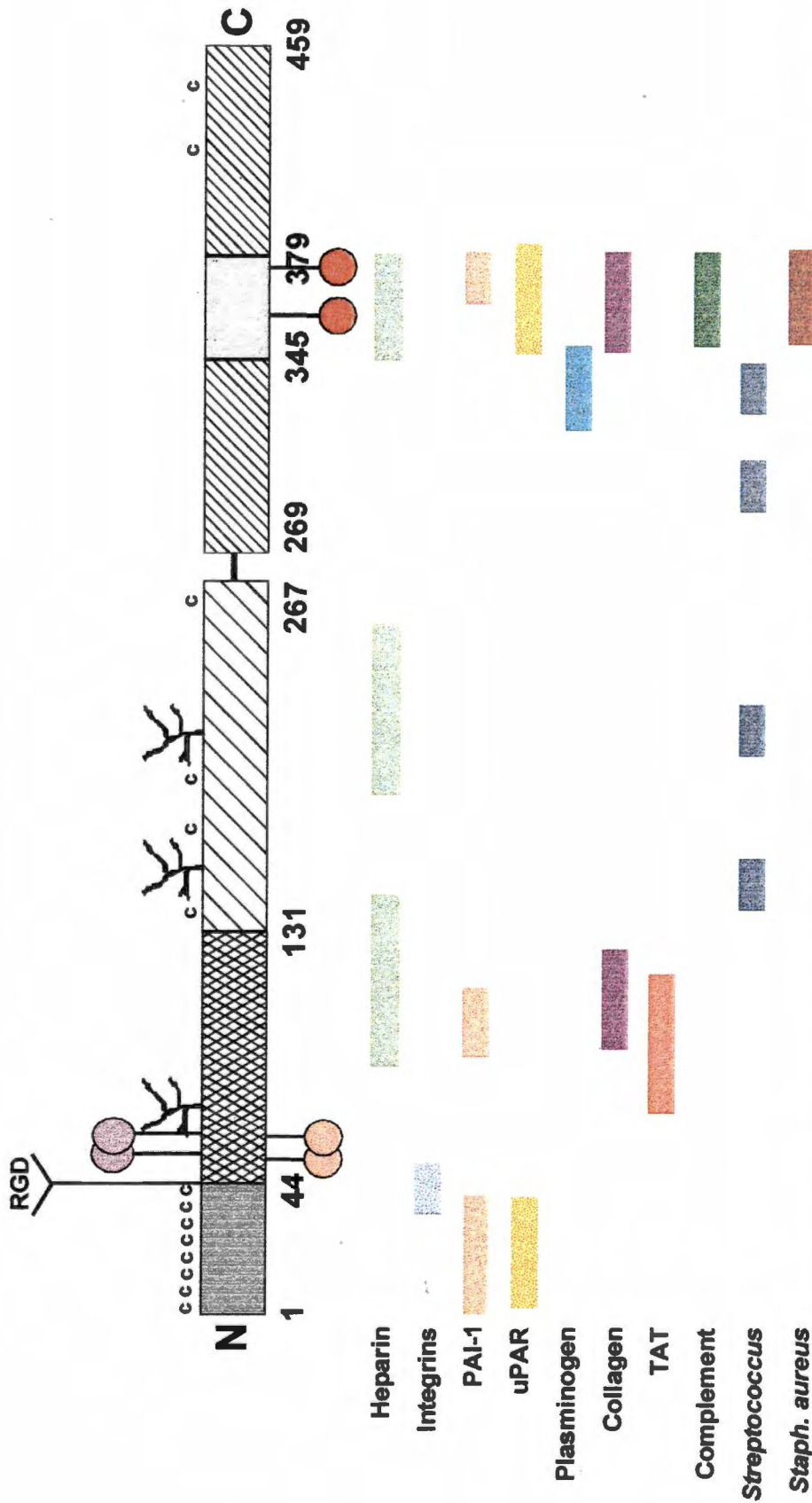
Figure 1-2: Post-translational Modifications and Proposed Ligand Binding Sites. The branched chains represent the sites of N-linked glycosylation on the proposed domain structure of vitronectin. The "c" denotes the location of the 14 cysteine residues in vitronectin. The lavender circles represent the two sulfated tyrosines, Tyr 56 and 59. The pink circles represent two threonine residues (Thr 50 and 57) that can be phosphorylated by casein kinase II. The orange circles in the heparin-binding domain are Ser 362 and 378, which can be phosphorylated by protein kinase C and protein kinase A, respectively. Below the domain structure with post-translational modifications are the proposed regions involved in ligand binding.

Cell Binding Sequence

Immediately following the somatomedin B domain is the arginine-glycine-aspartic acid sequence (RGD sequence). The RGD sequence is a common feature of many extracellular matrix proteins, including fibronectin, laminin and collagens. The RGD sequence is responsible for the integrin binding ability of vitronectin. Site directed mutagenesis of the RGD site has shown these three amino acids are necessary to promote integrin mediated cell adhesion and migration (22). Three integrins are capable of binding vitronectin, $\alpha_v\beta_1$, $\alpha_v\beta_3$ and $\alpha_v\beta_5$ (23). The integrin $\alpha_v\beta_3$ is commonly referred to as the "vitronectin receptor"; however, it binds at least 6 other ligands such as fibronectin and collagen.

Connecting Region

The "connecting region" of vitronectin between residues 46 and 130 links the somatomedin B domain to the hemopexin-like domains. A number of modifications to vitronectin take place within the connecting region. Asparagine 67 is post-translationally modified by N-linked glycosylation. Several acidic amino acids reside between amino acids 53 to 64, which many refer to as the "acidic" region of vitronectin. Within this acidic region, two tyrosine residues (Tyr-56 and Tyr-59) are post-translationally sulfated (24). Vitronectin is a substrate for both tissue and plasma transglutaminases *in vitro* (25). Vitronectin has been shown to form high molecular weight cross-linked multimers in the presence of transglutaminases. The putative cross-linking sites have been identified as glutamine 93, 73, 84 and 86 (26). Two threonine residues within the connecting region are substrates for casein kinase II, which is found in human serum and on the surface of blood cells. Phosphorylation of Thr-57 facilitates the phosphorylation of Thr-50 by

casein kinase II (*27*). The double mutant T50E/T57E expressed in the baculovirus system, which simulates phosphorylated threonine, promotes cell adhesion and accelerates the rate of cell spreading compared to the neutral T50A/T57A mutant or wild-type vitronectin. Phosphorylation of vitronectin at these threonine residues in such close proximity to the cell binding sequence may be responsible for promoting cellular adhesion.

Hemopexin-like Domains

The remaining sequence is homologous to the protein hemopexin, thus this region is referred to as the hemopexin-like domain (*28*). Two more sites for N-linked glycosylation, Asp150 and Asp223, are present in this domain. Six cysteine residues reside in this portion of vitronectin, taking part in two disulfide bonds. The two remaining free cysteines are buried within the vitronectin structure. Two phosphorylation sites are present in the second hemopexin-like domain. Protein kinase A phosphorylates vitronectin at Ser-378 ((*29-31*). Protein kinase A is found as an ectoenzyme in blood cells and is released into the blood from platelets once they are activated by thrombin [Korc-Grodzicki, 1988 #84]. Following the phosphorylation of Ser-378, one researcher found PAI-1 exhibited weaker binding to vitronectin (*30*). Vitronectin is also a substrate for protein kinase C *in vitro*, capable of being phosphorylated at Ser-362. Phosphorylation of vitronectin by protein kinase C was shown to attenuate the cleavage of vitronectin by the enzyme plasmin (*32*). The hemopexin-like domains are homologous to the heme transport protein, hemopexin. The division of the repeats is not straightforward, therefore, where the tandem repeats characteristic of hemopexin are aligned within the vitronectin sequence is fairly arbitrary.

Hemopexin is a serum glycoprotein that binds to heme reversibly and delivers it to the liver where it is taken up by receptor-mediated endocytosis. Removal of free heme is important, since it can catalyze free radical formation in the body. Hemopexin is synthesized as a single chain protein 440 residues in length. It is divided into two homologous domains that share approximately 25% sequence identity. The two domains are joined together by a hinge (*33, 34*). A four-fold internal sequence repeat is seen in each of the 200 amino acid domains (*28, 35*). This sequence repeat creates folds which are approximately 45 amino acids in length within which are conserved amino acids. It is this feature that allows identification of hemopexin-like domains in other proteins. The crystal structures of rabbit serum hemopexin, matrix metalloproteinase 2 (MMP2) and collagenase-3 (MMP-13) have been solved, with the structures of each being remarkably similar (*36-38*). The overall structure is disc-shaped, with a funnel-like tunnel in the middle of the each domain's disc that serves as an iron-binding site. The internal four-fold sequence repeats fold into four β-sheets. Each β-sheet is made of four anti-parallel β-strands. The β-sheets are arranged almost symmetrically about a central axis, creating a four-blade β-propeller structure (*37*). In hemopexin, the cyclic structure is stabilized by a disulfide bond between the first and last blades (*36, 39*). The apparent desire for ring closure suggests these circular structures are not entirely stable, and the addition of disulfide bonds could help avoid misassmbly

Heme binding is mediated primarily through the interdomain linker region between the two propeller domains, with residues from both domains involved (*39*). Both domains participate in conformational changes that are associated with heme binding and release (*40, 41*). Two histidines bind heme within the heme binding site,

which also contains a number of aromatic and basic residues (39). The positively charged environment around the heme acts to keep the histidines deprotonated and therefore stably coordinated to the iron above pH 5. Heme could then be released by decreasing the pH below 5, resulting in protonation of one or both of the histidines. This protonation could result in local unfolding, causing domain and/or linker movement and subsequent release of heme (39).

Interestingly, almost all of the β-propeller-containing proteins are multi-domain proteins (42). The β-propeller proteins that have been identified appear to be important in mediating protein-protein and protein-ligand interactions. Also of note, most of known β-propeller proteins have a way of bringing their first and last blades of the propeller together, either by extensive hydrogen bonding or disulfide bond formation (42). It is possible that the hemopexin-like domains of vitronectin also adopt a similar structure to that seen in hemopexin and could potentially explain the process of vitronectin multimerization. Indirect evidence from our laboratory support the theory that multimerization could be mediated through the hemopexin-like domains by excluding the involvement of other regions in multimerization (43).

Threading has been applied as a means to determine the three dimensional structure of vitronectin (C. Peterson, unpublished results). Since vitronectin shares such high homology with hemopexin, the crystal structure of hemopexin can be used as a template to "thread" vitronectin sequence. As a result of this threading, a total of 6 hemopexin-like repeats (blades) were elucidated (Figure 1-3). Four of the blades are in the central region between amino acids 129 and 323. A disulfide bond between amino acids 137 and 161 helps to constrain the modeling. The free sulfhydryl at amino acid 196

13
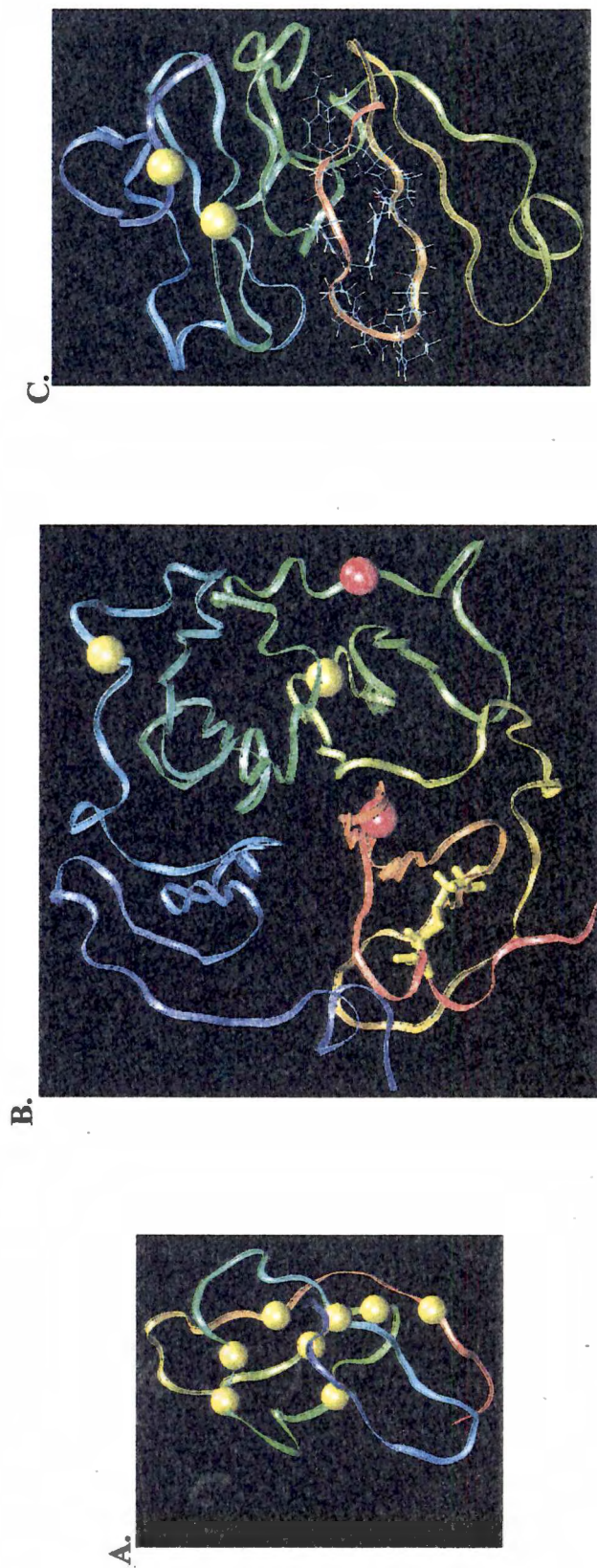
Figure 1-3: Model of Vitronectin Based on Threading. Molecular modeling of the domains of vitronectin. The somatomedin B domain is modeled in panel A. This structure is modeled with only 3 or the 4 proposed disulfide bonds. The central portion of vitronectin with 4 hemopexin-like repeats is shown in panel B. A four bladed β-propeller structure is visible. The last figure, panel C, shows the remaining hemopexin repeats, which form 2 blades of the β-propeller.

is buried in this model. The region between amino acids 354 and 456 contains 2

additional blades. The blades are interrupted by the heparin-binding domain. The free

sulfhydryl at 411 is buried in this model.

Heparin-Binding Domain

Within the second hemopexin-like domain is the heparin-binding domain. This

highly charged basic amino acid sequence spans residues 345 to 379 as identified by

affinity chromatography following cyanogen bromide digestion of vitronectin (*44*). The

heparin-binding site has been commonly referred to in the literature as being "cryptic"

within native vitronectin, becoming exposed upon denaturation and multimerization of

vitronectin. However, there is compelling evidence to suggest the heparin-binding site is

not cryptic, but exposed in both native and multimeric vitronectin. Titration curves

generated using fluorescently labeled heparin with native and multimeric vitronectin

demonstrated the two forms of vitronectin have the same binding affinity but have

different binding stoichiometries (*5*). This accounts for why many have seen an apparent

increase in binding affinity when using multimeric vitronectin. Other work by Gibson *et*

al. argues for a single exposed heparin binding site with no functional secondary binding

sites becoming exposed upon vitronectin multimerization (*45*). Monoclonal antibodies

specific for the altered form of vitronectin show that heparin can bind native vitronectin

(*46*). The serine residue at position 378 near the end of the heparin-binding domain can

easily be phosphorylated without denaturation (*31*). Other compelling evidence

supporting an exposed heparin-binding domain is the susceptibility of the region to

proteolytic digestion (see Figure 1-1). Both plasmin and thrombin cleave vitronectin in

the heparin-binding domain, with endogenous cleavage taking place at the end of the

domain. The susceptibility of this region to cleavage argues for an exposed heparin-binding domain.

Conformational Forms of Vitronectin

Vitronectin found in plasma is in its native, monomeric form. Upon denaturation by heat treatment, acid or chaotropic agents, vitronectin converts to a multimeric state following renaturation (*47*). Free cysteines exposed upon denaturation allow intermolecular disulfide bonds to be formed within some vitronectin multimers.

Early in the history of vitronectin research, it was discovered that denatured vitronectin bound to a heparin-Sepharose column more tightly than native vitronectin at physiological ionic strength (*46, 48*). Denatured vitronectin was also shown to more effectively neutralize the effects of heparin compared to native vitronectin (*48*). Complex formation between vitronectin and thrombin/anti-thrombin was shown to induce conformational changes in vitronectin, as monitored by increased reactivity with the conformationally sensitive antibody 8E6 (*46, 49*). These conformational changes also resulted in increased heparin binding. Based on these observations and the homology vitronectin shares with hemopexin, a model was put forth in which the heparin binding region is buried due to its interaction with acidic residues at the amino terminus and was therefore non-functional in native vitronectin (*50*). Upon denaturation, vitronectin would adopt a more open conformation, exposing the buried heparin-binding region. This model has been widely accepted by those doing vitronectin research, despite their own results, which often argue against it.

Although the encrypted-binding site model is popular among many researchers, another model is trying to emerge. As aforementioned, several pieces of evidence argue

against a buried heparin-binding region. Amino acids close to the region are available for phosphorylation as well as cleavage by proteases. More biophysical approaches have been used to study the heparin-binding ability of both native and multimeric vitronectin, and these measurements demonstrated both forms have the same binding affinity for vitronectin (5). Solution-based heparin-binding assays, NMR and expression of the carboxyl terminus (from Met 330 to Leu 459, encompassing the heparin-biding domain) of vitronectin support the defined heparin-binding domain as the primary site (45). This work also supports the contention that the heparin-binding domain is exposed in native vitronectin.

How does vitronectin multimerize? Comparison of unfolding and refolding curves for vitronectin shows they are not superimposable. This indicates the starting and ending products are not the same or the pathway for folding and unfolding is not the same (51). During refolding, the unfolded vitronectin is in equilibrium with a partially folded intermediate. This intermediate has a propensity to self-associate, but the refolding pathway favors the formation of multimers under physiological conditions. The formation of multimers upon refolding can be shifted toward monomeric vitronectin in the presence of high salt (47). Interestingly, inclusion of a heparin-binding peptide upon refolding does not prevent or promote multimerization. This argues against the encrypted-sites model, in which exposure of the heparin-binding domain causes vitronectin multimerization.

Ligand Binding Ability of Vitronectin

The multi-domain protein vitronectin is also conferred with multiple functions as well. Vitronectin is a difficult protein to assay since it exhibits no easily measurable activity of its own, but rather works to co-ordinate other proteins to perform a multitude of tasks. Coagulation, fibrinolysis, angiogenesis and cellular migration are several events that have been linked to vitronectin in the body. It is the proteins vitronectin interacts with in the bloodstream or in the extracellular matrix that are responsible for the above mentioned tasks to occur. The following section describes the ligand binding abilities of vitronectin by domain. A more thorough discussion of plasminogen activator inhibitor-1 (PAI-1) and its interaction with vitronectin will be explored in a separate section to follow.

Somatomedin B Domain

Two ligands have been shown to bind in the somatomedin B domain (Figure 1-2). PAI-1 binding has been localized to the somatomedin B domain as well as other regions of vitronectin. Further discussion of PAI-1 binding to vitronectin will take place later. The other ligand that binds to the somatomedin B domain is the urokinase-type plasminogen activator receptor (uPAR). As with PAI-1, the exact binding location of uPAR is controversial. The urokinase receptor is a glycosylated protein made up of three homologous repeats approximately 90 amino acids each, termed D1, D2 and D3. Linker regions tether the domains to one another. The linker region between domains 1 and 2 is sensitive to proteolysis, with low concentrations of chymotrypsin capable of cleaving this region (*52*). The amino-terminal repeat (D1) has been implicated in ligand binding (*52,*

53). The receptor is anchored to the membrane via a glycosyl-phosphatidylinositol (GPI) moiety *(54).* The GPI anchor is preferentially attached to residue Gly283 *(55).*

The uPA receptor binds both two-chain uPA and the single chain pro-uPA *(56).* uPA is released from cells in a single-chain form, which can be converted into its active two-chain form by limited proteolysis *(57, 58).* Binding of uPA to uPAR regulates uPA activity by either accelerating its conversion from pro-uPA to its active form *(59, 60)* or inhibiting the active enzyme with specific inhibitors *(61, 62).* Receptor bound uPA is accessible to and is capable of being inhibited by PAI-1, PAI-2 and PN-1 (protease nexin1) *(61-63).* When active uPA is bound to uPAR, the complex is not internalized and remains on the cell surface. However, when the receptor-bound uPA becomes complexed with one of its specific inhibitors, the complex is internalized and degraded *(64, 65).* Two transmembrane receptor proteins have been implicated in the clearance of the complexes, the α_2-macroglobulin receptor/low density lipoprotein receptor-related protein and the epithelial glycoprotein-330 *(66, 67).*

The uPA/uPAR system has a role in cellular migration, adhesion and signaling. The urokinase receptor has been shown to interact with vitronectin *(68).* PAI-1 binding blocks the binding of cells to vitronectin and soluble uPAR *(69, 70).* One model to explain these findings has the somatomedin B domain competing for both uPAR and PAI-1 binding. When excess PAI-1 is present, the PAI-1 will bind to the somatomedin B domain of vitronectin, leaving uPAR unoccupied and the cell less adhesive *(70).* The group led by Chapman agrees with this model; however, their data suggests PAI-1 interacts with vitronectin within the heparin binding domain which then decreases the affinity for uPAR.

Evidence supporting the localization of uPAR binding to the somatomedin B domain stems from competition experiments. The somatomedin B peptide 1-41 competes with immobilized vitronectin for uPAR binding (70). The same paper also demonstrates that the monoclonal antibody m153, specific for the somatomedin B domain, prevents uPAR binding to vitronectin.

Connecting Region

The binding sites for a number of different ligands have been localized to the connecting region. The acidic region may play a role in the initial binding of vitronectin to thrombin-anti-thrombin complexes (6). Collagen binding has been localized to the connecting region by using polypeptides derived from this region (71) and monoclonal antibody mapping (72). Another PAI-1 binding site was localized to residues 115 to 121 (73) using proteolytic fragments of vitronectin. The fragment competed for PAI-1 binding and also stabilized PAI-1 activity. A second heparin binding region (Asp82-Cys137) was localized to the connecting region using phage display to identify peptides that competed for heparin binding on immobilized vitronectin (74).

Hemopexin-like Domains

The first hemopexin-like domain binds several different ligands. A potential heparin-binding site has been localized to the first hemopexin-like domain between residues Lys-175 and Asp-219. This binding site was discovered using phage display (74) and was proposed to be cryptic in native vitronectin, however, the heparin binding affinity was not quantitated so the results may be misleading. Vitronectin has been shown to bind to bacteria, and two binding sites for *Streptococcus* have been identified in the first hemopexin-like repeat (12). Two additional *Streptococcus* binding sites are

located in the second hemopexin-like domain. The *Streptococcus* binding sites are characterized by their repetitive hydrophobic sequences. The binding site for plasminogen has been described in the second hemopexin-like domain (*75*). Limited digestion of vitronectin with plasmin generated a 61 kDa fragment that retained plasminogen binding ability until the terminus was digested with carboxypeptidaseB, at which point plasminogen no longer bound.

Heparin-binding Domain

The highly charged basic amino acid sequence of the heparin-binding domain has been implicated in the binding of many diverse ligands. The heparin-binding domain has been localized to this region based on its similarity to the heparin-binding sequences found in other proteins. In addition, a cyanogen bromide digestion fragment containing the heparin-binding domain has high affinity for heparin and competes with full-length vitronectin for heparin binding (*44*). Further competition studies using both synthetic peptides and monoclonal antibodies to the heparin-binding region also support the contention the heparin-binding domain contains the heparin-binding site in vitronectin (*75*). Cleavage sites within the heparin-binding domain have been used to demonstrate the heparin-binding ability of the region. Plasmin digestion of this region results in the loss of heparin-binding ability (*19, 75*). Digestion of vitronectin with both thrombin or elastase under non-reducing conditions which removes the heparin-binding domain but leaves the disulfide connecting the two chains intact generates forms of vitronectin that no longer retain heparin-binding ability (*19*).

Other ligands with localized binding to the heparin-binding domain include PAI-1 (*18, 75, 76*), uPAR (*77*), collagen (*71, 78*), complement complexes and perforin (*79*), and

Staphylococcus aureus (*11*). A series of synthetic peptides generated from the region surrounding a plasmin cleavage site (Arg361) were used to isolate the uPAR binding site in vitronectin (*77*). Two peptides, spanning residues 364-380 in the heparin-binding domain, blocked the binding of soluble uPAR to immobilized vitronectin. The collagen-binding ability of purified vitronectin fragments generated from formic acid cleavage was investigated by Ishikawa-Sakurai *et al*. Two groups of collagen-binding fragments were determined, with one group being localized to the heparin-binding domain (*71*). Full-length vitronectin as well as a cyanogen bromide digestion fragment from the heparin-binding domain (348-360) both inhibited the lytic activity of the membrane attack complex of complement as well as perforin secreted from cytotoxic T-cells (*79*). Finally, both heparin and a synthetic peptide from the heparin-binding domain inhibited *Staphylococcus aureus* adherence to vitronectin (*11*).

Multiple binding sites have been identified within vitronectin for several ligands. A single ligand may have more than one binding site within vitronectin, so the observation of multiple binding sites is feasible. However, it is the discrepancies that have been reported for the same sites within vitronectin that raise concern. It would appear that few results could be consistently repeated. The cause for these discrepancies could be due to the nature of the proteins involved, the design of the experiments and the personal bias of the researcher. For example, vitronectin is now described as a conformationally labile protein. Upon denaturation, vitronectin forms multimers. A common method for purification of vitronectin involves the addition of urea to serum followed by application to a heparin column. This form of vitronectin is easily purified, yet displays different ligand binding characteristics than native vitronectin. Therefore,

the conformational state of the vitronectin used in the studies must be properly evaluated. Vitronectin also undergoes some structural perturbations upon binding to plastic surfaces. This is usually not addressed in experimental design or interpretation. Lastly, many researchers interpret their results using encrypted-binding site models even though their results suggest otherwise. Therefore, the methodology and results should be carefully scrutinized before interpretation. Since this is not always possible, especially with early vitronectin research, it is often very difficult to draw conclusions from these studies.

PAI-1 and Vitronectin Interactions

The fact that vitronectin and plasminogen activator inhibitor-1 (PAI-1) interact has been well documented and is not a point of contention. However, the location of PAI-1 binding within vitronectin, the number of PAI-1 molecules that can bind vitronectin and even the downstream interactions of the complex are at the heart of a fevered debate. The problems of the conformational state of vitronectin as well as the techniques used to examine the interactions between PAI-1 vitronectin do more to complicate the debate and make comparison of results difficult. What follows is an overview of the structure of PAI-1, evidence for multiple PAI-1 binding sites within vitronectin and how the interaction of PAI-1 with vitronectin is important physiologically.

The human PAI-1 gene is composed of nine exons with eight introns (*80*). Full-length PAI-1 is synthesized as a 402 amino acid protein, with a 23 amino acid signal sequence. The mature protein is 379 amino acids in length. The mature protein contains

no cysteines, therefore the protein has no disulfide bonds. Three asparagine-linked glycosylation sites are present in PAI-1 but apparently do not affect its biological function. PAI-1 produced in *E. coli* lacking any glycosylation exhibits the same properties as glycosylated PAI-1 *(81)*.

PAI-1 functions to inhibit plasminogen activators. Plasminogen activators are serine proteases that activate the zymogen plasminogen to the broad-specificity enzyme plasmin. The two plasminogen activators found in mammals are tissue-type and urokinase-type plasminogen activators (tPA and uPA, respectively). PAI-1 is the most potent inhibitor of both tPA and uPA, preventing them from activating plasminogen. PAI-1 is secreted into plasma from hepatocytes *(82)*, endothelial cells *(83, 84)* and platelets *(85)*. The circulating concentration of PAI-1 is approximately 10 ng/ml, but localized concentrations can be much higher.

Mechanism of Action of Serpins

PAI-1 is a member of the serine protease inhibitor (serpin) family of proteins. Serpins are highly homologous proteins whose prime function is the inhibition of serine proteases. Serpins have a well-conserved tertiary structure *(86)*. Inhibition of serine proteases by serpins occurs through the interaction of the active site of the protease with the mobile reactive center loop of the serpin, which acts as a pseudo-substrate (see Figure 1-4) *(87, 88)*. Once bound to the protease, the reactive site residues on the mobile loop are accessible for cleavage. The residues that mimic the scissile bond (where the protease cleaves its substrate) are called the P1 and P1' residues *(89)*. The entire scheme for cleavage of the P1-P1' residue is unclear, but it is generally assumed the first step of the pathway is the binding of the mobile loop to the active site of the protease, forming a
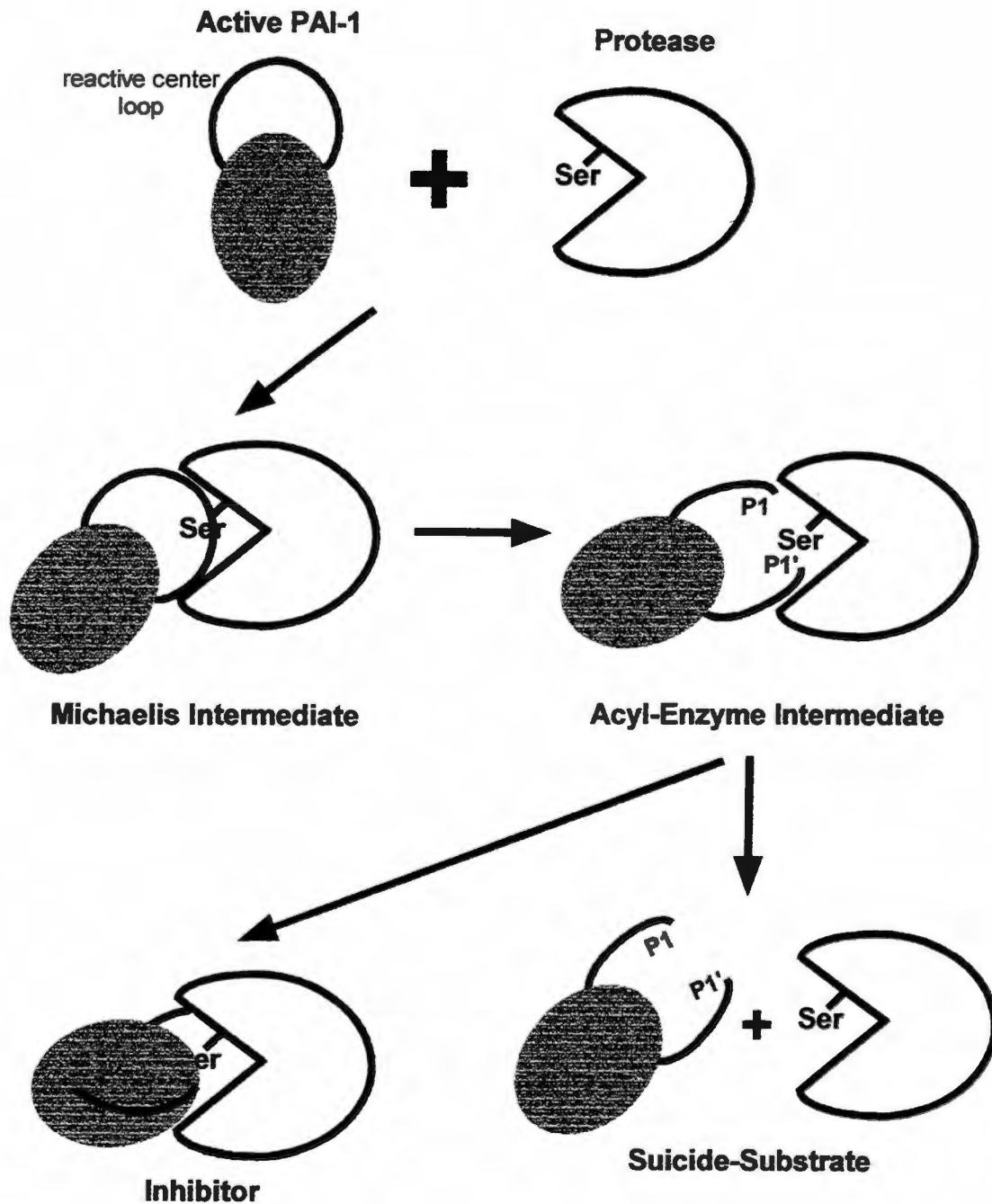
Figure 1-4: Mechanism of Serpin Action. The reactive center loop of active PAI-1 binds the protease to form a Michaelis type complex. The active site serine attacks the serpin, forming an acyl enzyme intermediate once the scissle bond is cleaved. The serpin can become either an inhibitor or a suicide substrate at this point. If the loop can insert into its central β-sheet, the serpin becomes an inhibitor. If insertion of the loop is blocked or if deacylation occurs before loop insertion, the serpin becomes a suicide substrate and is released from the active protease.

Michaelis-type intermediate. Following the formation of this complex, the serine in the active site of the protease attacks the carboxyl side chain of the P1 residue. An acyl-enzyme intermediate is formed once the P1-P1' bond is cleaved (*90, 91*). The cleavage of the P1-P1' bond is followed by a rapid insertion of the reactive center loop into the central β-sheet A (*92*). The five or six-stranded A sheet is the dominant feature of the molecule, with the reactive center loop extending from its fourth strand (*89*). If the reactive center loop is not able to fully insert into β-sheet A, the complex locks up. This event may prevent the deacylation of the acyl-enzyme intermediate, trapping the entire complex with no possibility of escape for the protease. However, if the insertion of the reactive center is blocked or if deacylation can occur before reactive center loop insertion, then the cleaved serpin is unable to bind the protease any longer and the protease is released from the inactive serpin (*93*). Therefore, the serpin can act as a substrate or an inhibitor based on the ratio of the rate of deacylation to the rate of loop insertion (*93*).

Structure of PAI-1

PAI-1 exists in two different conformations, an active form and a latent form. The active form of PAI-1 is relatively unstable and spontaneously converts to its inactive latent form without cleavage of its scissile bond between the P1 and P1' residues (Arg 358 and Met 359, respectively) (*81, 94*). The latent form can be partially reactivated by denaturation and renaturation (*95*).

The crystal structure of latent PAI-1 was solved in 1992. The structure was similar to the solved structures of other serpins and provided a glimpse into the mechanism of latency seen in PAI-1 (Figure 1-5) (*96*). The three core β-sheets, A, B and
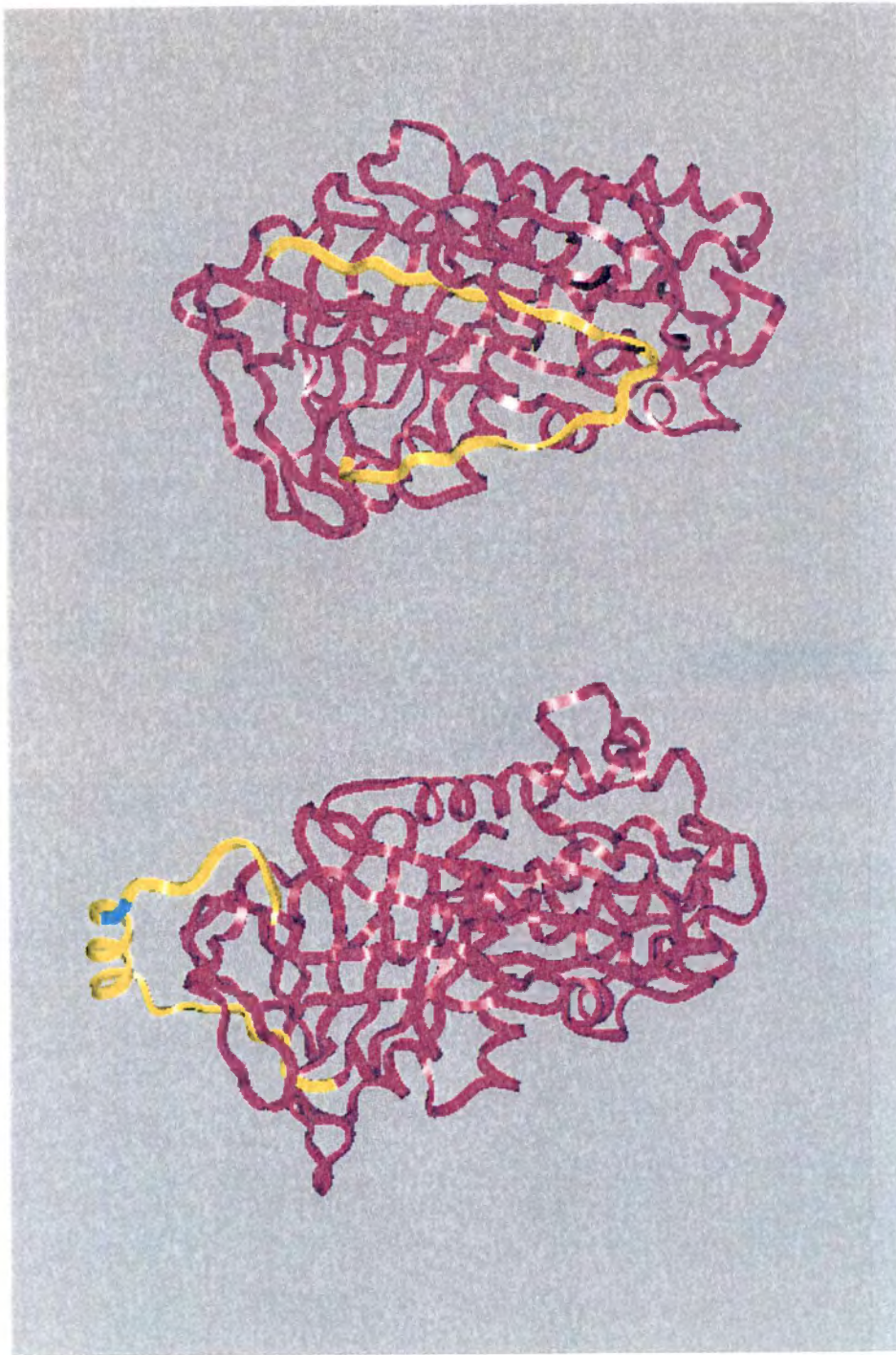
Figure 1-5: Structures of Ovalbumin and Latent PAI-1. Ovalbumin (structure on the right) is a non-inhibitory member of the serpin family. It is believed that active serpins resemble the structure of ovalbumin. The structure of latent PAI-1 is shown on the right. Both structures were modeled from their x-ray crystalographic coordinates (96) using the program Insight. The core of the proteins are both magenta ribbons. The reactive center loop in both proteins is modeled in yellow ribbon.

C, superimpose well with those of other serpins. The reactive center loop, between residues Ser 343 and Arg 368, was clearly resolved. The P16 to P4 residues (Ser 343 to Val 355) had become incorporated as a central β-strand (strand 4) in the central β-sheet A. The rest of the reactive center loop from P2 to P10' (Ser 356 to Arg 368) forms a loop on the surface of the protein. Interactions between the strands of the β-sheets and the reactive center loop stabilize the latent conformation.

Other evidence supports loop insertion causing latency in PAI-1. Limited protease digestion of the different forms of PAI-1, as well as PAI-1 complexed forms, allowed detection of conformational differences (*97*). PAI-1 in which the reactive center loop was cleaved had an indistinguishable digestion pattern from PAI-1 complexed to uPA. This result is in agreement with reactive center loop insertion into the central β-sheet, decreasing exposed regions for protease digestion. Mutagenesis of specific residues thought to be important in stabilizing the latent form of PAI-1 has been performed in an effort to increase the functional stability of the protein (*98*). Examination of the crystal structures of latent PAI-1 and the non-inhibitory serpin ovalbumin, which serves as a model for the active conformation of serpins, identified a salt bridge in latent PAI-1 that is not present in ovalbumin. Site directed mutagenesis was performed to disrupt this salt bridge between Glu-350 in the reactive center loop and Arg-30. All mutants constructed demonstrated an increased functional half-life compared to wild-type PAI-1, suggesting this salt bridge stabilizes the conformation of the latent form. Fluorescence spectroscopy was also employed to study loop insertion (*92*). A serine at the P9 position was changed to a cysteine, which was labeled with the fluorescent probe, NBD. An identical fluorescence increase and blue shift was seen in

cleaved PAI-1 and PAI-1 complexed with tPA or uPA. This data suggests that interaction with tPA or uPA results in insertion of the loop into β-sheet A, similar to latent PAI-1.

The crystal structure of a stable mutant of PAI-1 was solved in 1999. A stable quadruple mutant (Asn150→His, Lys154→Thr, Gln319→Leu and Met354→Ile) was made in bacteria and purified (99). The crystal structure revealed some interesting points (Figure 1-6). Two of the four independent molecules in the crystal had flexible reactive center loops, which were unconstrained by the packing of the crystal and hence were quite disordered. However, in the other two molecules of PAI-1, the reactive center loop is seen to interact with the central β-sheets of a different neighboring molecule of PAI-1, forming loop-sheet interactions. The result of this interaction was the generation of seemingly endless chains of PAI-1 molecules. The disorder seen in the two unconstrained PAI-1 molecules supports the notion that the reactive center loop of the active conformation of PAI-1 is flexible while the polymerization of the other two PAI-1 molecules gives insight into the mechanism of serpin polymerization seen in certain diseases.

Vitronectin Binding Site on PAI-1

Vitronectin binds PAI-1 with high affinity, with a K_d value equal to or lower than 100 nM (100). It has also been reported that vitronectin binds latent PAI-1, however, this interaction is weak when compared to active PAI-1 (101). The binding of vitronectin to active PAI-1 in solution increases the half-life of active PAI-1 by 2 to 3 fold (101, 102). The localization of the vitronectin-binding site within PAI-1 was investigated in order to gain some insight into the mechanism of PAI-1 stabilization imparted by vitronectin.
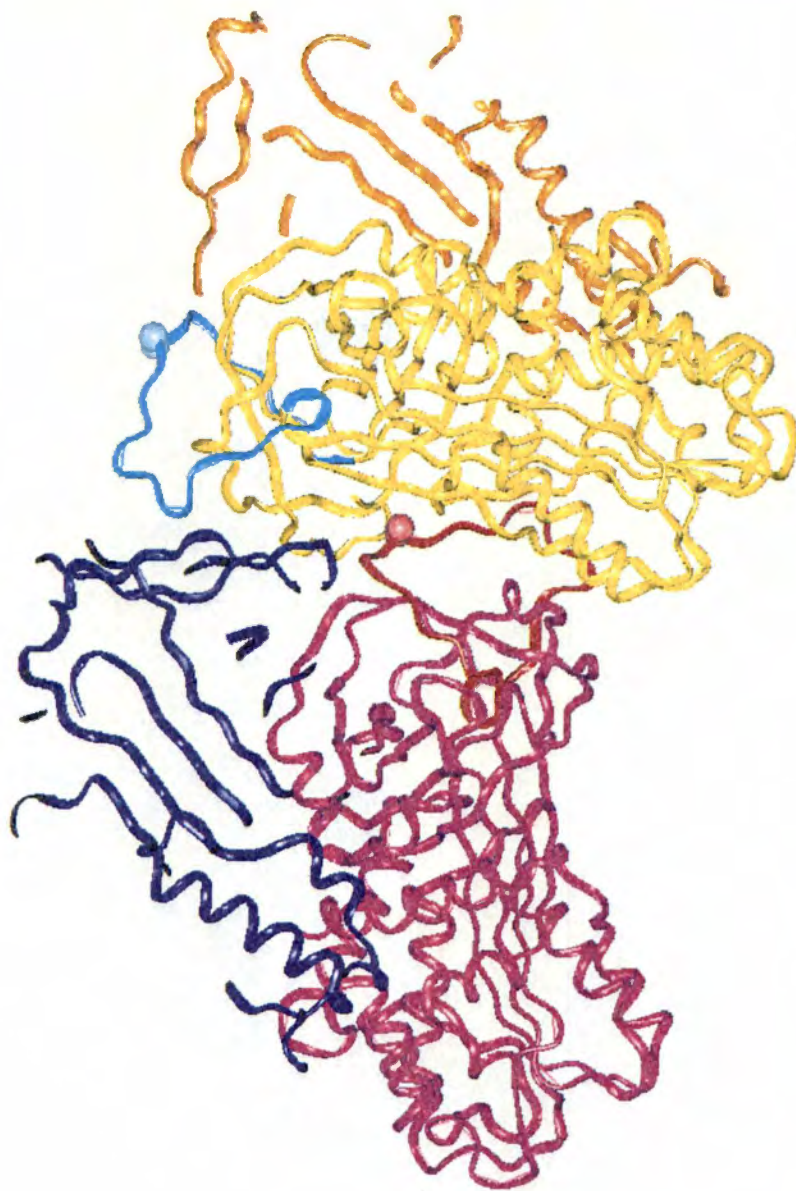
Figure 1-6: Structure of Active PAI-1. The structure of active PAI-1 was recently solved (99). In the crystals, four molecules could be resolved. Two of the PAI-1 molecules (in blue and orange) were resolved, however, their reactive center loops were disordered and could not be resolved. The other two molecules of PAI-1 (in magenta and yellow) were clearly resolved. The reactive center loops of each (in red and cyan) were found to interact with the β-sheets of a neighboring PAI-1 molecule, forming long polymers of PAI-1. For reference, the P1 and P1' residues are shown as spheres on the reactive center loops.

Three studies position the major vitronectin-binding site in the amino-terminal portion of PAI-1, with no involvement from the reactive center loop. Lawrence's group used random mutagenesis of approximately half (residues 13-147, nucleotides 248-650) of the cDNA of PAI-1 to find mutants that exhibit decreased binding to immobilized vitronectin yet still inhibited uPA(*103*). Five point mutations that each disrupt vitronectin binding were identified. The residues Gln-55, Phe-109, Met-110, Leu-116 and Gln-123 are all surface exposed residues, based on the crystal structure of latent PAI-1. These residues are located on helix C, helix E and β-strand 1A. In the second study, a series of well-characterized anti-PAI-1 monoclonal antibodies were used to localize the vitronectin binding site on PAI-1 (*104*). The epitopes of the antibodies that disrupted vitronectin binding mapped to the region between amino acids 110 and 145. These residues compose the subdomains helix E, β-strand 1A and helix F. Both the studies suggest a mechanism for the stabilization of the active form of PAI-1 by restricting the movement of β-sheet A which could prevent the insertion of the reactive center loop, thereby preventing latency. However, Lawrence's group only performed mutagenesis on approximately half of the PAI-1 cDNA and a Scatchard analysis performed on the vitronectin/PAI-1 interaction by van Meijer indicated there were two different dissociation constants. Therefore, the presence of another vitronectin binding site within PAI-1 cannot be discounted. Finally, protease digestion of PAI-1 and the construction of PAI-1/PAI-2 chimeras led to the localization of the vitronectin binding site between residues 115 and 130 (*105*). Limited proteolysis of PAI-1 by *Staphylococcus* protease V8 generated two fragments that retained vitronectin-binding ability. The fragments were predicted to overlap residues 91 to 130. PAI-2, which shares structural homology to PAI-

1 but does not bind vitronectin, was used to construct chimeras with portions of PAI-1. The only chimera that formed a complex with vitronectin contained amino acids 1 to 167 of PAI-1. Since a chimera with PAI-1 residues 1 to 114 did not bind vitronectin, this data predicts the vitronectin-binding site to be between amino acids 115 and 130.

PAI-1 Binding Site on Vitronectin

Perhaps nothing in the field of vitronectin research is as hotly debated as the location of the PAI-1 site (or sites?) on vitronectin. PAI-1 binding has been localized to three distinct sites within vitronectin, but the controversy does not end there. The number of PAI-1 molecules capable of binding to vitronectin is also contested. The following is a brief review of how the PAI-1 binding sites were elucidated and where they are potentially located.

Three distinct regions have been implicated in PAI-1 binding: the somatomedin B domain, the connecting region and the heparin binding domain. Proteolytic digestion and chemical cleavage have been used to determine the PAI-1 binding site is located in the somatomedin B domain. Seiffert first localized the PAI-1 binding site to the amino terminal 6-kDa fragment of vitronectin liberated in a cyanogen bromide digest (106). In PAI-1 far western blots of cyanogen bromide or formic acid cleaved vitronectin, it was demonstrated that PAI-1 bound to the fragments that contained the amino terminal portion of vitronectin (see Figure 1-7). A PAI-1 binding competition assay was also performed using cleaved vitronectin to compete with native vitronectin bound to the microtiter plate for PAI-1 binding. Only those fragments that contained the amino terminal somatomedin B region competed for PAI-1 binding. Vitronectin was also subjected to trypsin digestion (see Figure 1-1 for trypsin digestion) (17). The purified
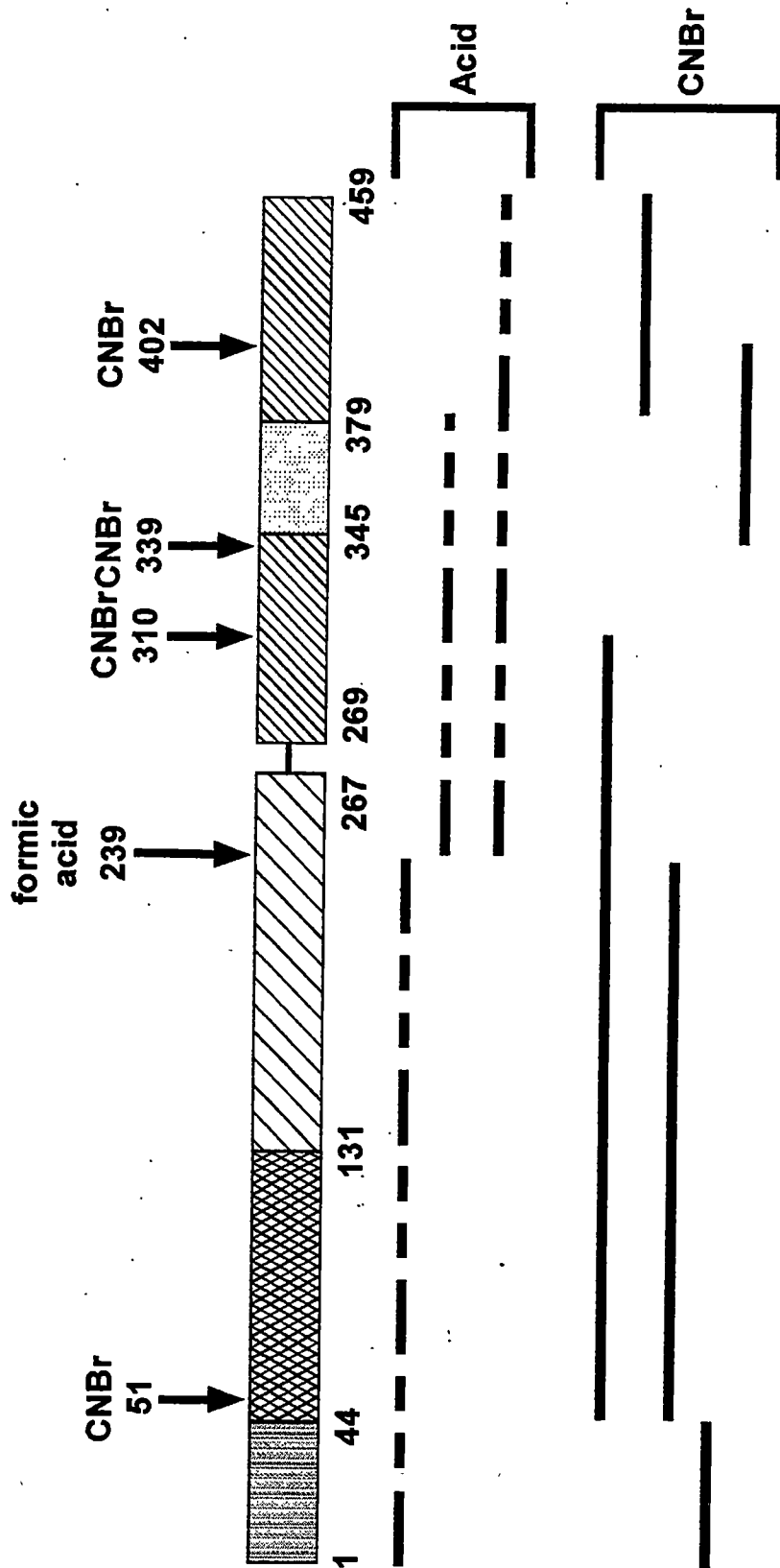
Figure 1-7: Location of Formic Acid and Cyanogen Bromide Cleavage Sites. The cyanogen bromide (CNBr) and formic acid cleavage sites are depicted with arrows. The fragments generated by the cleavage of vitronectin with either substance are shown below the vitronectin domain schematic. The dashed lines represent the fragments generated by acid cleavage of vitronectin. The solid lines represent the fragments generated in the CNBr digest.

33

amino-terminal portion of vitronectin (first 45 amino acids) caused a 50% reduction in PAI-1 binding to immobilized vitronectin and still stabilized PAI-1. Intact vitronectin (multimeric) also only reduced PAI-1 binding by 50%. This study suggests PAI-1 does interact with the amino-terminus, however, the 50% decrease in PAI-1 binding suggests another PAI-1 binding site may be present. Further studies using synthesized vitronectin fragments and monoclonal antibodies were employed to focus on the somatomedin B domain for PAI-1 binding. Amino-terminal fragments of vitronectin of various lengths were expressed in bacteria and tested for their PAI-1 binding ability (107). Vitronectin fragments between amino acids 1 and 52 were capable of binding and stabilizing PAI-1. Monoclonal antibodies were also used to determine the PAI-1 binding site. Monoclonal antibodies to the amino-terminus reduced PAI-1 binding to vitronectin whereas an antibody to the region between amino acids 52 to 239 did not prevent the interaction. Competitive binding assays using both heparin and PAI-1 demonstrate that heparin does not inhibit PAI-1 binding to vitronectin (43). Taken together, these three studies implicate the amino-terminal somatomedin B domain in PAI-1 binding.

A second putative PAI-1 binding site has been localized to the connecting region of vitronectin. Vitronectin fragments were generated by digestion with the *Staphylococcus* protease V8 and screened for their ability to bind to PAI-1 (73). The polypeptide consisting of amino acids 115 to 121 competed with PAI-1 for binding to immobilized vitronectin. PAI-1 activity was also stabilized using a synthetic peptide derived from the fragment. The polypeptide was shown to interact with a monoclonal antibody that has been shown to interfere with PAI-1 binding.

The last region of vitronectin with an alleged PAI-1 binding site is the heparin-binding domain. Preissner's group identified the PAI-1 binding site within the heparin-binding domain, however, the two sites do not overlap. Evidence for this claim comes from competition studies using both heparin and synthetic peptides derived from the heparin-binding domain (75, 108). Binding of heparin did not inhibit PAI-1 binding. Synthetic peptides of residues 348 to 370 did, however, block PAI-1 binding. This result is in agreement with that obtained by Gechtman et al. (76). Mapping with eight synthetic peptides from the area around the plasmin cleavage site identified the same high affinity PAI-1 binding peptide. Further evidence is from limited plasmin cleavage studies with vitronectin. Plasmin cleaves vitronectin within the heparin-binding domain. When plasmin cleaves the Arg-361 to Ser-362 bond, PAI-1 no longer binds vitronectin as well (18, 75). Finally, no complex formation was observed after vitronectin was treated with elastase or thrombin, which both cleave within the heparin-binding domain.

What could account for the discrepancy in the PAI-1 binding site? One possibility could be from experimental design. The conformational state of vitronectin used in these experiments is not always the same. There may be a difference in PAI-1 binding ability based on the ologomeric state of vitronectin. Chemical cleavage of vitronectin is performed under denaturing conditions. The epitopes identified with this method are therefore linear epitopes. These fragments may not retain the information necessary for PAI-1 binding. It is also possible that linear PAI-1 binding epitopes may come together to form a three-dimensional binding site.

Functional Consequences of the PAI-1/Vitronectin Interaction

PAI-1 and vitronectin both bind a variety of ligands. Vitronectin binding to PAI-1 stabilizes PAI-1 in its active conformation. This allows PAI-1 to interact with its ligands for a longer period of time. There is also evidence of overlapping binding sites within vitronectin, so when the PAI-1 binding site is occupied, other interactions cannot take place.

PAI-1 plays a role in the fibrinolytic system, which is responsible for the dissolution of blood clots. PAI-1 binds to tPA and inactivates it, preventing tPA from cleaving plasminogen into its active form plasmin. PAI-1 stabilized through its interaction with vitronectin has a longer functional half-life to find tPA and inactivate it. PAI-1 also inhibits α-thrombin with a relatively high affinity in the presence of vitronectin (*109, 110*). Active thrombin is rapidly endocytosed and degraded by the low density lipoprotein receptor-related proteins 1 and 2 (LRP 1 and 2) in the presence of both PAI-1 and native vitronectin (*111*).

Another role for vitronectin and PAI-1 in fibrinolysis is emerging. PAI-1 and vitronectin have both been found to associate with the fibrin in blood clots. By making clots *in vitro*, it was demonstrated that vitronectin is incorporated into the clot with fibrin (Podor, *et al.*, submitted for publication). Building on this study, the ability of PAI-1 to bind to the fibrin clots either with or without vitronectin present was investigated (Podor, *et al.*, also submitted for publication). PAI-1 by itself exhibited weak binding to the fibrin of the clot. However, when vitronectin was present, PAI-1 bound to the clot. Using confocal microscopy, PAI-1 was found to co-localize with the vitronectin bound to the fibrin. Also of note, fibrin clots with PAI-1 and vitronectin present inhibited the lysis

of the clots by tPA. Thus, vitronectin immobilized within a clot influences fibrinolysis by acting to retain PAI-1.

Vitronectin and PAI-1 have both been implicated in regulation of cell interactions with the extracellular matrix (ECM) of the vasculature. The balance between PAI-1 and vitronectin in the vasculature can influence the adhesive state of the cell. It has been reported that PAI-1 binding to vitronectin can cause a loss in cellular adhesion by several different mechanisms. First, it has been proposed that PAI-1 binds to the somatomedin B domain of vitronectin, which is also a proposed uPAR binding site. When PAI-1 binds to vitronectin in the ECM, it blocks the uPAR binding site (70). The cell can no longer use uPAR mediated adhesion to bind to vitronectin. The inhibitory effect of PAI-1 on cell migration is documented for both endothelial and uPAR-expressing cells (69, 77). Secondly, the plasminogen system has also been implicated in loss of cellular adhesion. Cell migration was associated with increased expression of uPA, plasminogen, uPAR and PAI-1 (112-114). Of note, uPA and uPAR have been localized to the leading edge of migrating cells. Increased plasmin activity, the result of low local PAI-1 concentration to inhibit its activation, has been shown to enhance cell migration and to cause vitronectin degradation (113, 115). This suggests that plasmin generated by uPA increases cellular migration by degradation of the ECM. A third mechanism is based on the observation that PAI-1 can inhibit cellular migration by interfering with the interaction between vitronectin and the vitronectin binding integrins (10, 116).

Of Mice and Protein

Knock-out mice are the new fad in science, used to elucidate the role of specific proteins in a whole animal model. In an effort to clarify the importance of both vitronectin and PAI-1, mice have been constructed that lack either one of the genes. Mice with targeted disruption of either the PAI-1 (*117*) or vitronectin (*118*) genes develop to term, grow to adulthood and are fertile. Sera from vitronectin-deficient mice completely lack vitronectin and PAI-1 binding abilities. The viability of these mice argues that vitronectin is not essential for cellular adhesion and migration during normal mouse development and suggests that other proteins overlap vitronectin's role in these processes. Further challenging of vitronectin-deficient mice with carotid artery injury suggests vitronectin plays an antithrombotic role *in vivo*, perhaps by inhibiting platelet-platelet interactions·or thrombin-substrate interactions (*119*). PAI-1 deficient mice have slight phenotypic abnormalities. The disruption of the PAI-1 gene in mice induces a mild hyperfibrinolytic state, in which clots were dissolved approximately twice as fast in PAI-1 deficient mice versus normal mice. PAI-1 deficient mice challenged with arterial injury have increased occlusion of blood vessels due to the accumulation and proliferation of smooth muscle cells at the injury site compared to wild-type mice (*120*). PAI-1 injected intravenously is able to suppress this occlusion in the deficient mice (*121*). The studies done with PAI-1 deficient mice collectively support the inhibitory role of PAI-1 in vascular wound healing and arterial occlusion due to inhibition of cellular migration.

Chapter 2

Expression and Characterization of a Somatomedin B Deletion Mutant of Vitronectin

Introduction

Vitronectin is currently purified from human plasma. The purification protocol has been optimized and high yields of pure, native vitronectin are attained. However, it is often advantageous to work with mutants of proteins. Careful mutagenesis of a protein can lead to a better characterization of both structure and function. Most vitronectin research has focused on vitronectin purified from plasma rather than engineering mutants. Recently, more researchers are becoming interested in expressing vitronectin mutants to better characterize the domain structure and explore ligand binding regions in more detail. In order to perform the desired mutagenesis on this protein, a suitable expression system needs to be found.

Several different expression systems have been used to express vitronectin. Bacteria are incapable of synthesizing full-length vitronectin and lack the machinery for post-translational modifications. However, bacteria have been used to express different domains of vitronectin, such as the somatomedin B domain, the hemopexin-like domains and the heparin-binding domain (*45, 107, 122*). Recombinant vitronectin has also been expressed in eukaryotic cells, using hamster kidney cells (*22*) or the baculovirus system

(*43, 123, 124*). Both Gibson and Zhao were able to successfully express and purify full-length and deletion mutants of vitronectin using the baculovirus system. Recombinant vitronectin was post-translationally modified and was functional in cell binding (*123, 124*). Further characterization of recombinant full-length vitronectin revealed it retained PAI-1-binding ability and bound to heparin in the same manner as multimeric vitronectin (*43*). Recombinant vitronectin produced in the baculovirus system mimics plasma derived vitronectin.

The amino-terminus of vitronectin contains the somatomedin B domain. The name is derived from the first isolation of the somatomedin B domain from plasma. Somatomedins are polypeptides that are believed to mediate the *in vivo* action of growth hormone (somatotropin) (*125*). Somatomedin B isolated from serum was characterized as a growth hormone-dependent trypsin-like protease inhibitor (*126*). Further studies of isoforms of this polypeptide revealed no growth-factor binding or action and implicated vitronectin degradation as the source of the somatomedin B polypeptide found in serum (*127*). The original activity of somatomedin B was therefore attributed to a contaminant in the preparation.

Statement of the Problem

Full-length vitronectin as well as a somatomedin B deletion mutant have been successfully expressed using the baculovirus system. Zhao expressed and purified a somatomedin B deletion mutant that was only used to characterize the regions or vitronectin important for cell binding ability (*124*). No further structural or functional characterization of the protein was attempted. Many ligands are proposed to bind to the somatomedin B domain so removal of the region can test for ligand binding abilities

retained within the remaining sequence. The deletion mutant must mimic vitronectin with respect to function for the regions not deleted for any conclusions to be drawn about the mutant protein. Does a somatomedin B deletion mutant expressed in the baculovirus system resemble vitronectin with respect to structure and function? Will this mutant retain similar ligand binding ability as plasma vitronectin? Can this mutant be used to draw conclusions about ligands that bind to the somatomedin B domain?

The localization of the PAI-1 binding site within vitronectin is the subject of much controversy. Attempts to localize the PAI-1 binding site have used techniques such as proteolysis, synthetic peptides and mutagenesis (see Chapter 1 for further discussion). The result of all these studies is the identification of three putative sites for PAI-1 binding: the somatomedin B domain, a site in the connecting region and the heparin-binding domain. The somatomedin B domain is commonly referred to as the primary or high affinity binding site for PAI-1. Does removal of one of the putative PAI-1 binding sites, the somatomedin B domain, result in total loss of PAI-1 binding ability?

Experimental Rationale

The baculovirus expression system utilizes insect cells for expression of recombinant proteins. In this system, proteins can be secreted into the medium. The cells can be grown in serum-free medium, making purification of the secreted protein easier. Another advantage of the baculovirus system is the cells are competent for performing post-translational modifications, such as N-linked glycosylation, phosphorylation, sulfation and disulfide formation. The insect cells are also capable of recognizing and cleaving the secretory signal sequence so secreted proteins are properly targeted. The baculovirus has been used successfully in our laboratory, so this system

was chosen for the expression of the recombinant vitronectin mutant lacking the somatomedin B domain.

Will deletion of the somatomedin B domain compromise the overall structure? This is a difficult question to address. Since there is currently no means of obtaining much information on the structural aspects of vitronectin, structural integrity is monitored by functional ability. Several pieces of evidence suggest removal of the somatomedin B domain will not adversely effect vitronectin structure. Proteolytic mapping, the presence of this polypeptide in serum as a proteolytic fragment and homology to somatomedin B-like domains in other proteins together suggest this amino-terminal polypeptide is its own domain. Therefore, removal of this amino-terminal domain is not expected to dramatically alter structure.

The somatomedin B deletion mutant was constructed with a histidine tag at the carboxy-terminus and synthesized in the baculovirus system as a secreted protein. Purified protein was characterized in terms of its ligand binding abilities. The results of these studies are presented in the proceeding sections.

Materials and Methods

Cell Culture

Cultures of *Spodoptera frugiperda* (Sf9) or *Trichoplusnia ni* (Hi5) cells (Invitrogen) were routinely grown as monolayers in Corning Ti-75 cm^2 culture flasks at 27°C or in suspension in side-arm spinner flasks with gentle stirring at room temperature. Sf9 cells were typically grown in serum-free Ex-Cell 420 medium (J.R.H. Biosciences)

supplemented only with the antibiotic gentamicin (20 μg/ml, Gibco BRL). The cells

were grown until near confluent, then split 1:5 into fresh medium. Hi5 cells were grown

in Ex-Cell 401 containing gentamicin (20 μg/ml) without the addition of serum. Hi5

cells were grown until approximately 80% confluent then the culture was split 1:5 into

fresh medium. Suspension cultures of Hi5 cells were prepared by pooling monolayer

cultures to the final concentration of $1x10^6$ cells/ml. Suspension cultures were split when

the cells reached a density of $2.0 - 2.5x10^6$ cells/ml into fresh Ex-Cell 401 medium.

Subcloning of Vitronectin Deletion Mutants into a Baculovirus Vector

The deletion mutant of vitronectin lacking the first 40 amino acids was

constructed using 3-step PCR with the plasmid pHILD-2/VN as the initial template. The

following primers were used:

ΔsomB sense	5' GGCTGTCGACAAGCCCCAAGTGACTCGCGG 3'
ΔsomB a.s.	5' GGGGCTTGTCGACAGCCAGAGCAACCCATG 3'
5' AOX1	5' GACTGGTTCCAATTGACAAGC 3'
3' AOX1	5' GCAAATGGCATTCTGACATCC 3'

The primers ΔsomB a.s. and 5' AOX1 were used to generate the N-terminal fragment of

vitronectin minus the somatomedin B domain of approximately 100 base pairs. The

primers ΔsomB sense and 3' AOX1 were used to generate a fragment consisting of the

majority of the vitronectin sequence of approximately 1300 base pairs. Both fragments

were gel purified using a Gel Extraction Kit (Qiagen). The purified fragments were

mixed and subjected to 15 cycles of PCR without the addition of any primers. To

amplify the full-length mutant, a third round of PCR was employed, using the 5' AOX1

and 3' AOX1 primers. The fragment was ligated into the PCRII vector (Invitrogen). The

mutant vitronectin was excised with EcoRI and ligated into pFASTBAC-1 digested with EcoRI. The resulting construct was named pFB/ssΔsBVN.

A version of pFB/ssΔsBVN was constructed with a histidine tag at the C-terminus. The plasmid pPicZαB/CT-his contains the full-length sequence of vitronectin with a C-terminal his-tag and a thrombin cleavage site. This construct was digested with BamHI and the ends were made blunt. The plasmid was then digested with ClaI, releasing a fragment of vitronectin of 820 base pairs plus 409 base pairs of the pPicZαB vector containing the his-tag. This 1229 base pair fragment was gel purified. The parent vector pFB/ssΔsBVN was digested with XbaI and the ends blunted. The singly digested vector was digested again with ClaI. The resulting digested vector was gel purified. The 1229 base pair fragment of vitronectin was ligated into the digested pFB/ssΔsBVN to create the his-tagged deletion mutant pFB/ssΔsBVN-his.

Full-length Vitronectin Constructs

The recombinant full-length vitronectin, pBlueBac/VN, was obtained from Dr. David Sane (*123*). A full-length vitronectin was also constructed with the addition of a histidine tag at the C-terminus. The same C-terminal 1229 base fragment described above digested from the plasmid pPicZαB/CT-his was employed. The vector pFB/597 contains full-length vitronectin within the pFASTBAC-1 vector. The plasmid pFB/597 was digested with HindIII and the ends were made blunt. The vector was then doubly digested with ClaI. The vector was gel purified and ligated with the his-tagged C-terminal portion of vitronectin. The resulting construct was named pFB/VN-his.

Virus Generation

The constructs made with the pFASTBAC-1 vector were transformed into the commercial bacterial strain, DH10bac (Gibco BRL). The DH10bac cells contain a large circular plasmid with the entire baculovirus genome. The gene of interest was able to recombine into the baculovirus plasmid within the bacteria. Transformed bacteria were plated on LB plates containing 10 µg/ml tetracycline, 7 µg/ml gentimicin, 50 µg/ml kanamycin, 40 µg/ml IPTG and 300 µg/ml Bluo-gal. The plates were incubated 18-24 hours at 37°C. Blue or white colonies were distinguishable after several more hours at room temperature. White colonies were grown and their DNA isolated. Sf9 insect cells were transfected with the recombinant bacmid DNA using Cellfectin (Gibco BRL). Production of recombinant vitronectin was monitored by Western blot and was used as an indication of virus production.

Virus Amplification and Infection

Initial viral stocks were amplified in Sf9 cells. From the initial viral stock, 200 µl was used to infect 10 mls at a concentration of a 1×10^6 cell/ml. The medium was collected after 72 hours and stored at 4°C protected from the light.

To determine the optimal amount of virus to add for protein production, test infections were performed using 3 ml cultures of Hi5 cells (at 1×10^6 cells/ml) and adding 5, 10, or 25 µl of amplified virus stocks. Seventy-two hours post-infection, the cells and medium were assayed for protein production by Western blot using rabbit polyclonal antibodies to human vitronectin. The amount of virus stock that produced the highest amount of undegraded protein in the medium was chosen for larger infections.

For large scale infections, Hi5 cells were grown in suspension as described above until the desired volume of cells was achieved. The cells were then infected with the pre-determined ratio of virus stock to cell density. The cells were allowed to grow for 72 hours. The cells were removed from the medium by centrifugation (5 minutes, 5000 rpm). The medium was tested for the presence of protein by Western blotting and stored at 4°C for purification.

Western Blotting

Cells and medium were boiled in 2X SDS sample buffer for 5 minutes. The samples were separated by SDS-PAGE and transferred to nitrocellulose using a Semi-Dry Blotter (BioRad). Nitrocellulose and filter paper were equilibrated in transfer buffer (0.35 M glycine, 25 mM Tris, 20% methanol) before transfer. A current of 15 volts was applied for 30 minutes. The nitrocellulose membrane was incubated in 10% non-fat dry milk in PBS at room temperature for 60 minutes. The membrane was washed three times with PBS/Tween (0.05%). Primary antibody of choice was diluted in PBS containing 2% non-fat dry milk (dilution varies with antibody used) and the filter was incubated for 60 minutes at room temperature. The membrane was washed and incubated in PBS containing 2% non-fat dried milk and 20 µl of the appropriate peroxidase-labeled secondary antibody (Vector) for 60 minutes at room temperature. After washing the membrane, any protein bands were visualized using developing solution (30 ml PBS, 50 mg/ml 4-chloro-napthol, 12 µl 30% H_2O_2).

PAI-1 Far-Western

An SDS-PAGE gel was run and transferred to nitrocellulose. The blot was blocked with 10% non-fat dry milk for an hour. Following the three washes in

PBS/Tween, the blot was incubated with a stable mutant PAI-1 (2.5 µg/ml) in 5 mls of 2% non-fat dry milk overnight. Anti-PAI-1 antibodies (Torrey Pines Biolabs, San Diego, CA) were diluted 1:1000 in 5 mls of 2% non-fat dry milk in PBS for one hour. Peroxidase linked anti-rabbit antibody (Vector, 1:1000 dilution in 2% non-fat dry milk) was added and allowed to incubate for an hour. Protein was visualized using the developing solution described above.

^{125}I-protein A Quantitative Western

An SDS-PAGE gel was run with a known vitronectin standard curve and proteins of unknown concentrations. The gel was transferred to nitrocellulose and blocked for one hour in 10% non-fat dry milk. The blot was incubated with primary antibody (rabbit #12, 1:2000 dilution, Rockland) to vitronectin in 2% milk, 0.1% Tween in PBS. This buffer was also used for all washes. The blot was washed extensively then ^{125}I-protein A (ICN) was added (1:10,000 dilution) and incubated at room temperature for an hour. The blot was extensively washed again and allowed to dry. The blot was then counted in a Instant Imager (Packard Instruments). A standard curve could be generated using the vitronectin of known concentrations and the unknown protein concentration could be determined.

ss∆sBVN Protein Purification

Infected cells were spun down at 5000 rpm for 10 minutes and the cleared spent medium was removed. A protease inhibitor cocktail was added to the spent medium (5 mM EDTA, 100 µg/ml PMSF, 1.0 µg/ml aprotinin, 1.0 µg/ml pepstatin A and 0.5 µg/ml leupeptin). The medium was mixed with 15 mls of Blue Sepharose CL-B resin (Pharmacia) in batch with gentle stirring at 4°C for 16 hours. The resin was then poured into a column and washed with Blue Sepharose Buffer (BSB, 50 mM Tris, 0.15 M NaCl,

0.1 mM EDTA, pH 7.4) until the absorbance was low. Bound protein was eluted with

BSB containing 2 M NaCl. A western was run to identify fractions containing protein.

These fractions were pooled and dialyzed into 20 mM sodium phosphate, pH 7.0.

Dialyzed protein was applied to a DEAE (Pharmacia) resin column equilibrated with 20

mM sodium phosphate, pH 7.0. The column was washed with 20 mM sodium phosphate,

pH 7.0 containing 0.15 M NaCl. Bound protein was eluted with 20 mM sodium

phosphate, pH 7.0 containing 0.3 M NaCl. Fractions containing protein were identified

by western blotting and pooled. Pooled fractions were dialyzed into 50 mM sodium

borate, pH 8.0. The protein was passed over an immunoaffinity column made from the

polyclonal rabbit #12 antibody linked to Affi-gel 10 (Bio-Rad). The column was washed

wash Gentle Binding buffer (Pierce) and bound protein was eluted using Gentle Elution

buffer (Pierce) in 1 ml fractions. Fractions containing protein were dialyzed into BSB

and concentrated. Protease inhibitor cocktail was added to the concentrated protein and it

was stored at 4°C until use.

ssΔsBVN-his Protein Purification

Infected cells were spun down at 5000 rpm for 10 minutes and the cleared spent

medium was removed. The cleared medium was mixed with Chelating Sepharose-Fast

Flow resin (Amersham Pharmacia Biotech) with gentle stirring for 16 hours at 4°C. No

protease inhibitors were added as binding of the protein to the nickel column could be

compromised. The resin was poured into a column and washed with 1X binding buffer

(5 mM imidazole, 0.5 M NaCl, 20 mM Tris, pH 7.9) followed by 1X wash buffer (60

mM imidazole, 0.5 M NaCl, 20 mM Tris, pH 7.9). The bound protein was eluted with

elution buffer containing 1 M imidazole. Fractions were analyzed by western blotting

and coomassie staining. Fractions containing protein were pooled and dialyzed. Protease inhibitor cocktail was added and the protein stored at 4°C.

BBVN Protein Purification

Spent medium from infected cells was cleared by spinning at 5000 rpm for 10 minutes. The medium was gently mixed with 15 mls Blue Sepharose CL-B resin for 16 hours at 4°C. The resin was poured into a column and washed with BSB. Bound protein was eluted with BSB containing 2 M NaCl. Fractions containing protein were pooled and dialyzed into 50 mM sodium borate, pH 8.0. The dialyzed pooled fractions were passed over an immunoaffinity column made by Dr. Angelia Gibson using the Pierce IgG orientation kit and a monoclonal antibody (Quidel) to vitronectin (*43*). The column was washed wash Gentle Binding buffer (Pierce) and bound protein was eluted using Gentle Elution buffer (Pierce) in 1 ml fractions. Fractions containing protein were dialyzed into BSB and concentrated. Protease inhibitor cocktail was added to the concentrated protein and it was stored at 4°C.

VN-his Protein Purification

Infected cells were spun down at 5000 rpm for 10 minutes and the cleared spent medium was removed. The cleared medium was mixed with Chelating Sepharose-Fast Flow resin (Amersham Pharmacia Biotech) with gentle stirring for 16 hours at 4°C. No protease inhibitors were added as binding of the protein to the nickel column could be compromised. The resin was poured into a column and washed with 1X binding buffer (5 mM imidazole, 0.5 M NaCl, 20 mM Tris, pH 7.9) followed by 1X wash buffer (60 mM imidazole, 0.5 M NaCl, 20 mM Tris, pH 7.9). The bound protein was eluted with elution buffer containing 1 M imidazole. Fractions were analyzed by western blotting

and coomassie staining. Fractions containing protein were pooled, dialyzed and concentrated. Protease inhibitor cocktail was added and the protein stored at 4°C.

Competitive PAI-1 Binding Assay (Microtiter Plate Assay)

Interactions between PAI-1 and native vitronectin or the recombinant vitroncetin samples were measured as described by Seiffert and Loskutoff (*106*) with slight modification. Microtiter plates were coated with 50 μl of a 1 μg/ml solution of native vitronectin in PBS overnight at 4°C. The wells were blocked with 200 μl of 3% BSA in PBS for and hour at 37°C after washing the wells three times with PBS. The wells were washed with PBS/Tw/BSA (PBS containing 0.1% BSA and Tween-20) three times. Vitronectin (280 nM starting concentration) was serially diluted down the plate in PBS/Tw/BSA pH 8.5 in a final volume of 50 μl. An additional 50 μl of PAI-1 (20 nM) was added to the wells and the plate was incubated at 37°C for 2 hours. Anti-PAI-1 antibodies (polyclonal antibody, a gift of Tom Podor, McMaster University and the Hamilton Civic Hospitals Research Centre, Hamilton, Ontario) were diluted (1:3000) into PBS/Tw/BSA and 100 μl were added after the plate was washed three times. After a one hour incubation at room temperature, the plate was washed again and an HRP- linked secondary antibody (1:1000) was added and incubated for an hour at room temperature. The plate was developed using a 0.2 mg/ml solution of ABTS in 50 mM sodium citrate, pH 5.5 containing 12 μl of 30% H_2O_2. Several absorbance readings were made at 405 nm in a microplate reader (Wallac, Victor^2).

Direct PAI-1 Binding ELISA

Vitronectin or recombinant vitronectin was diluted to 280 nM in PBS. The wells of a microtiter plate were coated with 50 μl of the dilute vitronectin and allowed to

incubate overnight at 4° C. The plates were washed three times with PBS. The plates were then blocked with 3% BSA in PBS for one hour at room temperature. After washing, a solution of 1 μM PAI-1 was serially diluted down the plate. The plate was placed at 37° C for 2 hours. The plate was rinsed and incubated with anti-PAI-1 antibodies (Podor, 1:3000) for one hour at room temperature. Peroxidase-labeled secondary antibody was added for one hour. The plate was read at several different times at 405 nm in a microplate reader.

Cell Binding Assay

The wells of a 24 well tissue culture plate were coated with a 10 nM solution of vitronectin or recombinant vitronectin diluted in PBS. The plates were coated overnight at 4°C. After rinsing with PBS, the wells were blocked with 500 μl of a 3.5% solution of BSA in PBS at room temperature for one hour. Rabbit smooth muscle cells were trypsinized and resupended in serum-free medium containing 1.5% BSA. The cells were counted and 25,000 to 75,000 cells were added to each rinsed well of the 24 well plate. The cells were allowed to adhere for 30 to 45 minutes. After rinsing the wells to remove any unbound cells, 10 mg/ml p-Nitrophenyl phosphate was added to 0.1M sodium acetate, pH 5.0 and 400 μl was added to the wells. The p-Nitrophenyl phosphate is converted into p-nitrophenol by alkaline phosphotase present on the cell membranes. Samples were taken at various timepoints by stopping the reaction with the addition of an equal volume of 1M Tris, pH 9.0, at which point the p-nitrophenol turns yellow and the absorbance can be measured at 405 nm.

Integrin Binding Assay (Microtiter Plate Assay)

Microtiter plates were coated with 100 μl of a 2.5 μg/ml solution of the integrin GPIIb/IIIa in binding buffer (50 mM Tris, pH 7.4, 0.1 M NaCl, 1 mM MgCl$_2$, 1 mM CaCl$_2$). Wells were blocked with 3.5% BSA in binding buffer for one hour at room temperature. Vitronectin and recombinant vitronectin was diluted to 500 nM in binding buffer plus 0.1% Tween and serially diluted down the plate. The plate was allowed to incubate for one hour at 37°C. After rinsing the wells, anti-vitronectin monoclonal anitbody (Quidel) was added to the wells for one hour at room temperature. Secondary antibody was added for one hour at room temperature. The plates were developed using a 0.2 mg/ml solution of ABTS in 50 mM sodium citrate, pH 5.5 containing 12 μl of 30% H$_2$O$_2$. Several absorbance readings were made at 405 nm in a microplate reader.

Heparin Neutralization (Thrombin/Anti-thrombin Kinetics)

A solution of thrombin (36,500 g/mol) was diluted in reaction buffer (PBS with 0.1% PEG-8000) to a concentration of 44 nM. A curve was generated with thrombin and varying concentrations of anti-thrombin ($\in$=0.65, 60,000 g/mol) diluted in reaction buffer to approximately 1.0 μM to determine the concentration of anti-thrombin which results in 70-80% inhibition of thrombin. The chromogenic substrate Chromozyme-TH and heaprin were included in the reaction to a final concentration of 0.19 nM and 0.9 μg/ml, respectively, in 1.1 ml. The reaction was monitored at 405 nm for 3 minutes at 30° C. For the competition experiments, the concentration of thrombin and anti-thrombin remain fixed while the concentration of vitronectin changes. Each reaction was performed in duplicate. The data was analyzed using a non-linear least squares equation with the program IGOR to determine the k_{app} for the reactions.

Results

Plasmid Generation

The vitronectin deletion mutant, ssΔsBVN, was generated by PCR to remove the somatomedin B domain. This deletion mutant was to include the signal sequence and the RGD sequence of vitronectin but lack the somatomedin B domain. The remainder of the protein was to be the same as native vitronectin. To accomplish this task, three-step PCR was employed (Figure 2-1). The plasmid pHIL-D2/VN was used as the source of native vitronectin for the PCR. Primers were engineered to remove the somatomedin B domain from amino acid 1 to 40. The 5' ends of the primers ΔsBVN anti-sense and ΔsBVN sense were designed to produce complementary ends once the individual fragments were synthesized (primer pairs used can be found in the Materials and Methods section). In the first round of PCR, two vitronectin fragments were made. One fragment, ssΔsB, encoded the signal sequence minus the somatomedin B domain to amino acid 40 plus a new SalI site and amino acid 41. The other fragment, VNΔsB, contained the new SalI site and amino acids 41 to 459 of vitronectin. In the second round of PCR, the two gel-purified fragments were added together without the addition of any primers. This self-priming reaction resulted in the generation of the deletion mutant. In the final round of PCR, the deletion mutant was amplified with the addition of the external primers. The ssΔsBVN PCR product was ligated into the PCR II vector (Invitrogen). The recombinant protein sequence was excised with EcoRI and ligated into pFASTBAC-1 so it could be expressed in the baculovirus system (Figure 2-2). The sequence of the deletion mutant pFB/ssΔsBVN was confirmed by sequencing.
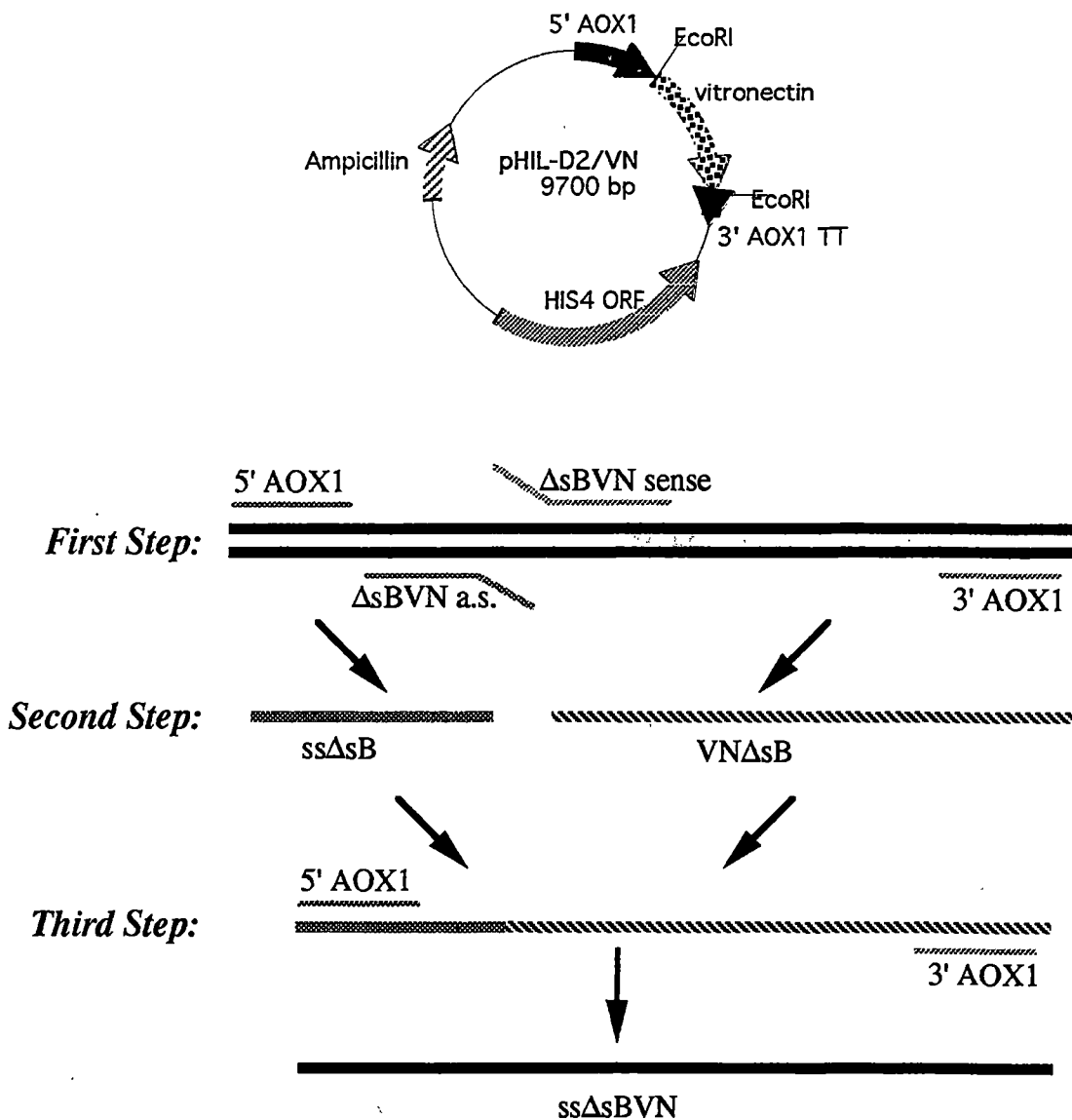
Figure 2-1: Generation of a Vitronectin Deletion Mutant Lacking the Somatomedin B Domain. The deletion mutant was created using three-step PCR. The plasmid pHIL-D2/VN was used as the template for the PCR reaction. The primers ΔsBVN sense and ΔsBVN a.s. have non-complementary ends that remove the somatomedin B domain yet are complementary to one another. The first round of PCR generated two fragments, one with the signal sequence lacking the somatomedin B domain and continuing after amino acid 40 while the other starts at amino acid 40 and continues until the end of vitronectin coding sequence. The fragment generated by PCR were gel purified and subjected to another round of PCR containing no primers. The reaction was self-primed. The final round of PCR utilized the second PCR reaction and the primers 5' AOX1 and 3' AOX1 to amplify the full-length deletion mutant, named ssΔsBVN.

54
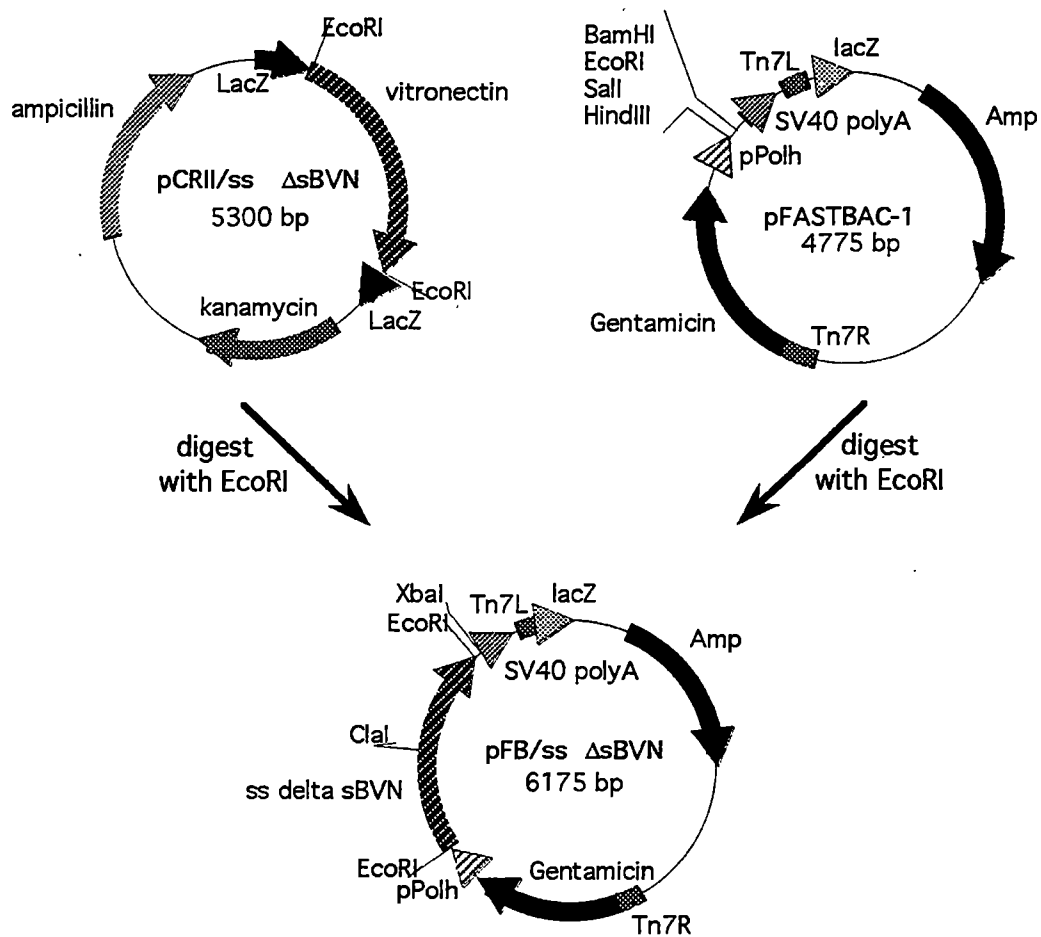
Figure 2-2: Construction of the plasmid pFB/ssΔsBVN. The plasmid PCRII/ssΔsBVN was digested with EcoRI to release the mutant vitronectin lacking the somatomedin B domain. The parent vector, pFASTBAC-1, was also digested with EcoRI and the ends dephosphorylated. The vitronectin deletion mutant, ssΔsBVN, was ligated into the digested parent vector to create pFASTBAC/ssΔsBVN.

A new recombinant vitronectin was constructed to facilitate protein purification. Due to the difficulties and lack of adequate purification of ssΔsBVN, a new strategy was sought to improve the ease of purification, the quality of purification and the yield. To this end, the recombinant protein ssΔsBVN-his was constructed. The plasmids pFB/ssΔsBVN and pPICZαB/VN-his were used to generate the new plasmid pFB/ssΔsBVN-his (Figure 2-3). Using the internal ClaI site in vitronectin and a BamHI site outside the coding region of vitronectin, the C-terminal portion of vitronectin including a histidine tag was excised from pPICZαB/VN-his. The BamHI site was blunted with Mung Bean Nuclease and the fragment gel purified. The parent vector was digested with ClaI as well as XbaI. The XbaI site from the multiple cloning region was blunted with Mung Bean Nuclease. The C-terminal portion of vitronectin containing the histidine tag was ligated into the digested pFB/ssΔsBVN resulting in the generation of the new plasmid pFB/ssΔsBVN-his.

Full-length vitronectin constructs were on hand to serve as controls. The full-length vitronectin construct BlueBac-VN was a gift from Dr. David Sane. The other full-length vitronectin construct was made with a C-terminal histidine tag. To generate this construct, the plasmids pFB/597 and pPICZαB/VN-his were used (Figure 2-4). The plasmids pFB/597 and pPICZαB/VN-his were digested with EcoRI and BamHI, respectively. The ends were then blunted with Mung Bean Nuclease. Both singly digested plasmids were digested again with ClaI. The C-terminal portion of vitronectin containing the histidine tag from pPICZαB/VN-his was gel purified and ligated into the

Xbal
Tn7L
lacZ
EcoRI
Amp
SV40 polyA
ClaI
ssΔsBVN
pFB/ss ΔsBVN
6175 bp
EcoRI
pPolh
Gentamicin
Tn7R

5' AOX1
pPICZ αB/
VN-his
5100 bp
α-factor ss
Zeocin
VN-his
AOX1 TT
ClaI
BamHI
myc & his-tag

digest with
Xbal & ClaI

digest with
BamHI & ClaI

Tn7L
lacZ
SV40 polyA
Amp
ClaI
ssΔsBVN-his
pFB/
ss ΔsBVN-his
6275 bp
pPolh
Gentamicin
Tn7R
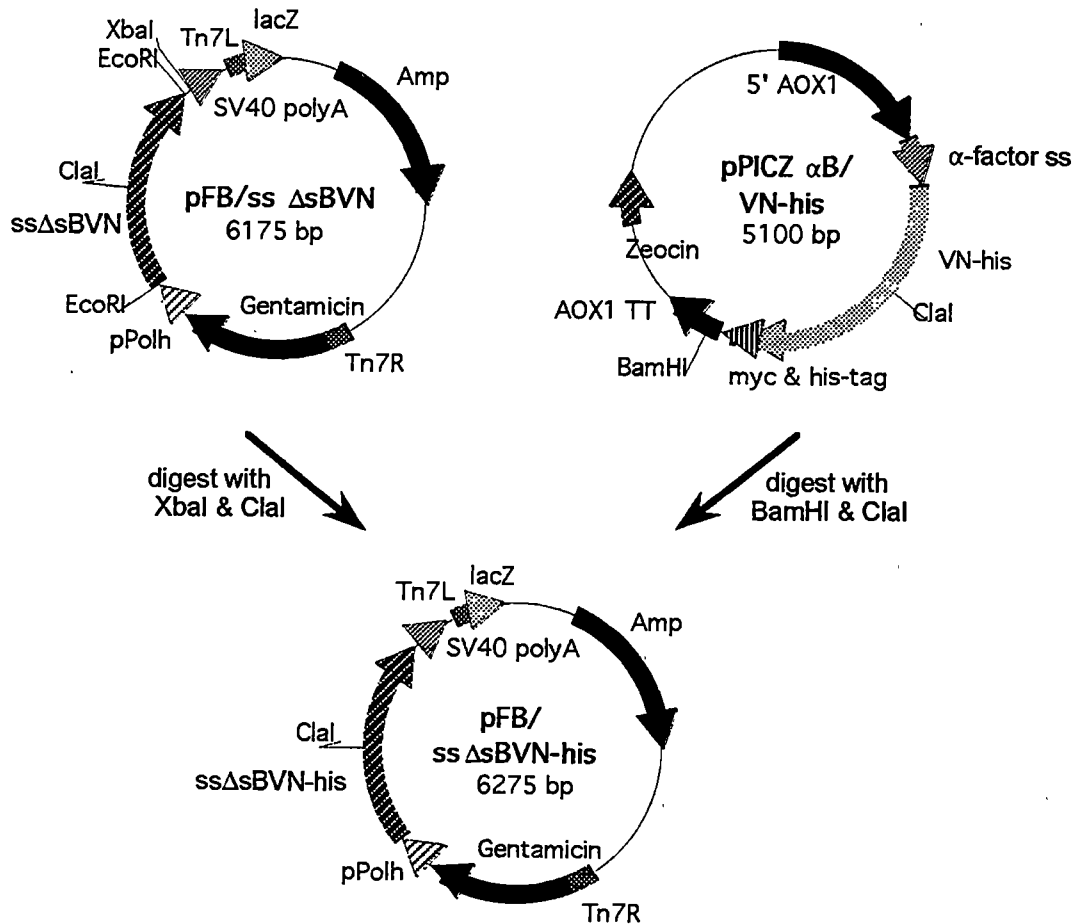
Figure 2-3: Construction of the Plasmid pFB/ssΔsBVN-his. The plasmid
pFB/ssΔsBVN-his was constructed from the two plasmids pPICZαB/VN-his and
pFB/ssΔsBVN. The plasmid pPICZαB/VN-his was digested with BamHI and the end
was blunted. A second digest with ClaI was performed resulting in the generation of a
his-tagged C-terminal vitronectin fragment. This fragment was ligated into the digested
parent vector pFB/ssΔsBVN. pFB/ssΔsBVN was digested with XbaI and blunted
followed by digestion with ClaI. The parent vector contains the N-terminal portion of
vitroncetin lacking the somatomedin B domain. The resulting construct was named
pFB/ssΔsBVN-his.
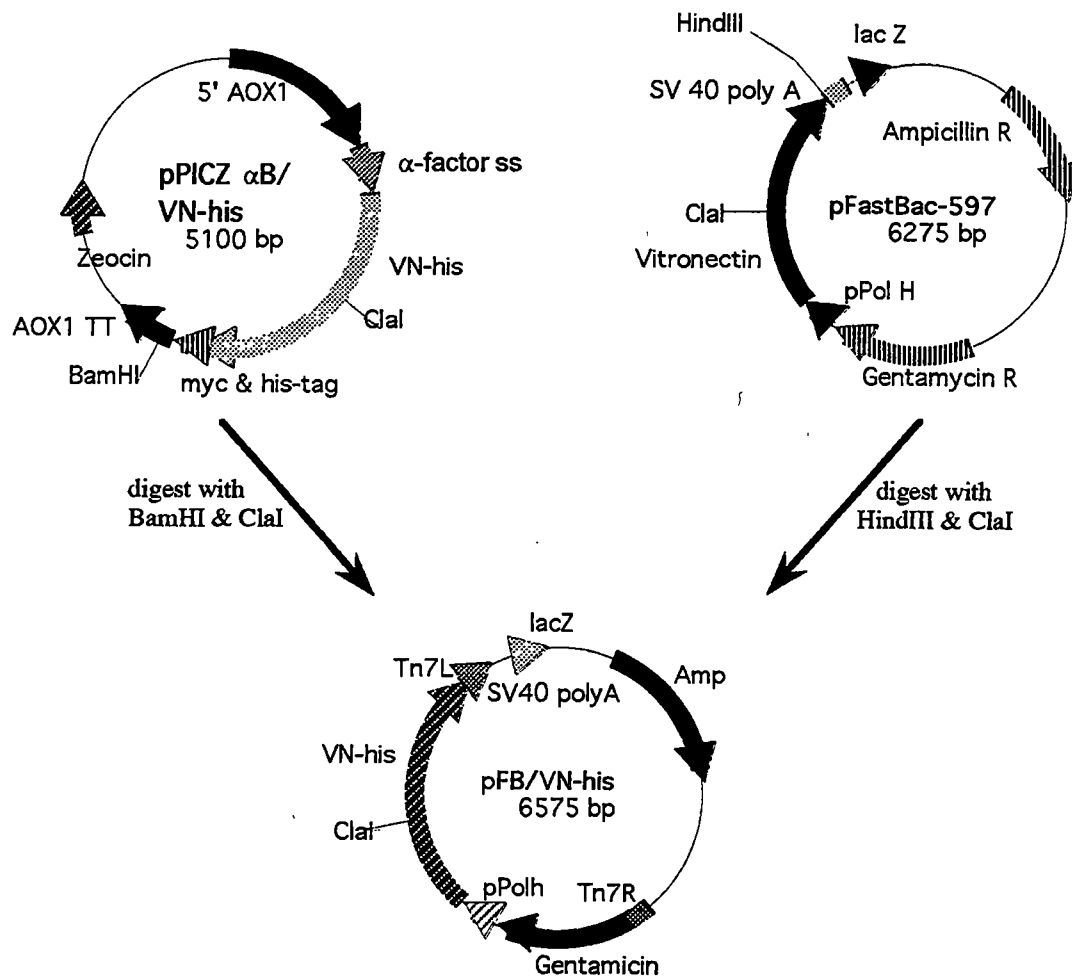
Figure 2-4: Construction of the Plasmid pFB/VN-his. Full-length vitronectin was constructed with a histidine tag on the C-terminus. pFB/597 contains the full-length vitronectin coding sequence and was chosen as the parent vector. It was digested wtih HindIII and the end was made blunt. It was further digested with ClaI and purified. The C-terminal portion of vitronectin with a his-tag was digested from the plasmid pPICZαB/VN-his. This plasmid was digested with BamHI and the end blunted. A second ClaI digest released the C-terminal his-tagged vitronectin fragment. The fragment was ligated into the digested pFB/597 to create the plasmid pFB/VN-his.

digested pFB/597 vector. The resulting plasmid, pFB/VN-his, was sequenced to confirm it was correct.

Transfection of Sf9 Cells and Viral Stock Generation

The three vitronectin coding sequences subcloned into the pFastBac-1 vector were transfected into the Sf9 cell line. The plasmids pFB/ssΔsBVN, pFB/ssΔsBVN-his and pFB/VN-his were transformed into DH10Bac cells, which contain the baculovirus genome on a very large plasmid known as the bacmid. After transformation of each individual plasmid into the DH10Bac cells, a recombination event occurs between the bacmid and the plasmid. The result is the incorporation of the protein coding sequence into the bacmid. The recombinant bacmids were purified from the DH10Bac cells and subsequently used in the transfection of Sf9 cells. Lipid-mediated transfections were performed for six individual bacmid isolates. Seventy-two hours post-transfection, the medium was removed and cleared by centrifugation. Production of the recombinant protiens was confirmed by Western blotting. After confirming the expression of the recombinant proteins, one of the transfectants was chosen for amplification. Sf9 cells (10 mls at 1 x 10^6 cells/ml) were infected with 200 μl of the initial viral stock. The cells were grown for three days. Immunoblotting confirmed the expression of the recombinant proteins in SF9 cells (Figure 2-5). This amplified virus was used as a viral stock for the infection of Hi5 cells for recombinant protein production.

Protein Expression

Test infections were performed with amplified viral stocks. Several different volumes of amplified viral stock were used to infect Hi5 cells (Figure 2-6). Immunoblotting detected the recombinant protein expression in the Hi5 cell line. The

59
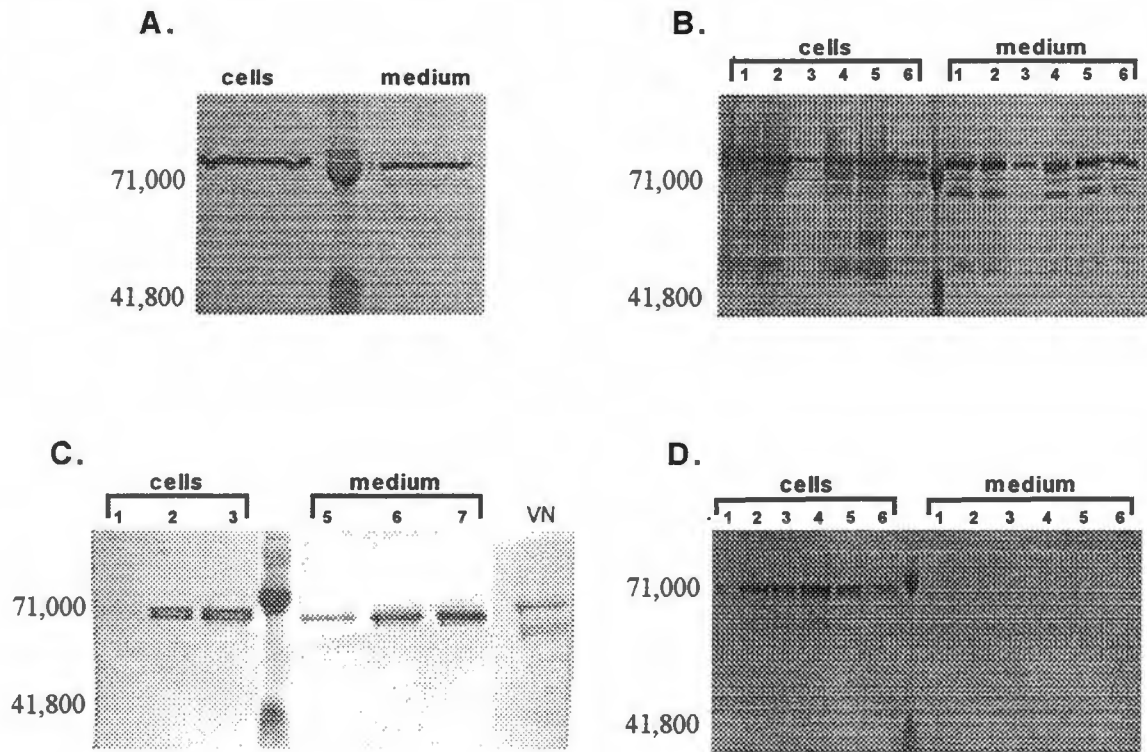
Figure 2-5: Transfection of Sf9 Cells. Recombinant vitronectin in the pFAST-Bac vector were transfected into Sf9 cells. The BBVN viral stock, however, is not in a pFAST-Bac based plasmid. Panel A shows the amplification of a BBVN viral stock in Sf9 cells. For this amplification, 200 µl of BBVN viral stock was added to 10 mls of Sf9 cells at 1×10^6 cells/ml. Full-length recombinant vitronectin can be seen in the cells and secreted into the medium. Panel B shows the transfection of the pFB/VN-his plasmid into Sf9 cells. All six of the transfections produced VN-his and secrete into the medium. Panel C shows the transfection of pFB/ssΔsBVN into Sf9 cells. Of the three transfections done, all make the vitronectin deletion mutant and secrete it into the medium. The last lane contains plasma vitronectin as a control. Panel D shows the transfection of the plasmid pFB/ssΔsBVN-his into Sf9 cells. The protein is clearly seen in the cell pellets. The amount of protein secreted into the medium, on the other hand, is rather low.
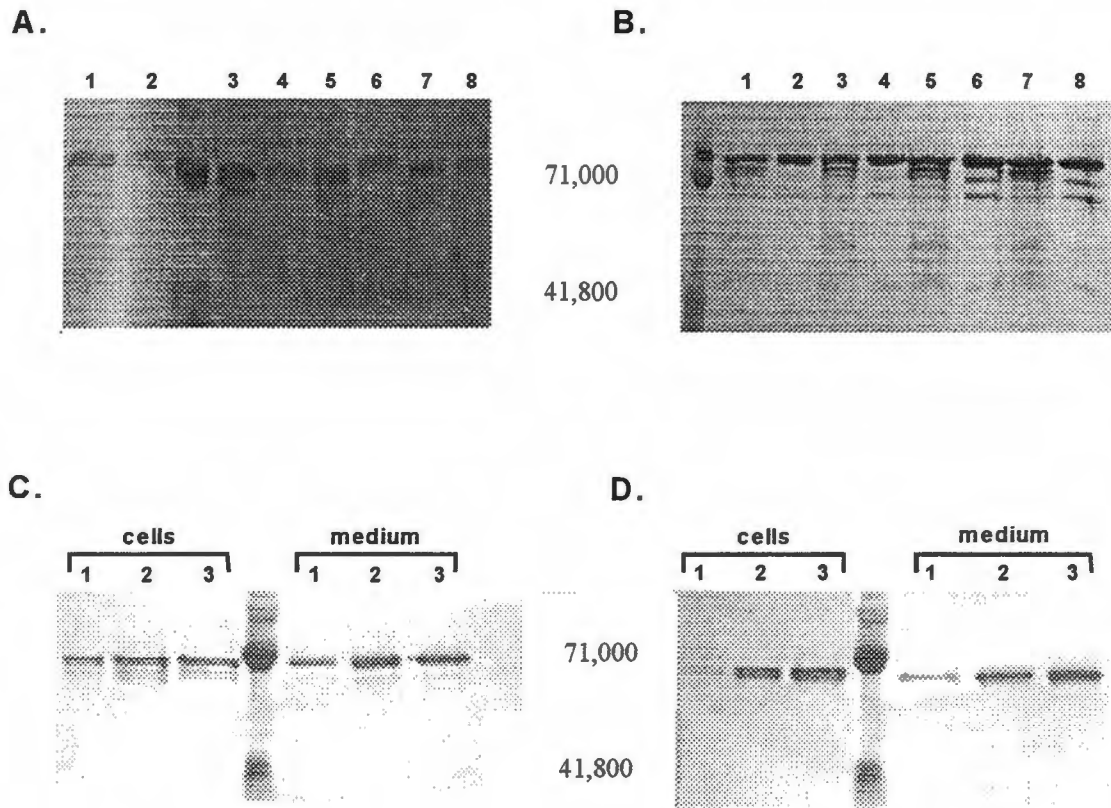
Figure 2-6: Test Infections of Viral Stocks. Amplified viral stocks were used to infect Hi5 cells (3×10^6 cells) to determine the optimum amount of viral stock to use in large scale infections. Kaleidoscope protein markers were used on all gels and the two markers seen on the gels correspond to 71,000 and 41,800 Daltons. Panel A shows the BBVN test infections. The first lane in the pair is the cell pellet and the second lane corresponds to the cleared medium. Lanes 1 and 2 were infected with 5 μl of viral stock. Lanes 3 and 4 were infected with 10 μl of viral stock. Lanes 5 and 6 were infected with 15 μl of viral stock and lanes 7 and 8 were infected with 25 μl. Panel B shows the test infections for VN-his. The first lane in the pair is the cell pellet and the second lane is the cleared medium. Lanes 1 and 2, 3 and 4, 5 and 6, and lanes 7 and 8 were infected with 5, 10, 15 and 25 μl of viral stock, respectively. Panel C shows the ssΔsBVN-his test infections. The first three lanes are the cell pellets while the last three are cleared medium. Lanes 1 were infected with 5 μl of viral stock, lanes 2 with 15 μl and lanes 3 with 25 μl. Panel D shows the test infections for ssΔsBVN. The first three lanes are the cell pellets and the last three lanes are cleared medium. Lanes 1 were infected with 5 μl of viral stock, lanes 2 with 15 μl and lanes 3 with 25 μl.

ratio of viral stock to Hi5 cells that generated the most non-degraded protein was used for larger infections of Hi5 cells.

For all large scale infections, the Hi5 cells were initially grown as monolayer cultures until there was a sufficient volume to add to a spinner flask for growth in suspension. Cells in suspension were grown to no more than 2.5×10^6 cells/ml and were split to 1×10^6 cells/ml. Once the desire volume was achieved, the cells at 1×10^6 cells/ml were infected with the viral stock. The infection was allowed to proceed for three days. Before the cells were spun down and the spent medium containing the secreted protein was recovered, a Western blot was performed to confirm the expression of the protein.

Monoclonal antibody 153 (mAB 153), which recognizes the somatomedin B domain of vitronectin, was used for Western blotting (Figure 2-7) in order to determine if the deletion mutant was indeed missing the somatomedin B domain. Immmunoblotting of plasma vitronectin, ssΔsBVN and ssΔsBVN-his using the mAB153 for detection confirmed that the deletion mutants were indeed lacking the somatomedin B domain. The full-length histidine tagged vitronectin protein (VN-his) was also probed with the mAB153 antibody. As expected, the antibody was able to recognize the somatomedin B domain within the full-length recombinant protein. Use of this antibody confirmed the deletion mutants were lacking the somatomedin B domain and the full-length recombinant retained the epitope. Two other antibodies were used to confirm the presence of the histidine tag (Figure 2-8) in ssΔsBVN-his. Since this construct also contains a c-myc epitope, an antibody for c-myc was also used (Figure 2-8). The
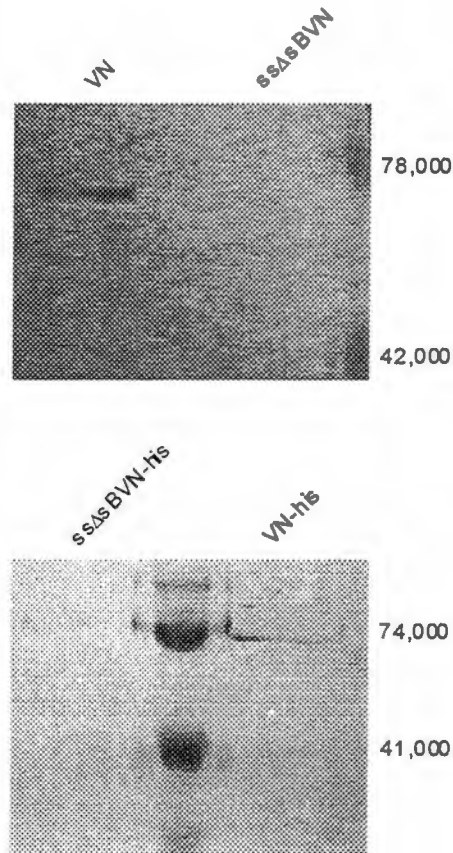
Figure 2-7: Detection of the Somatomedin B Domain Using the mAB153 Antibody.
The top panel in this figure has native vitronectin loaded into the first lane and the
recombinant protein lacking the somatomedin B domain in the second lane. In the lower
panel, an equal molar amount (2.5 uM) of both recombinant proteins was loaded into the
wells. Lane one contains the somatomedin B deletion mutant with a histidine-tag while
lane three has the full-length vitronectin with the histidine–tag. The monoclonal antibody
mAB153, which recognizes the somatomedin B domain of vitronectin, was used at a
1:500 dilution. The immunoblot was developed after incubation with a horseradish
peroxidase conjugated secondary antibody.

c-myc antibody

N-terminal his-tag antibody

C-terminal his-tag antibody
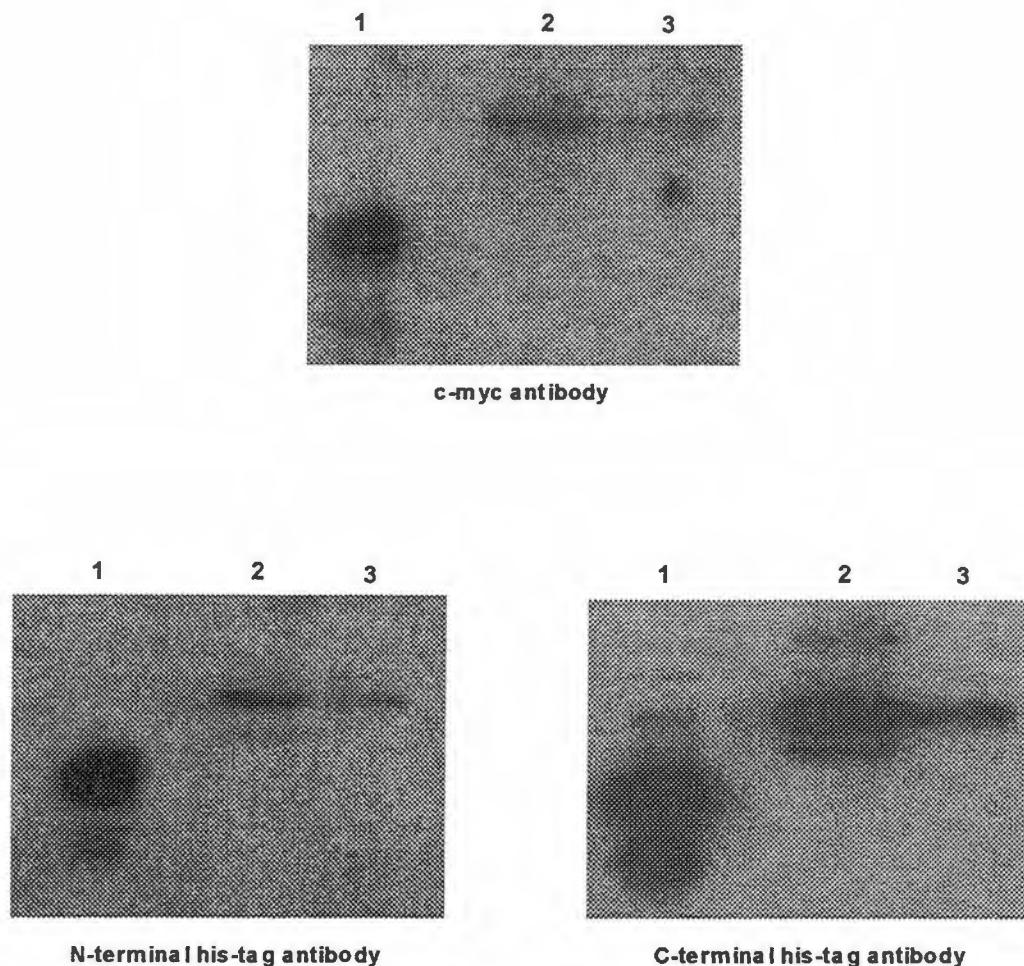
Figure 2-8: Recombinant Vitronectin Contains Epitopes for Both a Histidine and c-myc Tag. The purified and concentrated protein ssΔsBVN-his was run on an SDS-PAGE gel and transferred to nitrocellulose. Primary antibodies for either a C-terminal his-tag (1:5000, Invitrogen), an N-terminal his-tag (1:3000, Sigma) or a c-myc epitope tag (1:5000, Invitrogen) were incubated with the blot for one hour. Following several washes, the nitrocellulose was incubated with ^{125}I-protein A at a 1:10,000 dilution for one hour at room temperature. The nitrocellulose membranes were washed extensively then exposed to film overnight. Lane 1 is a his-tag positive control. Lane 2 is purified ssΔsBVN-his at a concentration of approximately 2 μg. Lane 3 is also purified ssΔsBVN-his, but it has been diluted 1:10 to a concentration of approximately 0.2 μg.

westerns show that both the histidine and c-myc epitope tags are present in the recombinant protein ssΔsBVN-his. Large-scale expression was then performed.

Protein Purification

Four different vitronectin constructs have been made. Two full-length vitronectin constructs were available, one with a histidine tag (VN-his) and the other with no tags (BBVN). The vitronectin deletion mutant lacking the somatomedin B domain was constructed without any tags (ssΔsBVN) and with a histidine tag (ssΔsBVN-his). The purification strategy for each of these proteins is outlined below.

BBVN:

The BBVN protein was expressed in Hi5 cells. Before the cells were spun out of the medium, protein expression was confirmed by Western blotting with a vitronectin polyclonal antibody. The cleared medium was spun with Blue Sepharose resin with the addition of protease inhibitors for approximately 16 hours. The beads were removed from the medium by pouring the slurry into a column. The column was washed with 1X Blue Sepharose buffer and all bound proteins were eluted with 2M NaCl in 1X Blue Sepharose buffer. Eluted protein was dialyzed into 50 mM sodium borate, pH 8.0. The dialyzed protein was applied to an oriented vitronectin monoclonal antibody column made by Dr. Angelia Gibson (Figure 2-9). A small amount of BBVN was eluted from the column, however, there were multiple lower molecular weight contaminating proteins that were not degradation products of the recombinant vitronectin. Due to the low yield and the presence of other contaminants, another oriented monoclonal antibody column made by Kenneth Minor was tried (Figure 2-10). Once again, the amount of BBVN that bound to the column was low as BBVN was still seen in the column flow through.
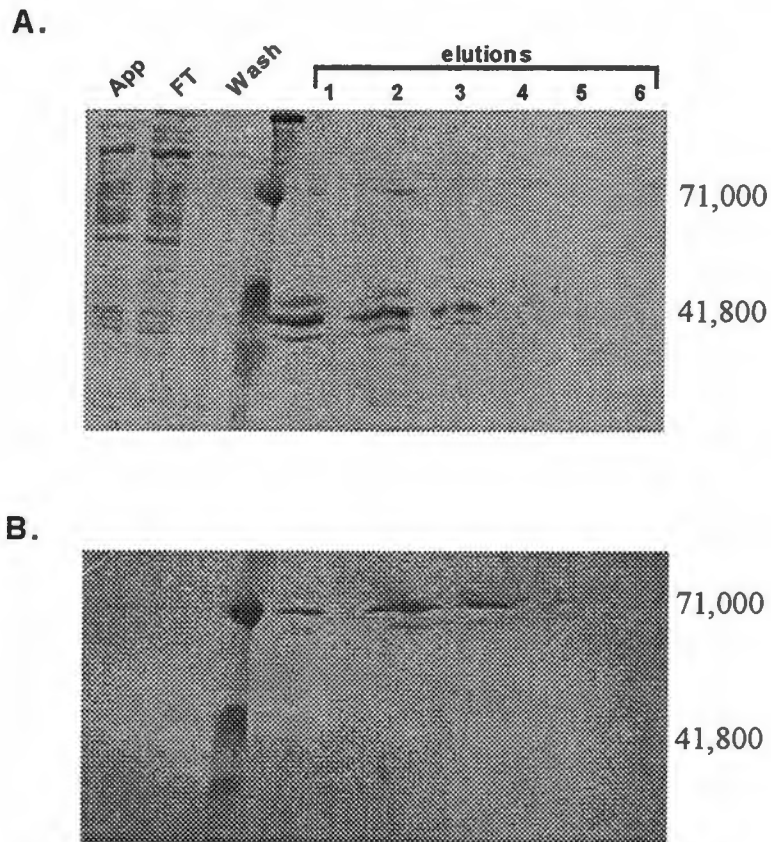
Figure 2-9: Purification of BBVN by Affinity Chromatography. An oriented monoclonal antibody column was made by Dr. Angelia Gibson to purify the recombinant protein, BBVN. This column was utilized to purify a large scale infection of BBVN. After the protein was concentrated from the spent medium by running a Blue Sepharose column, the protein was dialyzed and affinity chromatography performed. Panel A shows the Commassie blue stain of the monoclonal antibody affinity column fractions. The column was washed with Gentle Binding Buffer and the protein eluted with Gentle Elution Buffer. The Western blot in panel B has the same loading pattern as the stained gel.
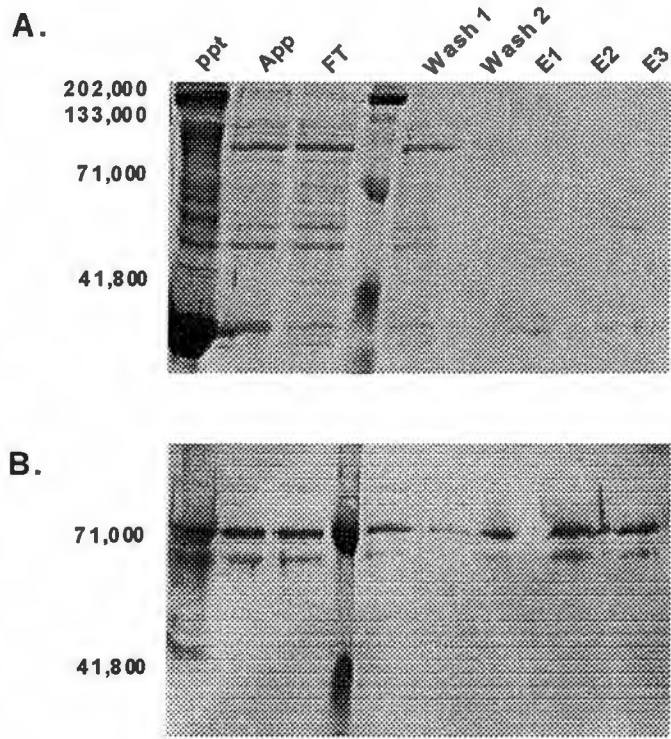
Figure 2-10: Purification of BBVN Using a New Monoclonal Antibody Column. A
new oriented vitronectin monoclonal antibody (Quidel) column was tested for its ability
to purify BBVN. Following concentration over a Blue Sepharose column, the protein
was dialyzed and loaded on the antibody column. Panel A is a Coomassie stained gel and
panel B is the corresponding Western blot. Lane 1 contains the precipitate following
dialysis. Lane 2 is a sample of the applied protein. Lane 3 is the flow through of the
column. Lane 4 is the protein standards. Lanes 5 and 6 are samples from the column
wash and lanes 7 through 9 are the column elutions.

Lower molecular weight contaminants were still seen using this column. Due to the low yield and impurity of the protein, a full-length vitronectin containing a histidine tag was constructed to ease the purification problems.

VN-his:

Medium containing the secreted VN-his was cleared by centrifugation. The cleared medium was spun with a Sepharose Chelating resin (Pharmacia) overnight at 4°C. The slurry was poured into a column the following morning. The column was washed with 5 mM, 25 mM and 50 mM immidazole before the final 1 M elution (Figure 2-11). The 25 mM to 1 M elution fractions were pooled. The protein was dialyzed into PBS with protease inhibitors. Following dialysis, the protein was concentrated. Gels were run to determine the purity of the concentrated protein (Figure 2-12). The amount of protein was determined by quantitative ELISA and total protein quantitated by the BCA assay. The amount of purified protein ranged from 4 to 8 mg, depending on the volume of cells used.

ssΔsBVN:

The first attempts to purify the somatomedin B deletion mutant did not involve the use of a histidine tag. The purification strategy for the mutant started by concentrating the protein from one to two liters down to approximately 50 mls by using a Blue Sepharose column. Proteins were bound to the column overnight in a slurry and all bound proteins were eluted with 2M NaCl in 1X Blue Sepharose Buffer (Figure 2-13). Protein was dialyzed into 20 mM sodium phosphate, pH 7.2 and applied to a DEAE column (Figure 2-14). Passing ssΔsBVN over the DEAE column removed some of the contaminating proteins to hopefully make purification over an antibody column better.
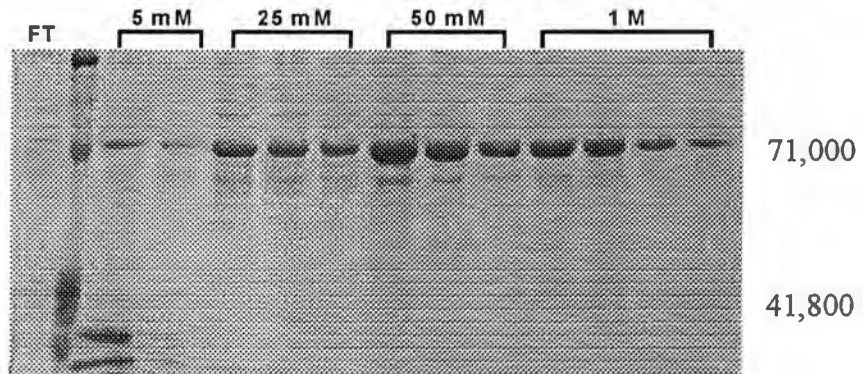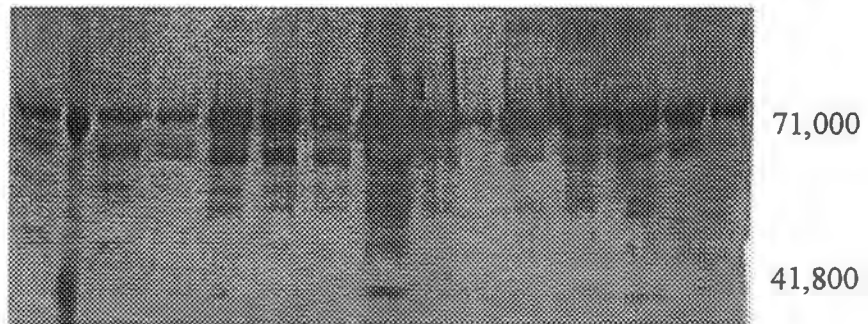
Figure 2-11: Purification of VN-his on a Chelating Column. SDS-PAGE gels were done after the column had run. Panel A shows the Coomassie stain while panel B is the Western blot. A polyclonal antibody was used to detect VN-his for the Western blot. Lane 1 is the column flow through. Lane 2 is the protein standards. Lanes 3 and 4 are a 5 mM immidazole wash. Lanes 5 to 7 are a 25 mM immidazole wash. Lanes 8 to 11 are a 50 mM immidazole elution. Lanes 12 to 15 are the 1 M immidazole elution.
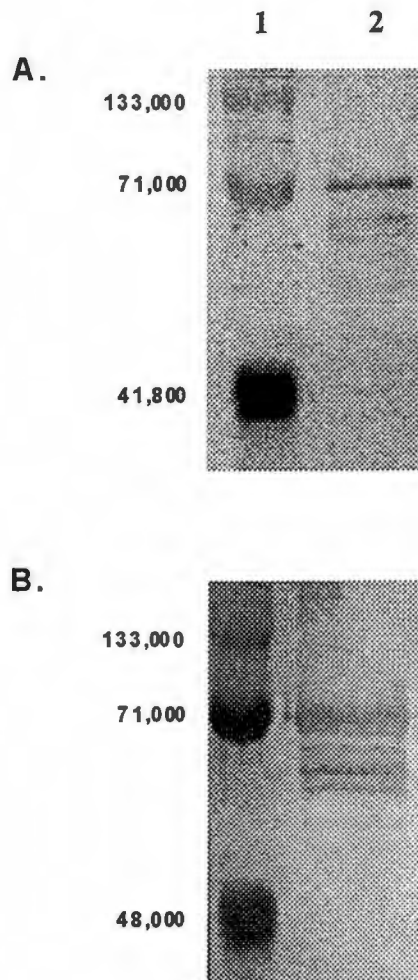
Figure 2-12: Purity of Concentrated VN-his. A total of 1 μg of VN-his was loaded on the SDS-PAGE gel. Panel A shows the Coomassie stain and panel B shows the Western blot. The Western blot was probed with a polyclonal antibody to vitronectin and developed using a horseradish peroxidase linked secondary antibody. Lane one is the protein standard while lane two is VN-his.
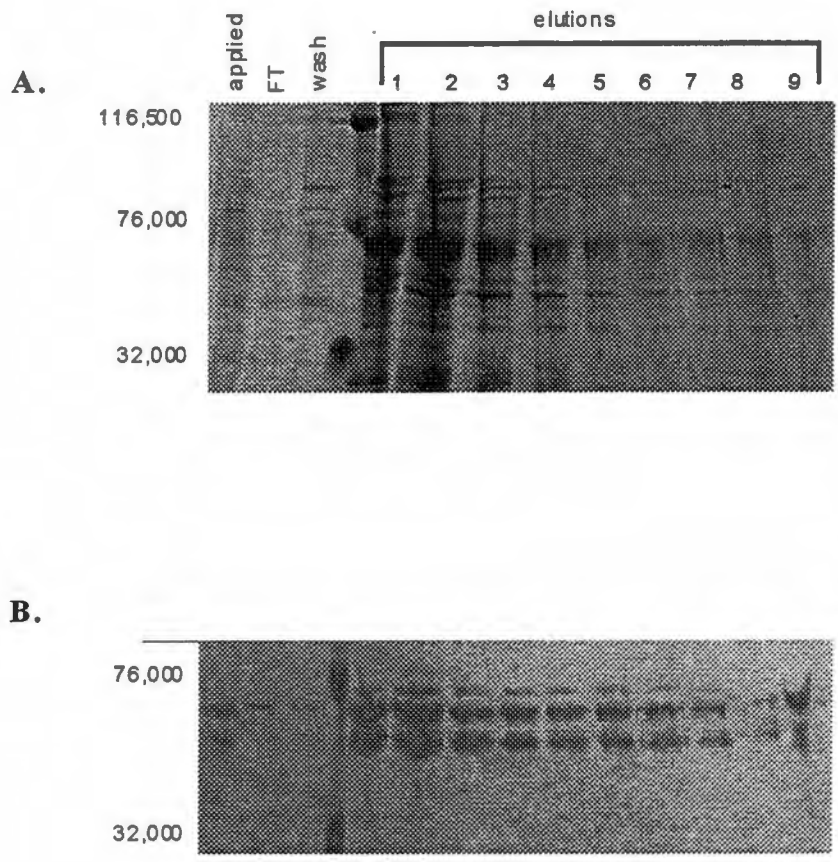
Figure 2-13: Concentration of ssΔsBVN from Medium on Blue Sepharose. Spent medium from Hi5 cells infected with ssΔsBVN was separated from cells by centrifugation at 4500rpm for 15 minutes. The cleared medium was spun with the Blue Sepharose resin overnight in the presence of protease inhibitors. The slurry was placed in a column and the resin washed with 1X Blue Sepharose buffer. Protein was eluted with 2M NaCl in 1X Blue Sepharose buffer. Panel A shows the Coomassie Blue stain of the column fractions. Panel B shows the corresponding Western blot of the column fractions. Polyclonal antibodies to vitronectin were used in the Western blot. Lane 1 is the sample applied to the column. Lane 2 is the column flow through. Lane 3 is the wash and lane 4 is the protein standards. The remaining lanes are the 2 M NaCl elutions.
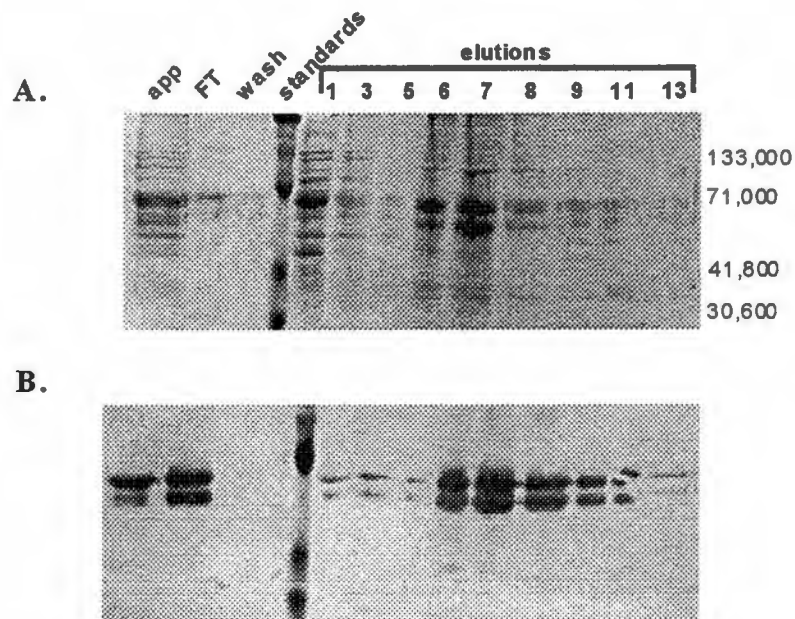
Figure 2-14: DEAE Purification of ssΔsBVN. The elution from the Blue Sepharose column was dialyzed into 20mM sodium phosphate, pH 7.2 and applied to the DEAE column. The column was washed with 0.15M NaCl in 20mM sodium phosphate. The vitronectin mutant was eluted from the column with 0.2M NaCl in 20mM sodium phosphate. Panel A shows the Commassie Blue stain of the column fractions. Panel B shows the corresponding Western blot probed with polyclonal antibodies to vitronectin.

The elution from the DEAE column was dialyzed into 50 mM sodium borate, pH 8.0. The dialyzed ssΔsBVN was applied to a polyclonal antibody column (Figure 2-15). The antibody column was generated by coupling of the antibody to Affi-Gel 10 (Bio-Rad). Some relatively pure ssΔsBVN protein was purified following this procedure. However, as with the other antibody column, the capacity of the column was low so the yield was low. Also, several other contaminating proteins were visible. Perhaps the greatest problem with the antibody columns was their degeneration over time. The binding and purification capacity of the columns deteriorated over time to the point they were no longer effective at purification. The purification the deletion mutant was attempted again, this time with a construct containing a histidine tag.

ssΔsBVN-his:

The somatomedin B deletion mutant containing a histidine tag was expressed in Hi5 cells. The cleared medium containing the secreted protein was spun overnight in the presence of activated Sepharose Chelating resin at 4°C. The following morning, the resin was collected in a column. The column was washed with 5 mM immidazole buffer and the protein eluted off with 1 M immidazole (Figure 2-16). The ssΔsBVN-his protein eluted from the column is not pure, however, the yield of protein from the column was much higher compared to ssΔsBVN purified over the antibody column. The protein was dialyzed into PBS with protease inhibitors and concentrated (figure 2-17). The ssΔsBVN-his protein was quantitated using an ELISA and total protein determined using the BCA assay. As with VN-his, the quantity of protein purified varied from 4 to 8 μg depending on the volume of cells used for the infection.
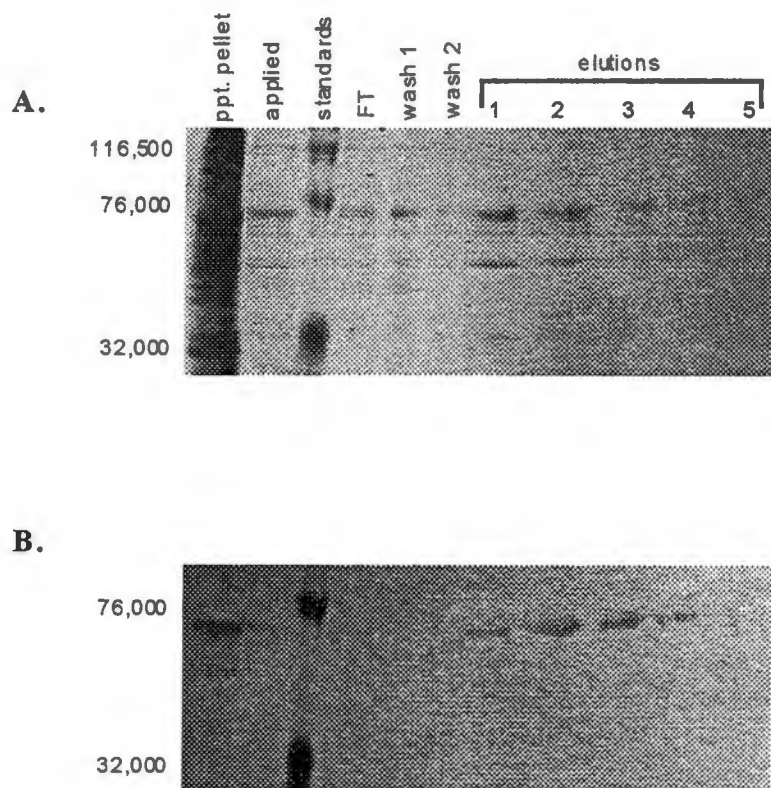
Figure 2-15: Purification of ssΔsBVN on a Vitronectin Polyclonal Antibody Column.
Polyclonal antibodies to vitronectin were first purified over a vitronectin column. The
antibodies were then linked to Affi-gel 10 resin. The DEAE elution was dialyzed into
50mM Sodium Borate, pH 8.0 with the addition of protease inhibitors. After dialysis,
some precipitate was present. The precipitate was removed by centrifugation and the
saved for gel analysis. The cleared dialyzed protein was applied to the antibody column.
The column was washed with Gentle Binding Buffer and the protein bound to the column
was eluted with Gentle Elution Buffer. Panel A shows the Coomassie Blue stain of the
column fractions. The Western Blot of the column fractions is shown in panel B.
Polyclonal antibodies to vitronectin were used for the detection of the recombinant
protein.
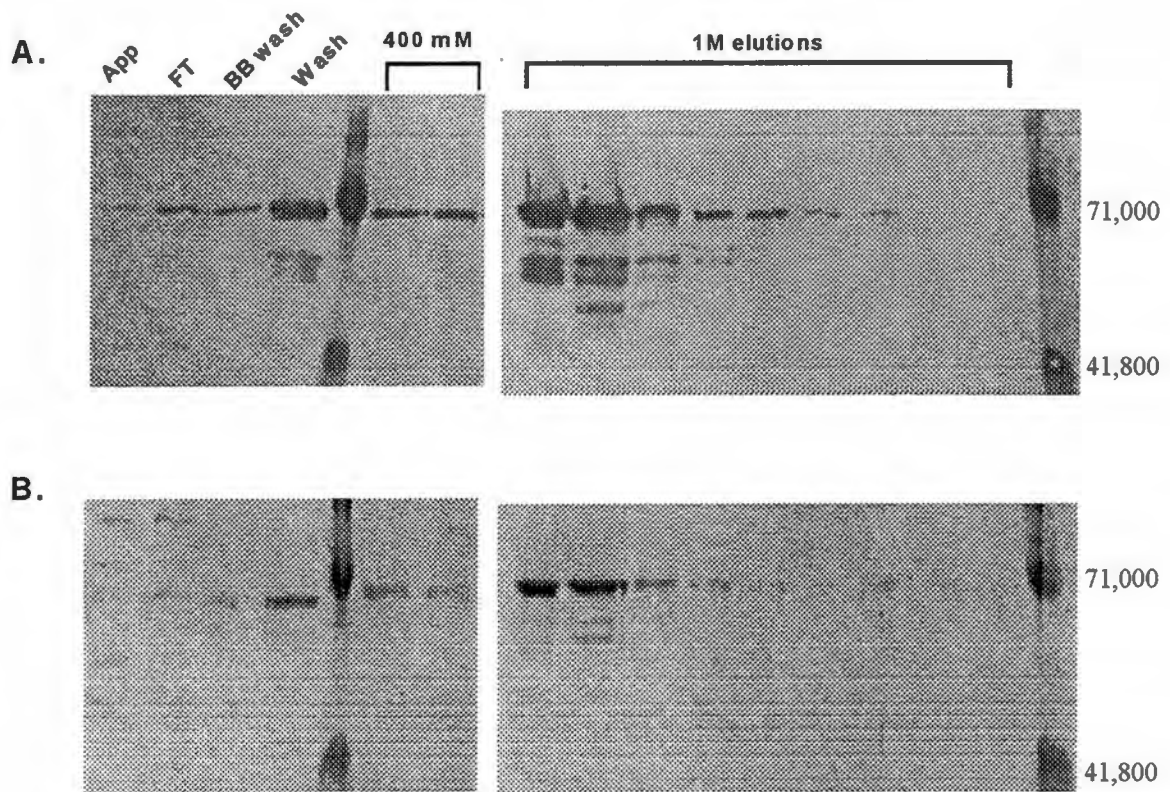
Figure 2-16: Purification of ssΔsBVN-his on a Chelating Column. Spent medium from a ssΔsBVN-his infection was clarified by centrifugation. The cleared medium was spun overnight with the activated chelating resin. The resin was washed extensively then the protein was eluted with 400 mM and 1 M immidazole. Panel A is the Western blot and panel B is the Coomassie stain of the column fractions. Lane 1 a sample of the applied protein. Lane 2 is the column flow through. Lane 3 is the binding buffer wash (5 mM immidazole) and lane 4 is the wash buffer (60 mM immidazole). Lanes 6 and 7 are a 400 mM immidazole elution and lanes 8-16 are 1 M immidazole elutions.
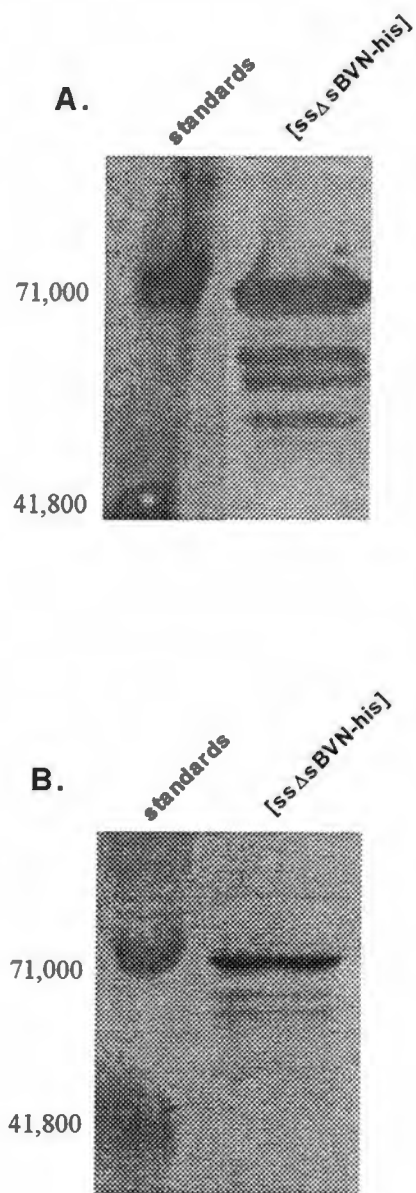
Figure 2-17: SDS-PAGE of Purified and Concentrated ssΔsBVN-his. Protein eluted from the chelating column was dialyzed into PBS. The dialyzed protein was concentrated down to 2-3 mls. Protease inhibitors were added after concentration. A total of 0.5 µg of protein was loaded on the gel. Panel A shows a Western blot of the concentrated ssΔsBVN-his while panel B is the Coomassie stained gel.

Gel Filtration Chromatography of Purified ssΔsBVN and ssΔsBVN-his

Recombinant vitronectin expressed in the baculovirus system is not in a monomeric state (*43*). Using both antibodies sensitive to the conformational state of vitronectin and gel filtration on an HPLC, Gibson determined that the recombinant vitronectin was more similar to multimeric rather than native vitronectin.

The size of the purified ssΔsBVN and ssΔsBVN-his was determined using gel filtration on an HPLC (Figure 2-18). Western blots using polyclonal antibodies showed that vitronectin was contained in the major peak at retention time around 6.2 minutes. The other prominent peak at a retention time of approximately 12.2 minutes contains no vitronectin and is most likely derived from protease inhibitors added to the purified protein. Protein standards were run twice for each standard in order to generate a standard curve (Table 2-1). The standards are accurate for values between 35 and 700 kDa. After 700 kDa, the accuracy of the column is compromised as the retention time approaches the void volume of the column. Therefore, an exact size for the recombinant proteins cannot be obtained. The retention time for the recombinant proteins is almost identical to that of multimeric vitronectin. This confirms that the three proteins are similar in an oligomeric form.

Cell Binding

The cell binding ability of the recombinant vitronectin proteins was determined. Both recombinant proteins contain the RGD site for integrin binding, however, the somatomedin B deletion mutant has only a few amino acids preceeding the RGD. The ability of rabbit smooth muscle cells to bind immobilized vitronectin was examined (Figure 2-19). Equal molar amounts of plasma vitronectin, multimeric vitronectin, VN-
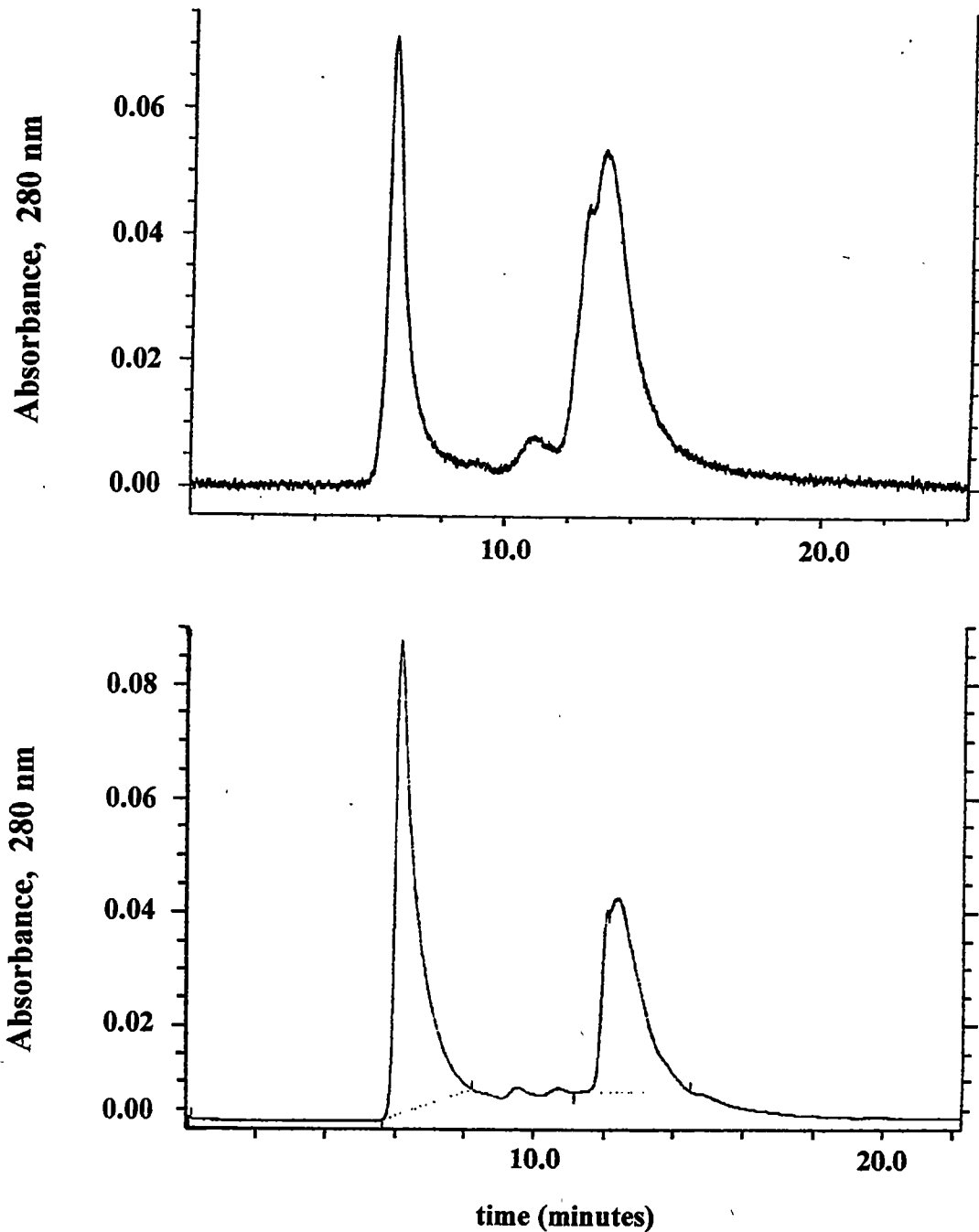
Figure 2-18: Gel Filtration Profiles for the Somatomedin B Deletion Mutants.
Purified proteins were concentrated before application to the gel filtration column. The
upper panel shows the profile for the deletion mutant containing the histidine tag,
ssΔsBVN-his. The lower panel is the elution profile for ssΔsBVN, which lacks a
histidine tag. Fractions were analyzed for the presence of vitronectin by immunoblotting
and confirm that the fraction eluting at approximately 6 minutes contains vitronectin.

Table 2-1: Determination of the Molecular Weight of the Recombinant Proteins.

Standard	Molecular Weight (Daltons)	Average Retention Time (min)
Blue Dextran	2,000,000	5.978
Thyroglobin	669,000	6.773
Ferritin	440,000	7.923
Catalase	232,000	8.722
BSA	67,000	9.587
Ovalbumin	43,000	10.080
Chymotrypsinogen	25,000	11.105
Native Vitronectin	74,000	9.350
Multimeric Vitronectin	> 669,000	6.145
ssΔsBVN	> 669,000	6.160
ssΔsBVN-his	> 669,000	6.250
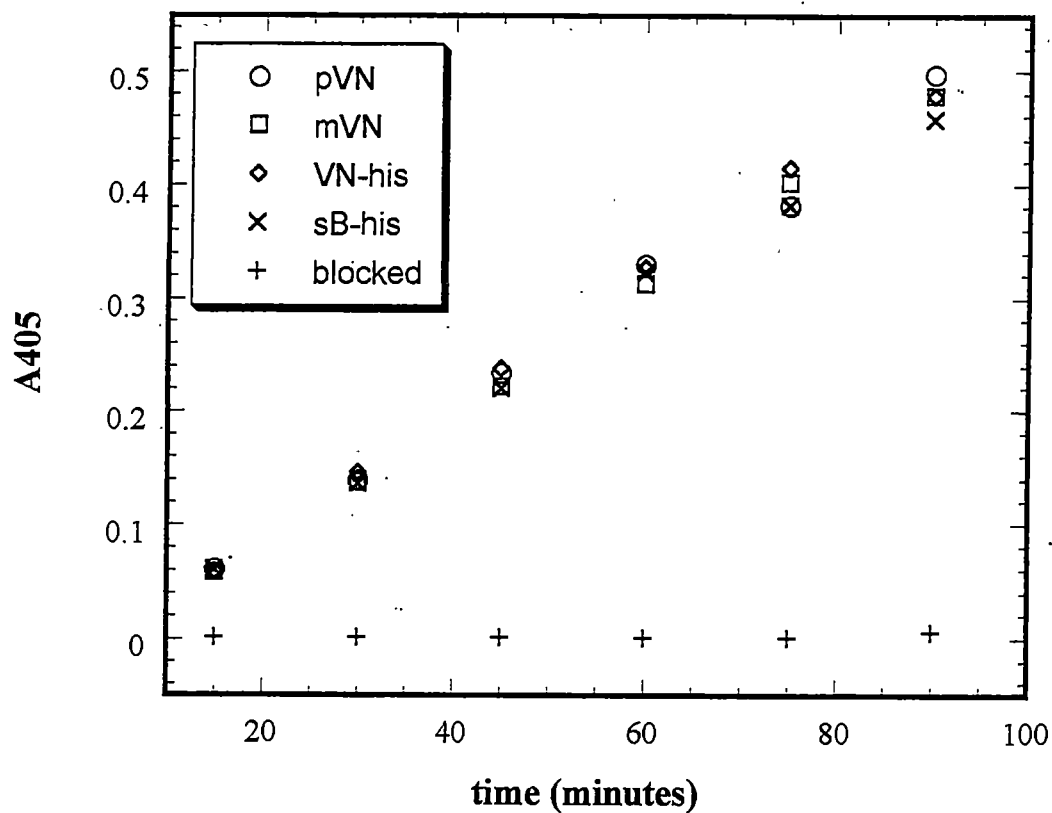
Figure 2-19: Cell Binding Ability of Recombinant Vitronectin. The binding of rabbit smooth muscle cells to immobilzed plasma vitronectin (pVN), multimeric vitronectin (mVN), VN-his, ssΔsBVN-his (sB-his) or blocked wells was determined in this cell binding assay. Equal molar amounts (8 nM) of protein were immobilized to the wells. The conversion of p-nitrophenyl phosphate to p-nitrophenol by alkaline phosphotase on the cell was monitored by the absorbance at 405 nm.

his and ssΔsBVN-his were immobilized to the plates. Figure 2-19 demonstrates there is no appreciable difference in the cell binding ability of any of the proteins.

Integrin Binding

A direct integrin binding ELISA was performed to determine the integrin binding ability of the recombinant vitronectin. The ability of vitronectin to bind the immobilized integrin GPIIb/IIIa was tested. Both recombinant proteins, ssΔsBVN-his and VN-his, retained integrin binding ability (Figure 2-20). The recombinant proteins bind to GPIIb/IIIa essentially identically. However, the binding is approximately 2-fold better than the binding of plasma vitronectin to the integrin.

Heparin Neutralization

The recombinant proteins were tested for their ability to bind heparin in order to determine if they were functionally similar to plasma or multimeric vitronectin. A solution-phase heparin neutralization assay was performed. This assay measures the activity of thrombin in the presence of its inhibitor, antithrombin, and heparin. Heparin acts as a catalyst in the reaction, bringing thrombin and antithrombin together more rapidly, resulting in increased inhibition of thrombin. When vitronectin is added to the mixture, vitronectin competes with both thrombin and antithrombin for heparin binding, reducing the rate of interaction between thrombin and antithrombin (its K_{app}). The effects of adding varying concentrations of vitronectin and the recombinant vitronectin are shown in Figure 2-21. Both VN-his and ssΔsBVN-his compete for heparin binding, however, the concentration needed to inhibit heparin activity by 50% is different. The concentration of VN-his and ssΔsBVN-his needed to inhibit heparin activity by 50% is approximately 0.04 and 0.2 μM, respectively. The corresponding value for multimeric

81
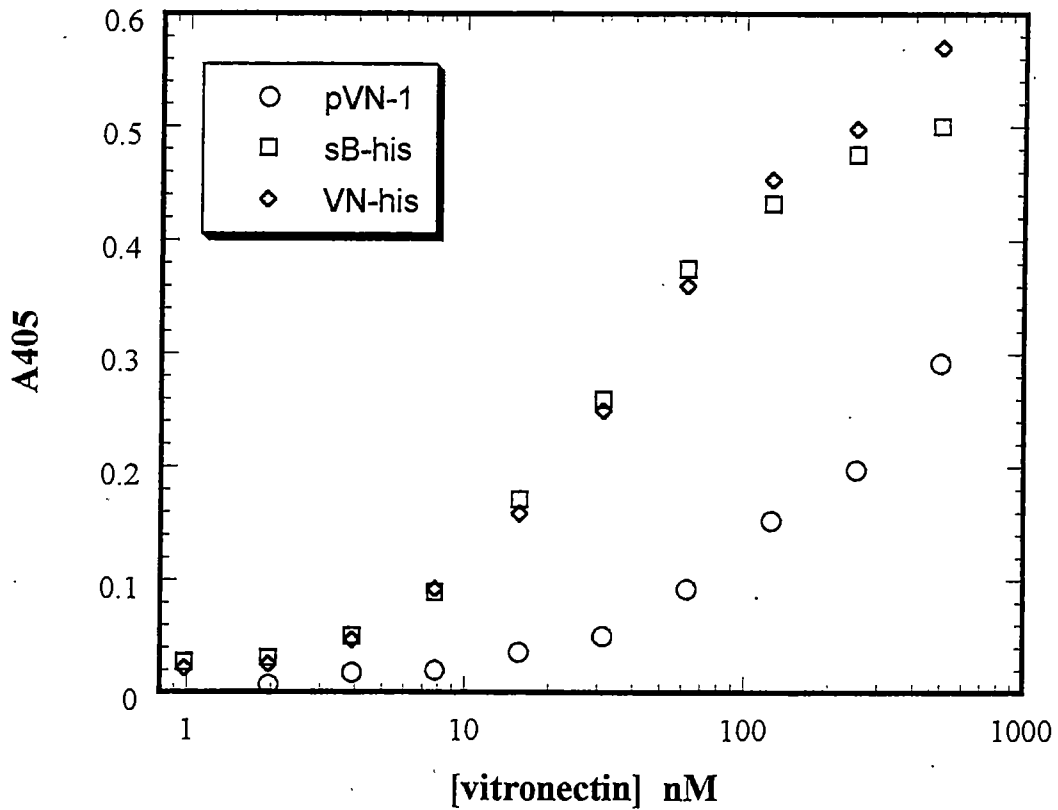
Figure 2-20: The Integrin GPIIb/IIIa Binding Ability of Recombinant Vitronectin.
The integrin GPIIb/IIIa is immobilized in a microtiter plate. Plasma vitronectin (pVN),
ssΔsBVN-his (sB-his) or VN-his (VN-his) is serially diluted down the plate. Bound
vitronectin is detected with an anti-vitronectin monoclonal antibody (Quidel).
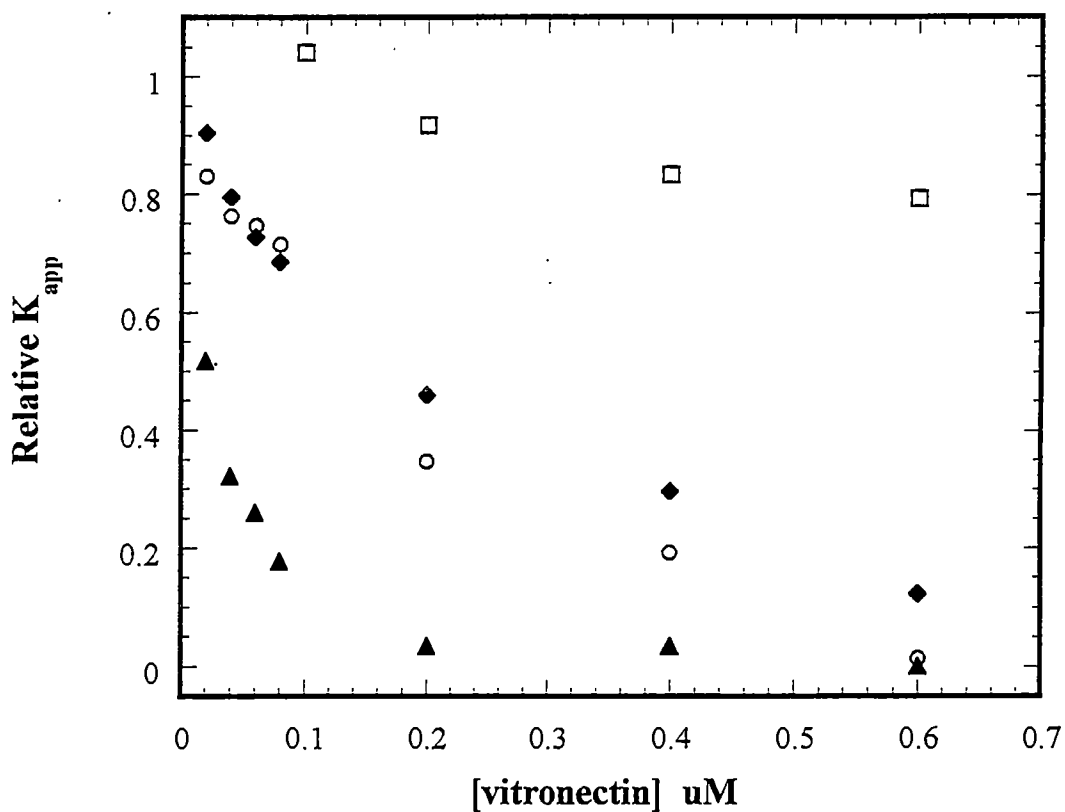
Figure 2-21: Heparin Neutralization Assay for Recombinant Vitronectin. Heparin activity was measured by observing a decrease in thrombin activity due to inhibition by antithrombin. Thrombin activity was continuously monitored over time by observing the hydrolysis of the chromogenic substrate Chromozyme-TH. Variations in the Kapp were measured at various concentrations of vitronectin. Kapp rates were determined using the program IGOR and standardized to the reaction rate of heparin-catalyzed inhibition in the absence of vitronectin. Data points are given at varying concentrations with the addition of plasma vitronectin (□), multimeric vitronectin (O), VN-his (▲) and ssΔsBVN-his (◆).

vitronectin is approximately 0.16 μM. The value of 0.16 μM for multimeric vitronectin is in close agreement with the observed 0.1 μM (*5, 43*). The concentration of ssΔsBVN-his needed to inhibit heparin activity by 50% is approximately 0.2 μM, which is comparable to that of multimeric vitronectin. The concentration of 0.04 μM for VN-his is comparable to other recombinant proteins expressed in the baculovirus system without a histidine tag, which demonstrated 50% inhibition at 0.05 μM (*43*).

PAI-1 Binding (Far-Western, Solid Phase, Competitive ELISA)

Several assays were performed in order to determine the PAI-1 binding ability of the recombinant proteins. A PAI-1 far-Western was done initially to analyze PAI-1 binding. As shown in Figure 2-22, the full-length recombinant protein VN-his and the somatomedin B deletion mutant both bound PAI-1. A control gel showed no background contribution from the PAI-1 polyclonal antibody binding any vitronectin sample (data not shown).

A direct PAI-1 binding ELISA was also performed. In this assay, vitronectin is immobilized on the microtiter plate. PAI-1 was then serially diluted down the plate. A control was also included so any non-specific PAI-1 binding to the plate could be corrected. As shown in Figure 2-23, VN-his and plasma vitronectin bind PAI-1 similarly. However, the somatomedin B deletion mutant has a greatly reduced PAI-1 binding ability. The absorbance values were comparatively low, but still above background PAI-1 binding. The data plotted in Figure 2-23 is for low concentrations of PAI-1, as higher concentrations of PAI-1 contribute too large a background absorbance.

A solution based competitive PAI-1 binding assay was also performed. In this assay, plasma vitronectin is immobilized on a microtiter plate. Recombinant, plasma or
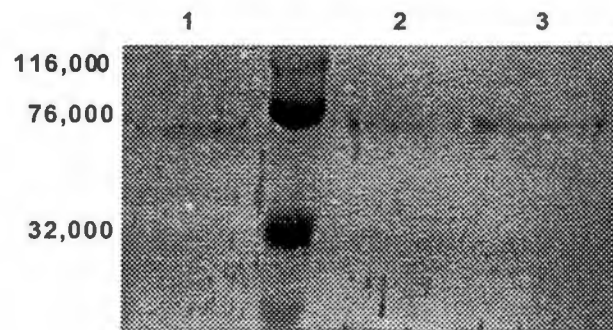
Figure 2-22: PAI-1 Far-Western of Recombinant Proteins. An equal molar amount (500 nM) of ssΔsBVN-his (lane 1), VN-his (lane 2) or plasma vitronectin (lane 3) was loaded on an SDS-PAGE gel. Following transfer, the blot was incubated with 2.5 µg/ml of a stable mutant of PAI-1. Polyclonal anti-PAI-1 antibodies (Torrey Pines Biolabs) were used at a 1:1000 dilution to detect any PAI-1 bound to the vitronectin immobilized on the nitrocellulose. Horseradish peroxidase conjugated secondary antibodies were used for colorometric detection.
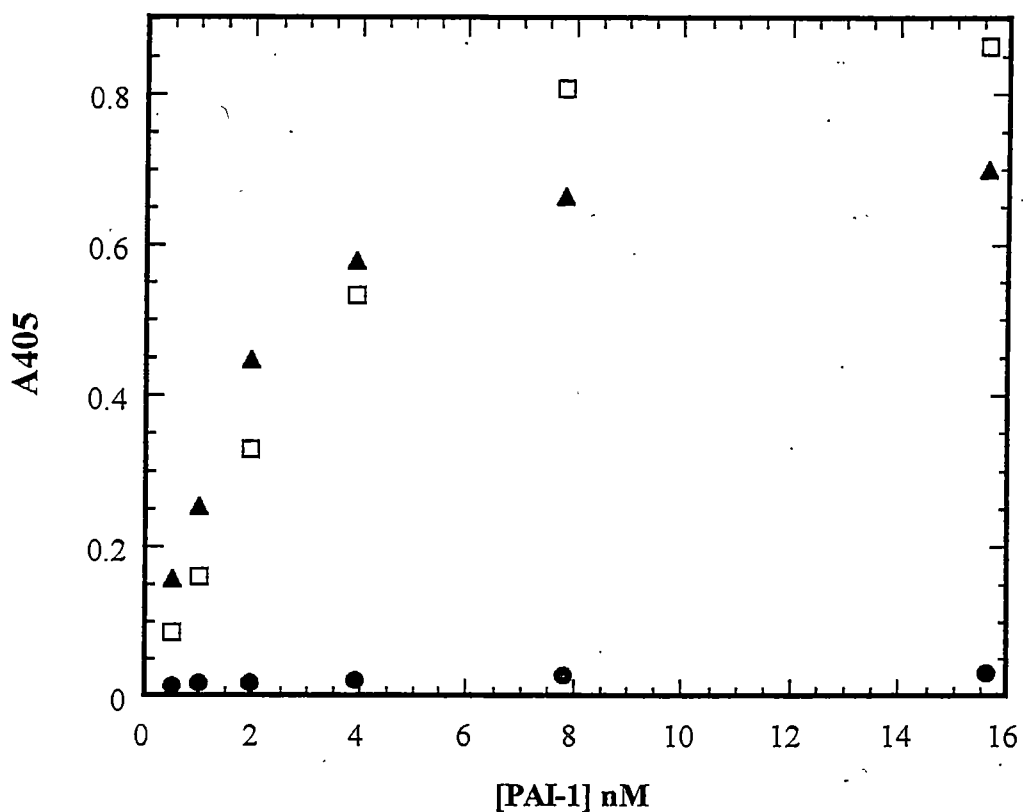
Figure 2-23: Direct PAI-1 Binding Immunoassay. A direct PAI-1 binding immunoassay was performed to determine the PAI-1 binding ability of the recombinant · proteins. An equal molar amount of vitronectin (280 nM) was used to coat the wells of a microtiter plate. A solution of plasma vitronectin (□), VN-his (▲) or ssΔsBVN-his (●) was used to coat the plate. PAI-1 (500 nM final concentration in the first well) was serially diluted down the plate and the PAI-1 detected with a polyclonal antibody (from Tom Podor, 1:3000). Each data point was corrected to remove the contribution from non-specific PAI-1 binding to the plate.

multimeric vitronectin was serially diluted and incubated with active wild-type PAI-1. The vitronectin in solution competes for PAI-1 binding with the vitronectin immobilized on the microtiter plate. PAI-1 bound to the vitronectin on the plate was detected with polyclonal PAI-1 antibodies. Both recombinant proteins competed for PAI-1 binding to different degrees (Figure 2-24). Whereas plasma and multimeric vitronectin are virtually indistinguishable in PAI-1 binding ability, VN-his exhibits a slight decrease in its PAI-1 binding ability. The somatomedin B deletion mutant, on the other hand, shows a marked decrease in PAI-1 binding ability compared to plasma vitronectin, multimeric vitronectin and recombinant vitronectin (VN-his).

Discussion

While eukaryotic expression systems are used extensively in the study of proteins, very few researchers are employing them in the study of vitronectin. Full-length vitronectin has been produced by transfected hamster kidney cells (*22*). However, expression levels of the protein were low, approximately 1 µg/ml. This recombinant full-length vitronectin exhibited similar cell binding to vitronectin purified from plasma. Interestingly, no further studies were ever pursued. The other system that has been used successfully is the baculovirus system. Zhao expressed a recombinant full-length vitronectin in this system and characterized it for correct post-translational modifications (*123*). Vitronectin was shown to be glycosylated, sulfated at the two appropriate residues and phosphorylated at Ser 378. This recombinant protein also retained cell and PAI-1 binding ability. This group also expressed several mutants of vitronectin, with one
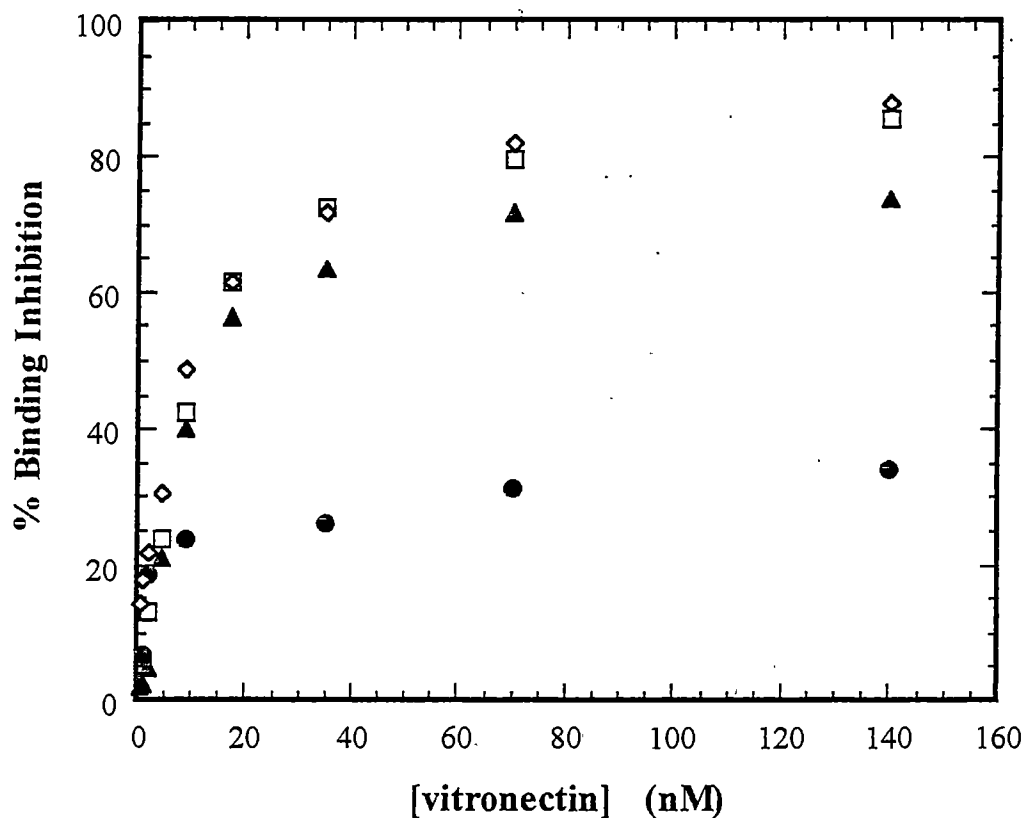
Figure 2-24: Competitive PAI-1 Binding Assay. Multimeric vitronectin (□), plasma vitronectin (◇), VN-his (▲) or ssΔsBVN-his (●) were tested for PAI-1 binding in a competitive assay. A constant amount of PAI-1 (10 nM) is added to decreasing concentrations of vitronectin in solution. The data is plotted as percent binding inhibition, which is calculated using data from wells with no added vitronectin representing 100% binding.

lacking the heparin binding domain and another lacking the somatomedin B domain (*124*). These proteins were expressed as fusion protein, using a histidine tag. These deletion mutants were used to characterize cell binding ability. No further characterization was performed on the mutants.

The most popular method for expressing vitronectin is in bacteria. Although bacteria cannot produce full-length vitronectin, many researchers express recombinant domains in the bacteria. The effects of a lack of post-translational modifications on vitronectin function have not been well characterized. Likewise, it is not known how important the post-translational modifications are for proper vitronectin function. The somatomedin B domain, as a whole, with point mutations or with deletions, has been expressed in bacteria and used to determine the PAI-1 binding site (*107, 128*). These polypeptides were expressed as fusion proteins and tested for PAI-1 binding ability, however, no characterization of the disulfide arrangement or oxidation state of the cysteines was performed.

The goal of this project was to express and characterize a deletion mutant of vitronectin lacking the somatomedin B domain. The ligand binding ability of the somatomedin B deletion mutant was evaluated. The study was aimed at determining the similarity of recombinant vitronectin to that obtained from plasma in order to answer the pertinent question: Does removal of the somatomedin B domain result in the loss of PAI-1 binding ability?

Can a Recombinant Vitronectin Be Expressed and Easily Purified Using the Baculovirus System?

Four baculovirus viruses were used in this study. Two were full-length vitronectin and the other two were somatomedin B deletion mutants. The first somatomedin B construct lacked a histidine tag (ssΔsBVN). This protein proved to be difficult to purify. The protein was too impure to put directly over an affinity column, so Blue Sepharose was used to concentrate the medium. A second DEAE column removed some contaminating proteins. The final column, an immunoaffinity column made from rabbit polyclonal antibodies to vitronectin, worked to purify the ssΔsBVN. However, the capacity of the column was low and its ability to successfully bind and purify the protein grew progressively worse over time until it became ineffective. Yields were very low even when the antibody column was working, with 300-500 μg of protein isolated from one liter of spent media.

The full-length vitronectin, BBVN, was also expressed to serve as a baculovirus expressed vitronectin control. Although it expressed well, it too was difficult to purify. The strategy employed by Gibson using a monoclonal antibody column was ineffective for the purification of BBVN. A new monoclonal antibody column generated by Kenneth Minor did no better so a histidine tagged full-length vitronectin was constructed.

Histidine tagged constructs were made for both full-length (VN-his) and the somatomedin B deletion mutant (ssΔsBVN-his). Both expressed well in Hi5 cells, with optimum expression seen after 72 hours. Purification by a chelating resin resulted in relatively pure protein. Protein concentration as determined by ELISA and the BCA assay were generally indistinguishable. The protein was not purified to homogeneity,

however. Some degradation products are present after purification, as seen by Western and Coomassie stained gels. Typical protein yield after purification was 3-4 mg protein per liter of spent medium. These trials in protein purification indicate that recombinant vitronectin expressed in the baculovirus system that contain a carboxy-terminal histidine tag are easily purified.

Are the Recombinant Vitronectin Proteins More Similar to Native or Multimeric Vitronectin with Respect to their Oligomeric State?

Structural studies performed on BBVN previously (*43*) demonstrated the protein produced in the baculovirus system was more similar to multimeric than native vitronectin. Two different recombinant vitronectin samples were subjected to gel filtration chromatography. Molecular weight estimations from the gel filtration column estimated the size of ssΔsBVN, ssΔsBVN-his and multimeric vitronectin to be greater than 669,000 Daltons.

The recombinant protein also behaved more similarly to multimeric vitronectin with respect to heparin binding. The somatomedin B deletion mutant, ssΔsBVN-his, and the full-length vitronectin, VN-his, both neutralized heparin activity to a similar degree as multimeric vitronectin.

Are There Functional Differences between the Recombinant Forms of Vitronectin and Plasma Vitronectin?

Several assays were performed to evaluate whether the recombinant vitronectin was similar to plasma vitronectin. The cell binding, integrin binding and heparin binding ability of the recombinant proteins was evaluated in parallel with native and multimeric

(denatured/renatured) vitronectin. Both recombinant proteins contain the RGD sequence necessary for integrin binding and the heparin binding domain for heparin binding.

The cell binding ability of both recombinant proteins, VN-his and ssΔsBVN-his, as well as native and multimeric vitronectin was investigated using rabbit smooth muscle cells. There was no appreciable difference in the cell binding ability of any of the vitronectin samples. Deletion of the somatomedin B domain did not compromise the cell binding ability of this mutant. Therefore, the determinants necessary to promote cellular adhesion are contained outside the somatomedin B domain. This result is consistent with the work of Zhao (*123, 124*). Several recombinant vitronectin constructs were expressed using the baculovirus system to examine cell binding ability (using hybrid endothelial cells): native vitronectin, recombinant full-length, a somatomedin B deletion mutant, a heparin binding deletion mutant, and two full-length vitronectin with the RGD sequence mutagenized to either RAD or RGE. Deletion of either the somatomedin B or heparin binding domain had no effect on cell binding or spreading. The RAD and RGE mutations, on the other hand, were severely impaired in their ability to bind cells. Additionally, human fibrosarcoma cells were found to bind denatured vitronectin (*129*). This interaction could be compromised with the addition of antibodies to the amino-terminus (amino acids 1-51), which resulted in attenuation of cell binding at high antibody concentrations.

The integrin binding ability of the recombinant proteins was also compared to that of native vitronectin. The platelet integrin GPIIb/IIIa (also referred to as $\alpha_{IIb}\beta_3$) was used in these assays. This integrin, expressed on the surface of platelets, binds vitronectin and facilitates their adhesion to sites of injury during thrombus formation (*130*). The

GPIIb/IIIa integrin was immobilized to the wells of a microtiter dish and the vitronectin in solution was allowed to incubate with the bound integrin. All three of the proteins bound to the integrin. Both of the recombinant proteins, VN-his and ssΔsBVN-his, exhibited similar binding to the immobilized platelet integrin. The binding of plasma vitronectin to the integrin was approximately 10-fold lower than that of the recombinant proteins. The oligomeric state of the recombinant proteins may promote their increased binding to the integrin. Integrins often bind their ligands more efficiently when there is a clustering of the recognition site. The oligomeric state of the recombinant proteins may mimic this clustering so they are better able to bind the integrin. The results of this study indicate that the cell binding sequence (RGD) necessary for integrin adhesion is exposed in both native and oligomeric vitronectin. Other studies, using multimeric vitronectin, have demonstrated binding to GPIIb/IIIa (*129*) as well as the $\alpha_v\beta_3$ and $\alpha_v\beta_5$ integrins (*116*) using immobilized integrin and soluble vitronectin.

There is only one other report investigating the integrin binding ability of native vitronectin. In this study, both plasma and multimeric vitronectin were incubated with immobilized GPIIb/IIIa. Plasma vitronectin was shown to bind 5 to 10-fold less than multimeric vitronectin and said to saturate at approximately 140 nM even though the plotted data did not indicate any leveling in the binding curve to suggest saturation had been approached. This contrasts the results of the present study, in which plasma vitronectin is not saturated at a concentration of 500 nM but does differ significantly from the binding of the recombinant proteins.

A solution-phase kinetic assay was performed to compare the rates of heparin neutralization for the recombinant, native and multimeric vitronectin. The heparin

neutralization assay provides more evidence that the recombinant vitronectin binds to heparin with an affinity similar to multimeric vitronectin. The midpoints for inhibition for multimeric, VN-his and ssΔsBVN-his were 0.14, 0.04 and 0.18 μM, respectively. The midpoint for inhibition for multimeric vitronectin is in close agreement with the reported midpoint. The midpoint for inhibition for the multimeric form of vitronectin has been reported to be between 0.1 and 0.2 μM (5, 43). The midpoint for inhibition by native vitronectin could not be determined from the results presented in this dissertation, but has a published value of 0.6 μM (5). Two other recombinant vitronectins characterized by Angelia Gibson, one a full-length and the other truncated after the heparin binding domain at the endogenous cleavage site, shared the same midpoint for inhibition of 0.05 μM. This agrees closely with the value obtained for VN-his. Essentially, there are no significant differences in the ability of the recombinant proteins, VN-his and ssΔsBVN-his, and multimeric vitronectin to neutralize heparin.

The difference in the apparent reaction rates for the somatomedin B deletion mutant and the full-length protein could be attributed to differences in the oligomeric state. The size of the proteins was determined to be greater than 669,000 by gel filtration chromatography. Therefore, the VN-his protein may be a larger multimer than either multimeric vitronectin or the ΔsBVN-his. The difference in the K_{app} may be attributed to avidity, rather than an increased affinity. In this case, the apparent affintiy is greater when many binding sites are clustered together compared to one or two binding sites. In other words, the effective binding of heparin to multimeric vitronectin is tighter than the measured binding affinity of the heparin to monomeric vitronectin.

The results of this study thus far support the contention that the recombinant vitronectin produced in the baculovirus system effectively mimics vitronectin, being more similar to the multimeric state of the protein. The assays used to address ologomeric structure and vitronectin function have up to this point involved ligand binding to areas outside of the somatomedin B domain. The results indicate that deletion of the somatomedin B domain do not adversely effect vitronectin function. Therefore, this deletion mutant can serve as an effective tool in teasing out the ligand binding ability of vitronectin.

Does Removal of the Somatomedin B Domain Result in Loss of PAI-1 Binding Ability?

The location and the number of PAI-1 binding sites within vitronectin remains shrouded in controversy. The approach used in this dissertation research to provide some insight into the nature of the PAI-1 binding site was to generate a mutant form of vitronectin that has one of the putative binding sites removed. This deletion mutant, ssΔsBVN-his, has removed the proposed high affinity PAI-1 binding site. Will this mutant bind PAI-1? This is the question that begs to be answered.

PAI-1 binding ability of the recombinant proteins has been tested using three separate methods. Initially, PAI-1 binding was examined by Far-Western analysis. A PAI-1 stable mutant was able to bind plasma vitronectin, VN-his and ssΔsBVN-his. Therefore, all three proteins retain PAI-1 binding ability. This method does not reveal any information about differences in PAI-1 binding ability, it only states that PAI-1 can bind to these proteins. This technique has been used previously to isolate fragments of vitronectin that retained PAI-1 binding activity (*106*).

In order to see if ssΔsBVN-his has weaker binding to PAI-1, two different immunoassays were performed: a direct PAI-1 binding and a competitive PAI-1 binding immunoassay. For the direct PAI-1 binding immunoassay, vitronectin is coated to a polystyrene dish followed by incubation with dilutions of PAI-1 in solution. This being a solid-phase assay, true ligand binding affinities cannot be determined from this data as vitronectin binding to the plastic can result in conformational changes or adhesion may leave ligand binding inaccessible. Despite the pitfalls, this assay can supply some information about the PAI-1 binding ability of the somatomedin B deletion mutant. There is virtually no difference seen in PAI-1 binding to immobilized VN-his and native vitronectin. With the somatomedin B deletion mutant, however, binding of PAI-1 was significantly reduced. The concentration of PAI-1 used to bind the immobilized vitronectin started at 500 nM and was serially diluted. At PAI-1 concentrations above approximately 20 nM, however, background binding of PAI-1 to the microtiter plate made interpretation of the results difficult. Therefore, comparisons between the proteins could only be made with very low concentrations of PAI-1. This could mask PAI-1 binding to the ssΔsBVN-his protein if higher concentrations of PAI-1 are necessary for binding.

The last test for PAI-1 binding activity utilized a competitive PAI-1 binding ELISA. In this assay, vitronectin in solution competes with immobilized vitronectin for soluble PAI-1 binding. The binding of PAI-1 to immobilized vitronectin is monitored. Both vitronectin and PAI-1 are in solution, so there are no conformational changes associated with binding to plastic. Native plasma vitronectin, multimeric vitronectin and VN-his all inhibit PAI-1 binding to a similar extent. The PAI-1 binding ability of

ssΔsBVN-his, on the other hand, is clearly reduced. Addition of ssΔsBVN-his results in approximately 35% binding inhibition. In other words, the deletion mutant only binds to enough PAI-1 in solution to cause a 35% reduction in PAI-1 binding to immobilized vitronectin, while 65% of the PAI-1 binds to the vitronectin immobilized on the plate. This result is significant in that it demonstrates a protein lacking the somatomedin B domain still retains PAI-1 binding activity, albeit to a lower extent than vitronectin containing the somatomedin B domain. This current study indicates that PAI-1 binding is not solely contained within one linear epitope of vitronectin.

Three distinct regions have been implicated in PAI-1 binding: the somatomedin B domain, the connecting region and the heparin binding domain (see Chapter 1). Briefly, the PAI-1 binding site has been investigated using proteolysis, synthetic peptides as well as recombinant and site directed mutants. Using these approaches, the PAI-1 binding site has been localized to the somatomedin B domain and the heparin binding domain. The other proposed PAI-1 binding site was localized using phage display, however, little research has continued on this site after its description. Instead, most of the controversy revolves around the somatomedin B and heparin binding domains. Despite the similar tests used to identify the PAI-1 binding site, the discrepancy still exists.

Threading of the vitronectin sequence to determine structure has been attempted (C. Peterson, unpublished results). Only one of the proposed epitopes for PAI-1 binding has been modeled, the heparin-binding domain (see Figure 1-3). PAI-1 has yet to be docked to this region, so no information is available about PAI-1 binding to this site. The somatomedin B domain has been modeled. In this model, only 3 of the 4 proposed disulfide bonds have been modeled. Unfortunately, there is not enough information about

the interaction between the somatomedin B domain and the rest of the protein to permit docking of the domains. The connecting region between amino acids 55 and 125, which contains another putative PAI-1 binding site, is unable to be modeled. The results of the threading of vitronectin sequence do not reveal any clues as to the PAI-1 binding site as of yet. As more information becomes available, the modeled structure may prove more useful for the examination of PAI-1 binding sites.

Recent results from our laboratory in collaboration with Dr. T. Podor suggest a reason why the PAI-1 binding site has been so difficult to localize. The size and stoichiometry of the PAI-1/vitronectin complexes was analyzed using analytical ultracentrifugation (Podor, T.J. *et al.*, manuscript submitted). The results indicate vitronectin forms a 2:4 complex with PAI-1. In other words, two PAI-1 molecules bind a single vitronectin molecule. Furthermore, two monoclonal antibodies previously shown to inhibit PAI-1 binding to vitronectin (*75, 107*) were used to determine if there was more than one PAI-1 binding site within vitronectin. The antibodies map to the somatomedin B domain (mAB 153) or a large central fragment of vitronectin beginning after the somatomedin B domain and ending before the heparin binding domain (*107, 131*). Both of the monoclonal antibodies interfered with PAI-1 binding, however, neither one completely abolished binding. Intriguingly, each monoclonal antibody reduced PAI-1 binding by approximately 50 percent. The observation that a somatomedin B deletion mutant of vitronectin still retains some PAI-1 binding ability supports the two binding site model.

The idea that PAI-1 binding induces multimerization of vitronectin was first investigated by Seiffert (*132*). Addition of active PAI-1 to plasma resulted in the

formation of disulfide-linked vitronectin dimers and large noncovalently linked multimers, as evidenced mainly by native electrophoresis. The formation of these dimers and multimers was also associated with the expression of new epitopes for conformationally sensitive antibodies. Work by Kenneth Minor in our laboratory agrees with the studies performed by Seiffert. Using gel filtration chromatography, K. Minor demonstrated that PAI-1 induces multimerization of vitronectin (unpublished results). Vitronectin remains in the multimeric state even after PAI-1 is dissociated.

A model demonstrating the possible mechanism of PAI-1 induced vitronectin multimerization is shown in Figure 2-25. According to this model, PAI-1 induces structural changes within vitronectin that eventually causes it to self-associate. This self-association event may be induced by the binding of one or both of the PAI-1 molecules to vitronectin. When PAI-1 becomes latent, it dissociates from vitronectin, leaving vitronectin in its multimeric state.

Concluding Remarks and Future Directions

A recombinant form of vitronectin lacking the somatomedin B domain can readily be expressed using the baculovirus system. This mutant containing a histidine tag, ssΔsBVN-his, is easily purified from the spent medium of the cells. The ssΔsBVN-his protein is functional with respect to heparin binding, cell binding and integrin binding. Removal of the somatomedin B domain did effect PAI-1 binding ability. The ssΔsBVN-his mutant exhibited weaker binding to PAI-1 than native, multimeric and recombinant
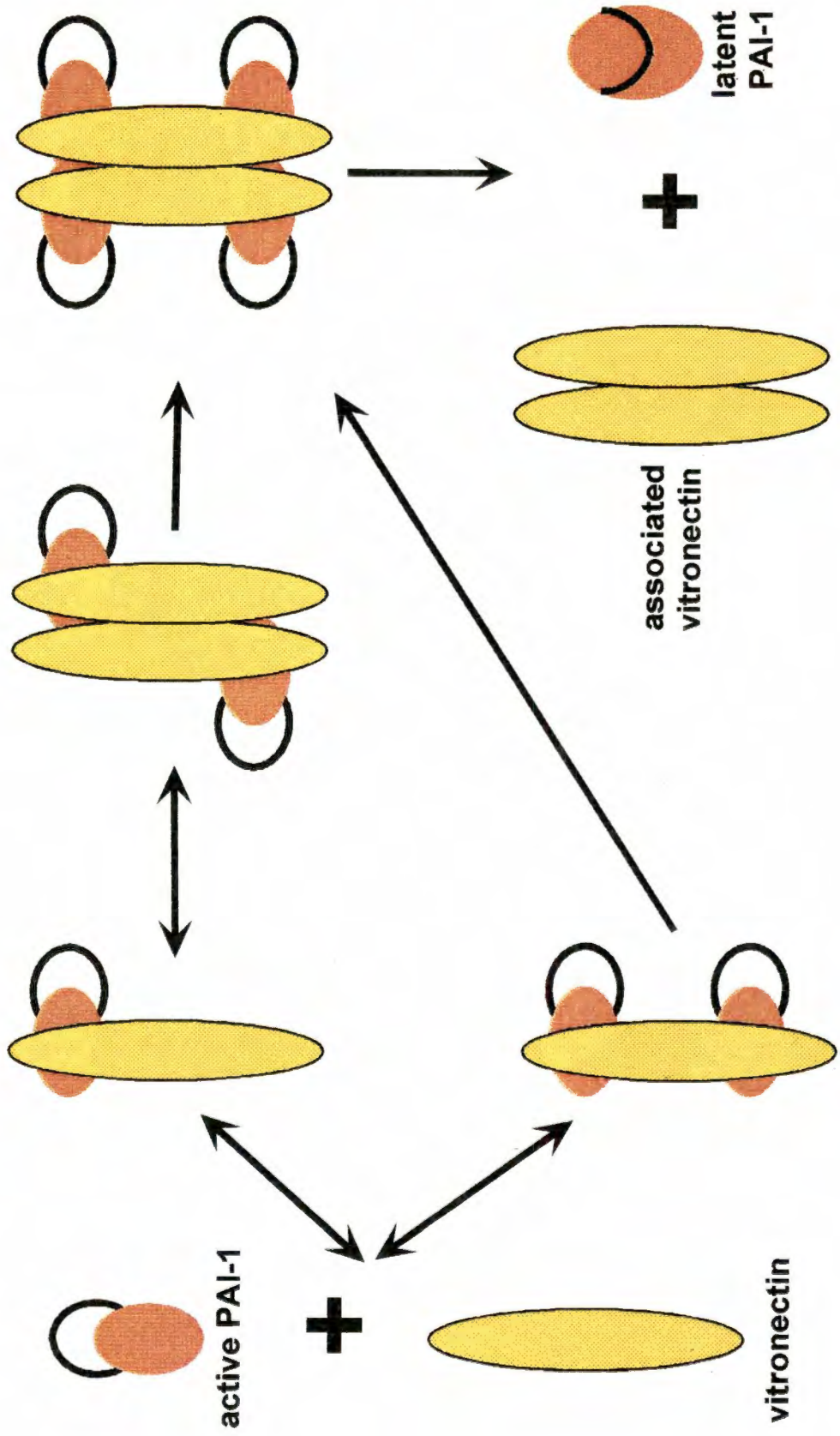
Figure 2-25: Model of PAI-1 Induced Vitronectin Multimerization.

full-length vitronectin (VN-his). The results of these studies support a model of two PAI-1 binding sites resident within vitronectin.

The ssΔsBVN-his recombinant protein has been initially characterized and analyzed for PAI-1 binding ability. This mutant could also be useful in identifying the urokinase receptor (uPAR) binding site. Much like PAI-1 binding, the location of the uPAR binding site has been suggested to be in either the somatomedin B domain or the heparin binding domain (*70, 77*). The ability of the somatomedin B deletion mutant to bind the urokinase receptor can be tested using biotinylated uPAR. This protein could also be useful in understanding the relationship between PAI-1 and vitronectin in cellular migration and adhesion. It has been shown that ssΔsBVN-his retains cell binding ability, but does it promote cellular migration? In the presence of PAI-1? For cells expressing uPAR? Further characterization of this recombinant somatomedin B deletion mutant is certainly worthwhile to address these questions and gain further insight into the function of vitronectin.

Chapter 3

The Use of Retroviral Vectors to Introduce Vitronectin or PAI-1 into Endothelial Cells

Introduction

Synthetic vascular grafts have commonly been used in humans for the replacement of diseased or injured arteries. The use of synthetic vascular grafts, however, has met with only limited success. Whereas grafts placed in high flow arteries are successful, those placed in low flow arteries rarely survive more than a few years. The following is a brief review of the history of vascular grafts, their promise, and their pitfalls for use in human beings.

History of Vascular Grafts

The field of vascular surgery had its beginnings at the turn of the century when surgeons learned it was possible to directly suture blood vessels. It soon became apparent that excision of discrete areas of arteries could not all be repaired by a direct end-to-end suture. Following this revelation, surgeons in the early 1900s soon began using normal human arteries and non-essential veins in the body to replace arteries. Attempts to transplant normal human arteries were short lived due to their antigenic properties. The transplanted arteries rapidly underwent rejection and dissolution. The denaturation of the protein within the transplant graft was attempted yet did not overcome

the problem of rejection. Venous grafts, on the other hand, were far more successful. The venous grafts in the arterial system, however, had only restricted applicability due to the limitations of obtaining sufficient lengths and sizes of non-essential veins. In the late 1940s and early 1950s an observation by Voorhees founded the modern era of reconstructive arterial surgery. Voorhees noted that a synthetic fabric made from Vinyon "N" became coated with a smooth, relatively nonthrombogenic surface when implanted in the aorta of a dog (133). The graft also displayed fibrin deposition within the pores of fabric, therefore, it was assumed that fibroblasts and endothelial cells could migrate onto the graft. This theory proved itself to be true. A completely confluent endothelial layer can be seen on the synthetic grafts of dogs in three to six months and in as little as two weeks in calves or pigs (134). The future of reconstructive arterial grafts seemed bright indeed.

Synthetic vascular grafts were used throughout the body to treat diseased arteries, especially those with excessive atherosclerosis. However, over time it became apparent that the synthetic vascular graft worked very well in some situations, but not others. Synthetic grafts with high life spans, or patency rates, over many years are ones with large diameter (generally greater than 10-12 mm), high flow and low resistance situations, such as aortic grafts. In small caliber grafts (4 mm or below) where the flow is low and the resistance is high, synthetic vascular grafts fail miserably. A study by Sauvage's group using Dacron® grafts studied the patency of synthetic grafts in humans of progressively smaller arteries. Grafts in the aorto-iliac (or abdominal cavity) position exhibited a 99% patency rate over ten years, a 51% patency rate in the femoro-popliteal (between the pelvis and the knee) position over ten years, and a patency rate of 15-20%

in the distal calf in less than three years (*135*). Choice of material for the synthetic graft

did not appreciably alter the above result. Expanded polytetrafluoroethylene (PTFE) or

Teflon® grafts placed below the knee had a patency rate of approximately 25% after three

years (*136*).

How Do Synthetic Vascular Grafts Heal?

A graft that has healed is no longer thrombogenic or antigenic. These properties

can be attained when the graft develops a full endothelial cell lining. There are three main

ways grafts are believed to endothelialize in humans: by pannus ingrowth from the ends

of the grafts, intravascular fallout of cells from the bloodstream, and transmural capillary

ingrowth (*137*)(Figure 3-1). Before the graft can develop an endothelial lining in the

intima, the surface must be rendered nonthrombogenic. Following implantation of the

graft, a thick layer of fibrin is deposited on the intima, resulting in the attraction of

platelets. The platelets in turn secrete growth factors, such as platelet derived growth

factor, which stimulate the growth and migration of smooth muscle and endothelial cells

(*138*). Pannus ingrowth, the migration of endothelial cells from the native artery, is

generally only seen a few millimeters from the junction of the graft and the artery, the

anastomosis. With pannus ingrowth, the cells should eventually proliferate from the graft

ends to cover the graft, rendering it non-thrombogenic. Intravascular fallout can deposit

cells in the midgraft regions so the graft can heal from the middle out to meet the pannus

ingrowth. Transmural capillary ingrowth relies on the migration of capillary endothelial

cells through the pores of the graft to provide a source of cells for surface

endothelialization (*139, 140*). This type of growth is affected by the porosity of the

membrane used (*140*). The larger the pores in the material, the greater the ability of cells
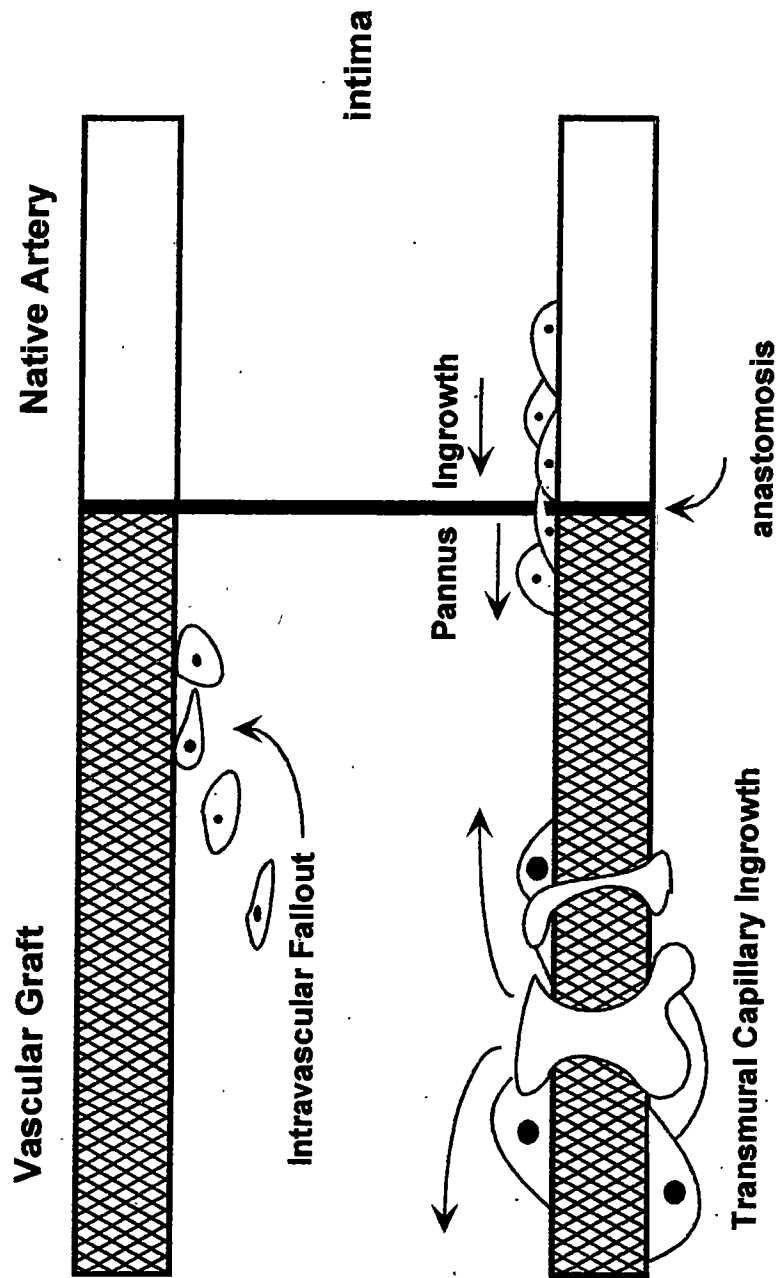
Figure 3-1: Mechanisms of Endothelialization of Vascular Grafts. Three mechanisms of healing are shown in the figure above. 1) Pannus ingrowth of cells from the native artery onto the vascular graft. 2) Intrasvacular fallout of cells from the bloodstream onto the vascular graft. 3) Transmural capillary ingrowth of cells through the pores of the vascular graft material. The anastomosis, where the native artery has been surgically connected to the synthetic graft, is shown as the solid black line.

105

to cross the membrane, resulting in cellular and capillary ingrowth. When healing of the graft does not occur, graft failure takes place.

Why Do Synthetic Vascular Grafts Fail?

Graft failure can be attributed to several events. The synthetic materials used for vascular grafts are hydrophobic, which adversely affects cell adhesion. Whereas the porous structure of PTFE would appear to be an ideal material for cellular and capillary ingrowth, this event is seldom complete in humans (140). These synthetic materials are also inherently thrombogenic. This effect is intensified in the small diameter vascular grafts, which have a lower flow rate than the larger, higher flow grafts. The patency of these small diameter vascular grafts without the use of drugs to limit platelet adhesion and aggregation is limited (141). Late graft failure is commonly due to anastomotic neointimal hyperplasia, an abnormal increase in normal cells of the inner blood vessel at the junctions of the graft. Neointimal hyperplasia is generally attributed to smooth muscle cell proliferation. The proliferation of smooth muscle cells may be stimulated by the changes in shear rates at the anastomosis of the graft to the artery or by growth factor release from activated platelets or vascular wall cells (137, 142). Macrophages also mount a response to the exposed foreign PTFE grafts. This response includes the release of growth factors, which results in non-specific stimulation of the surrounding vessel wall (137). If this response is prolonged, it may contribute to a thickened neointima, which could lead to vascular occlusion. In the case of severe atherosclerosis, downstream progression of the disease also could account for the failure of grafts. A possible solution to these problems is the maintenance of a functional endothelial cell monolayer coating the synthetic vascular graft that could potentially act as a buffer zone between platelets

and the graft surface. The antithrombotic proteins secreted by the endothelial cells could reduce the thrombotic events which lead to occlusion and therefore failure of the grafts.

Gene Therapy to Improve Vascular Graft Patency

Gene therapy has been suggested as a way to improve the patency of synthetic vascular grafts. This powerful tool could potentially be used to modify vascular endothelial cells which are subsequently used to seed synthetic grafts. Genes may be introduced into the vascular endothelial cells to inhibit cell growth, promote migration or adhesion of endothelial cells, or promote anti-thrombogenic activities. These modified cells could then constituatively express protein derived from the introduced gene to render the graft non-thrombogenic and therefore aid in the healing of the graft.

A vector is defined as the vehicle used to introduce the gene of interest into the target cell. Disabled viruses are commonly used, as well as non-viral based vectors, such as naked DNA or DNA complexed with lipids. Viral vectors are generally more efficient in introducing DNA into the target cells than naked or complexed DNA, however, engineered viral vectors have the potential to illicit an immunological response. Several viral vectors also have the potential to integrate into the cell's genome, which extends the duration of the target gene's effects. Viral vectors are therefore more commonly chosen for gene therapy. The three most commonly used viral vectors are retroviruses, adenoviruses and adeno-associated viruses. The lentivirus, the family of virus that HIV belongs to, is now emerging as a promising viral vector.

Retroviruses have a single stranded RNA genome which is transcribed into double-stranded DNA with the help of reverse transcriptase supplied by the virus. The double-stranded DNA can be integrated into the host cell's genome. Theoretically, the

introduced retroviral DNA can be maintained in the cell over its entire life span (*143-145*). The major drawback involved with the use of retroviral vectors is target cells must be actively dividing for the DNA to integrate into the genome (*146*).

Adenovirus is a double-stranded DNA virus that cannot be incorporated into the host cell genome. Since the double-stranded DNA is not integrated, it has the potential to infect non-dividing cells. However, there is only transient expression from the non-integrated double-stranded DNA (*147*). The largest problem with adenoviral vectors is they stimulate an immune response, which shortens the life span of the transferred gene.

Adeno-associated viruses are small single-stranded DNA parvovirus. The virus is non-pathogenic to humans. Gene expression is achieved by both integration into host DNA and episomal transcription. High efficiency expression has been achieved in non-replicating cells as well as longer-term expression compared to adenovirus (*148-150*).

Lentivirus based vectors are single-stranded RNA retroviruses. Double-stranded DNA made by the virus' reverse transcriptase is integrated into the target cell genome. As with a retrovirus, it is possible to retain the integrated DNA throughout the lifetime of the cell. Perhaps the biggest advantage of the lentiviral vectors is their ability to infect non-dividing cells.

A variety of vectors are available for gene therapy and several phase I clinical trails in humans are underway utilizing this technology. It appears as if the introduction of genes into vascular endothelial cells to relieve the problems associated with graft failure is a viable solution. However, there have been problems associated with the transduction of vascular endothelial cells and their use on synthetic vascular grafts.

Using the dog as a human model for the study of vascular grafts, it has been noted that seeded transduced vascular endothelial cells exhibit only minimal luminal endothelialization (151), despite the fact that grafts seeded with non-transduced cells develop a full endothelial cell lining. This limited luminal endothelialization results regardless of the vector used, the seeding cell density of the graft, or the seeding substrate (151). These results lead to the suggestion that retrovirally transduced vascular endothelial cells have an impaired ability to adhere to and proliferate on vascular grafts *in vivo*.

Adhesive Ability of Transduced Endothelial Cells

In order to more thoroughly investigate the adhesive ability of retrovirally transduced vascular endothelial cells, neoR gene-transduced, "mock"-transduced (cells that were exposed to the medium of PA317 cells that serve as a control to determine if the manipulation of the cells has any affect), and naïve endothelial cells were exposed to physiologic shear stress when adhered to extracellular matrix proteins (151). All three cell types were allowed to adhere to either collagen IV, laminin or fibronectin. The shear stresses used were 20 and 90 dyn/cm^2, which simulate the mean and peak aortic shear stresses in large canine arteries. To summarize the work of this study by Sackman, *et al.*, the neoR transduced cells had significantly reduced adhesion on fibronectin under shear stress than both the naïve and "mock" infected cells. This once again points to an impaired adhesive ability of transduced endothelial cells that is not dependent upon the gene transduced into the cell. The fact the neoR transduced cells do not adhere as well to fibronectin indicates there may be a problem with either the fibronectin receptor or its interactions with the cell or the extracellular matrix.

Following up on the above studies, Sackman *et al.* attempted to correlate the expression of cellular receptors responsible for adhesion, integrins, with the adhesive ability of the endothelial cells (*152*). The results of this study are summarized below. Both canine and human endothelial cells were transduced by one of three following vectors: LN (containing only the neoR gene), LtSN (containing the human tPA gene and neoR), or LHL (with the hygromycin B resistance gene). Naïve and mock transduced cells were also analyzed. The expression of the integrin subunits in the above cells for fibronectin ($\alpha_5\beta_1$), collagen IV ($\alpha_2\beta_1$) and vitronectin ($\alpha_v\beta_3$) were tested by using Western blotting. The alpha subunits (α_5, α_2 and α_v) of naïve and transduced cells were all expressed in an intact form. Both the β_1 and the β_3 integrin subunits were found to be intact in naïve and mock transduced cells. The β_1 subunit, however, was not intact in any of the transduced cells. Transduced cells failed to express the β_3 subunit.

What are the implications of transduced cells having degraded or non-existent β integrins? Integrins are integral membrane glycoproteins involved in adhesion to the extracellular matrix and to one another (for review see (*23, 153, 154*)). All integrins are non-covalently linked heterodimers consisting of both an α and a β subunit. Currently, seventeen α and eight β subunits are known (see Table 3-1). The specificity of ligand binding is determined by the α subunit. The overall structure of the both the α and the β subunits are similar, each having a large extracellular domain, a single hydrophobic transmembrane region, and a short cytoplasmic domain.

The amount of structural information on integrins is increasing (for review see (*155*). The structures of different domains found in integrins have been solved by NMR

Table 3-1. Integrins and Their Ligands.

β-subunit	α-subunit	Ligands and Other Cellular Receptors
β_1	α_1	collagen, laminin
	α_2	collagen, laminin
	α_3	fibronectin, laminin, collagen
	α_4	fibronectin, VCAM-1
	α_5	fibronectin
	α_6	laminin
	α_7	laminin
	α_8	unknown
	α_v	*vitronectin*, fibronectin
β_2	α_L	ICAM-1, ICAM-2
	α_M	C3b complement component (inactive), fibrinogen, factor X, ICAM-1
	α_x	fibrinogen, C3b complement component (inactive)
β_3	α_{IIb}	fibrinogen, fibronectin, von Willibrand factor, *vitronectin*, thrombospondin
	α_v	*vitronectin*, fibrinogen, von Willibrand factor, thrombospondin, fibronectin, osteopontin, collagen
β_4	α_6	laminin
β_5	α_v	*vitronectin*
β_6	α_v	fibronectin
β_7	α_4	fibronectin, VCAM-1
	α_{IEL}	unknown
β_8	α_v	unknown

111

and x-ray crystallography. Seven of the seventeen α subunits known contain a 200 amino acid domain, referred to as the I (or A) domain. It has homology with the collagen binding domain of von Willibrand factor and is involved in ligand binding. The crystal structures of several I-domains have been solved (*156, 157*). The I-domain folds into a central six-stranded β-sheet surrounded by seven α-helices. Structural predictions of the ligand-binding domain of β-subunits suggest they adopt a structure similar to the I-domain (*158*). The remaining α-subunits are non-I-domain integrins. However, approximately 440 amino acids at the amino-terminus on non-I-domain integrin α-subunits are predicted to fold into a β-propeller structure composed of seven four-stranded β-sheets (*159*). Once again the β-propeller structure is implicated in mediating ligand-binding interactions.

The association between the α and β subunits occurs within the extracellular domains. When the receptor is bound by its ligand, other bound integrins aggregate together in organized complexes known as focal adhesions. In addition to bound integrins, signaling molecules also gather in focal adhesions, resulting in the activation of a number of tyrosine kinases, such as focal adhesion kinase and c-src. Also present in the focal adhesions are cytoskeleton-associated proteins, including paxillin and tensin. The cytoplasmic domains are believed to interact with these cytoskeleton and cytoplasmic transduction pathways to transfer external signals into the cell. Likewise, intracellular events can trigger the association of integrins to alter specificity so the cell can transfer signals outside to structure its external environment or control its adhesion. Cells lacking these crucial mediators of cell adhesion and signal transduction may have drastically altered phenotypes.

Other proteins are available to help mediate and maintain the adherent state of cells, such as the urokinase receptor (uPAR, see Chapter 1). The urokinase receptor may play a more important role in cellular adhesion if the integrins are not functioning properly. Without functional or intact β subunits, the adhesive ability of cells could be compromised. This could account for the lack of adhesive ability Sackman noted above. Since the work by Sackman only specifically included the β_1 and β_3 subunits, the other β subunits may be intact. Although fibronectin, collagen and vitronectin have been implicated as being major players in the extracellular matrix, other proteins are present and their recognition by the remaining intact integrins and other membrane-bound glycoproteins permit adhesion of the impaired transduced endothelial cells to culture flasks.

The question remains as to why the β_1 and β_3 subunits of transduced endothelial cells are truncated or not expressed. The presence of the *neo* gene used for cell selection has been shown to alter the expression of genes in several cell lines (*160*). This gene, upon introduction in human cells, contains a phosphotransferase activity which could inappropriately alter the phosphorylation state of the cell. The presence of this gene in transduced cells may lead to the inappropriate phosphorylation of the β integrin subunits. It has been noted by Tapley et al. that phosphorylation of the β_1 subunit leads to inactivation of the receptor (*161*). Using the Rous sarcoma virus for oncogenic transformation, it was seen that $pp60^{src}$ phosphorylates a tyrosine residue in the β_1 subunit. This phosphorylation event leads to decreased binding to both talin and fibronectin. Another phosphorylation event occurs on a serine residue within the β_1 subunit which specifically leads to the inability of the integrin $\alpha_v\beta_1$ to no longer bind

fibronectin. Therefore, a phosphorylation event on the β subunits could lead to the decreased adhesive ability of the transduced endothelial cells.

Statement of the Problem

Transduced endothelial cells have impaired adhesive ability potentially due to the loss of integrin integrity. Since integrins are important in mediating interaction between the cell and the extracellular matrix (ECM), the question is: Can over-expression of proteins that regulate cell:matrix interactions be effective at improving the adhesive properties of transduced endothelial cells? Vitronectin and PAI-1 have both been implicated in regulation of cell interactions with the ECM of the vasculature. Therefore, both vitronectin and PA1-1 have a potential therapeutic value in restructuring the vasculature by mediating cellular adhesion and migration or pericellular proteolysis. The balance between PAI-1 and vitronectin in the vasculature can influence the adhesive state of the cell. Can this balance be exploited to confer an adhesive character to transduced cells? Another question that arises is: Will cells that over-express PAI-1 cause a decrease in cellular adhesion? Since excess PAI-1 has been implicated in decreased cellular adhesion, cells that over-express PAI-1 may exhibit an altered adhesive phenotype.

Experimental Rationale

Vitronectin circulates within the bloodstream and can be found in the extracellular matrix. The integrins $\alpha_v\beta_1$, $\alpha_v\beta_3$, $\alpha_v\beta_5$ and $\alpha_{IIb}\beta_3$ have all been shown to bind to vitronectin (*162*). The interaction between vitronectin and the integrins on cells could be important for cellular adhesion, angiogenesis or migration. The process of angiogenesis, the growth of new capillaries from the existing vessels, is commonly used as a system to study factors that regulate migration and adhesion. Angiogenesis is a complex process

involving endothelial cell proliferation, migration and differentiation (*163*). The surrounding extracellular matrix must be degraded to free the cells for migration. The endothelial cells must proliferate and migrate, in addition to synthesizing new extracellular matrix components. Finally, the endothelial cells form new vascular sprouts that become capillaries. A possibility is that the balance between stimulators and inhibitors of angiogenesis control the adhesive state of the cell. These events that take place during angiogenesis also need to occur in a healing graft, so this serves as an appropriate model system for graft healing.

The actions of PAI-1 and vitronectin appear to be influential in determining the adhesive state of the cell. There is a large body of literature devoted to elucidating the roles of vitronectin and PAI-1 on cellular migration and angiogenesis. Vitronectin interacts with the integrins via its RGD binding site. The integrin $\alpha_v\beta_3$, which binds vitronectin, is the major integrin found on endothelial cells (*164*). Stefansson et al. have shown that using vitronectin-coated plates enhances the migration of smooth muscle cells (*10*). Also in this study, it was found that PAI-1 binding to vitronectin was sufficient to block the ability of vitronectin to bind to $\alpha_v\beta_3$. Therefore, the secretion of vitronectin from transduced endothelial cells could stimulate smooth muscle cell coverage of the graft surface as well as provide a matrix surface for endothelial cell adhesion as long as the immediate concentration of PAI-1 is such that little PAI-1 binds vitronectin.

The conversion of inactive plasminogen into its active form, plasmin, has been reported to increase cell migration. This results from the proteolysis of vitronectin and other matrix proteins, releasing the cell from its surrounding for migration (*116*). Since PAI-1 inhibits the serine proteases urokinase- and tissue-type plasminogen activators and

115

prevents the conversion of plasmin into its active form plasmin, PAI-1 transduced

endothelial cells may increase cellular adhesion by reducing pericellular proteolysis of

the extracellular matrix and integrins (Figure 3-2). However, PAI-1 may prevent

interaction of the urokinase receptor on cells with vitronectin in the matrix by competing

for overlapping binding sites in the somatomedin B domain of vitronectin (*10, 69, 128*).

When the concentration of uPA is greater than that of PAI-1, uPA binds to uPAR (Figure

3-3). This event changes the conformation of the receptor so it promotes binding to

vitronectin (*165*). When the concentration of PAI-1 exceeds that of uPA, it competes

with and displaces uPAR binding to vitronectin. If this is the case, then over-expression

of PAI-1 by the endothelial cells could lead to decreased cellular adhesion.

Human umbilical vein endothelial cells were transduced with a recombinant

retroviral vector containing either PAI-1 or vitronectin (details of the procedure are

outlined in the results section). The genes of interest integrate into the HUVEC genome

behind a retroviral promoter. To ensure the HUVECs have been successfully transduced

with PAI-1 or vitronectin, Western blots were performed to detect secreted protein and

polymerase chain reaction was used to confirm the introduction of the target genes. Once

the transduction of the HUVECs was confirmed, Western blots using antibodies specific

for α2, α5, αv, β1 and β3 integrin subunits were performed to evaluate the integrity of

the α and β subunits in the transduced cells. The PAI-1 and vitronectin transduced

endothelial cells were tested for their ability to withstand a physiological shear stress of

90 dynes/cm^2 in flow experiments in an effort to determine if the adhesive ability of the

transduced cells was comparable to that of naïve endothelial cells.
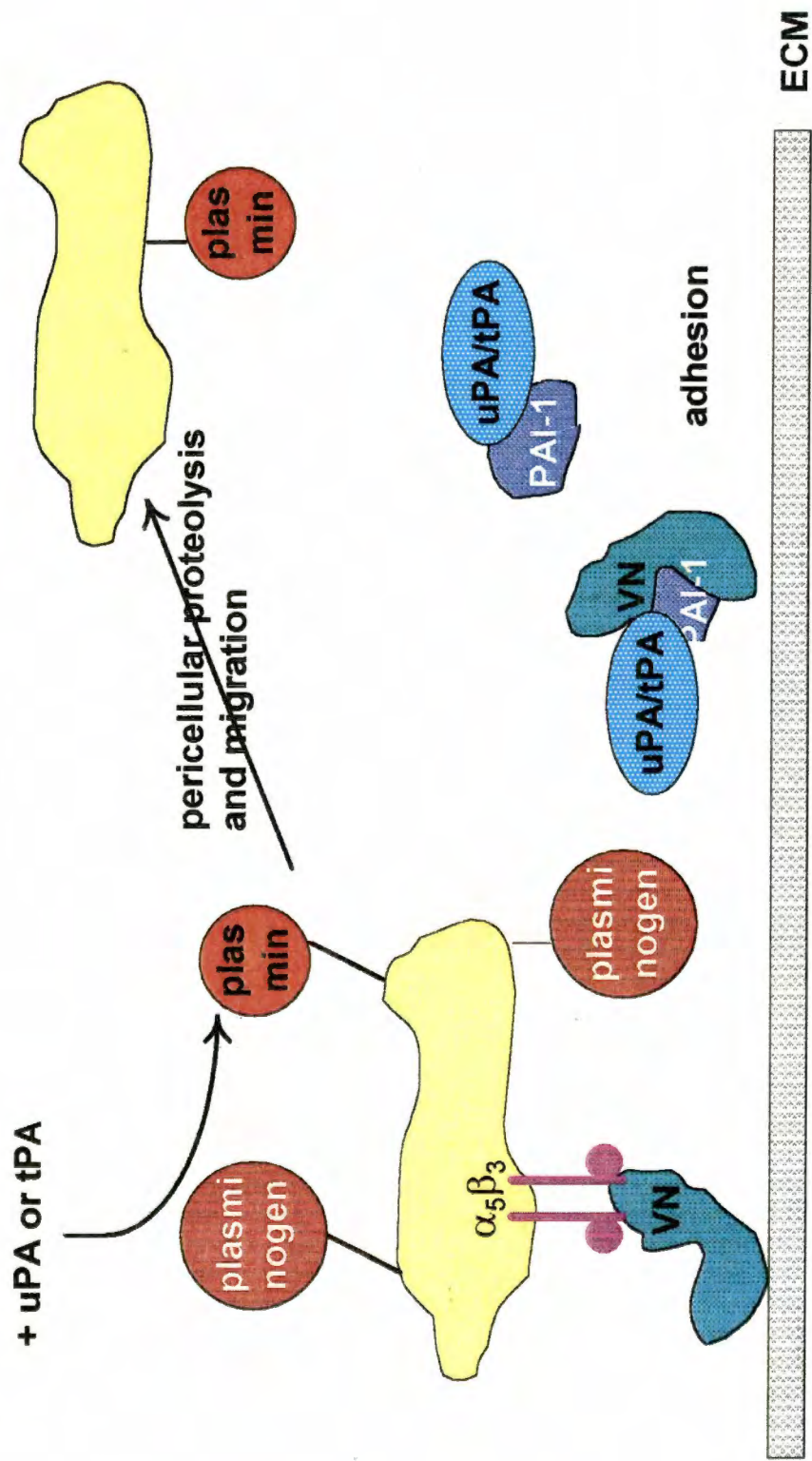
Figure 3-2: Plasminogen System in Regulating Pericellular Proteolysis. The schematic above represents the roles of the components of the plasminogen system in regulating cellular adhesion and migration. Without much PAI-1, the serine proteases uPA and tPA can cleave plasminogen into its active form, plasmin. Plasmin then degrades the ECM and the cell is free to migrate. If PAI-1 is present, it binds to and inactivates uPA and tPA, preventing the activation of plasmin. The cell remains attached to its surroundings and adhesion is maintained.

117
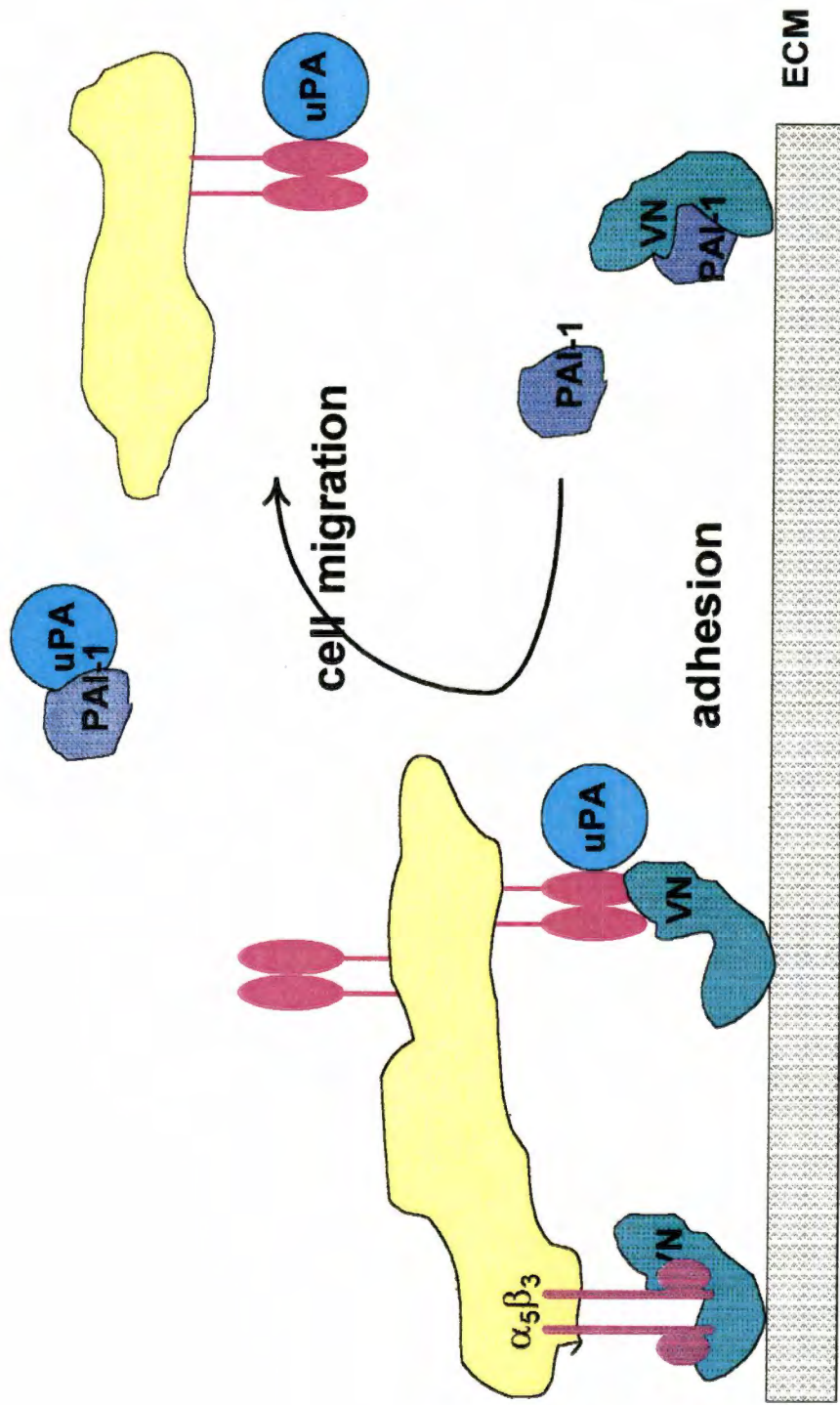
Figure 3-3: uPAR Regulation of Cellular Adhesion. Binding of uPA to uPAR increases the affinity of uPAR for vitronectin. This promotes cellular adhesion. When the concentration of PAI-1 is greater than that of uPA, the PAI-1 competes for vitronectin binding with uPAR. PAI-1 now binds vitronectin while uPAR is released. Upon release of uPAR from vitronectin, the cell is free to migrate.

Materials and Methods

Cell Culture

The GP&E, PA317 and NIH3T3 cell lines (supplied by Dr. Jill Sackman, Ethicon Endo Surgery, Inc., Cincinnati, OH) were grown in Dulbecco's Modified Eagle's Medium (DMEM, Sigma) supplemented with 10% fetal bovine serum (Biowhittaker), penicillin and streptomycin (Gibco BRL). Human umbilical vein endothelial cells (HUVEC) were obtained from a commercial supplier (Clonetics). Human endothelial cells were grown in fully supplemented endothelial growth medium (EGM Bullet Kit, Clonetics). All cell cultures were grown at 37°C in a humidified chamber with 5% CO_2.

Construction of the Recombinant Retroviral Vectors

The cDNA for human PAI-1, PAI-B6, was obtained from Dr. David Ginsburg (University of Michigan Medical School) and subcloned into the retroviral vector pLXSN (supplied by Dr. Jill Sackman). The full-length PAI-1 coding sequence including the signal sequence was excised with EcoRI and ligated into EcoRI digested pLXSN. The resulting plasmid was named pLXSN/ssPAI-1. The plasmid pBlueBacVN encoding full-length human vitronectin (obtained from Dr. David Sane, Department of Medicine, Duke University Medical Center) was digested with NheI. The ends of the resulting fragment containing full-length vitronectin were filled in and the fragment was ligated into the PCR2.1 vector (TA Cloning Kit, Invitrogen), creating the PCR2.1/ssVN plasmid. This plasmid was digested with EcoRI to release vitronectin and ligated into EcoRI digested pLXSN, subsequently known as pLXSN/ssVN.

Transfection of GP&E Cells

GP&E cells were transfected with recombinant retroviral vectors pLXSN/ssPAI-1 and pLXSN/ssVN using the Superfect Transfection Reagent (Qiagen). The day before the transfection, 6×10^5 cells were seeded in 60-mm petri dishes and grown at 37°C with 5% CO_2. The following day, the cells were approximately 75% confluent. DNA (2.5 μg) was diluted into media containing no serum or antibiotics then 5 μl of the Superfect Transfection Reagent was added. Samples were incubated for ten minutes at room temperature. The growth medium from the GP&E cells was aspirated and the cells washed once with PBS. Following the ten minute incubation, 1 ml of growth medium containing serum and antibiotics was added to the reaction then transferred to the cells. The cells were incubated for 3 hours at 37°C with 5% CO_2. After 3 hours, the medium was removed and the cells were washed once with PBS. Fresh growth medium was added and the cells were grown until confluent.

Generation of Producer Cell Lines

PA317 cells were infected with the virus generated from the transfected GP&E cells. The conditioned medium from the GP&E cells transfected with pLXSN/ssPAI-1 or pLXSN/ssVN was removed and spun at 3000rpm for 5 minutes to clear any GP&E cells. The medium with polybrene added to 8 μg/ml was then placed on PA317 cells that were approximately 70% confluent. After 24 hours, fresh medium was added and the cells were grown until nearly confluent. The cells were trypsinized from the plate and diluted 1:100 into medium containing G418 (500 μg/ml). The cells were selected for 7 to 10 days until G418-reistant colonies had grown. The resistant colonies were trypsinized from the petri dishes using cloning rings. The colonies were expanded and frozen for

titering. Approximately 40 of each PA317/PAI-1 and PA317/VN G418-resistant colonies were frozen.

Titering Viral Supernatants

NIH 3T3 fibroblast cells were plated in a six well dish at 2.5 x 10^4 cells per well. Virus-containing supernatant from the producer cells was collected and spun at 3000 rpm for five minutes to remove any cells. The virus-containing supernatant was serially diluted into 2.5 mls DMEM to final dilutions of 10^{-2}, 10^{-4}, 10^{-5} and 10^{-6}. The media from the NIH 3T3 cells was removed and 1 ml of each diluted virus-containing supernatant was added to the wells. Polybrene, which aids in viral attachment to the cell membrane, was added to a final concentration of 8 μg/ml. The cells were incubated for 2 hours at 37°C then an additional 1 ml of DMEM was added. After 24 hours, the media was removed and 2 mls of DMEM with 0.5 mg/ml G418 (Geneticin, Gibco BRL) was added. After 7 to 10 days, the cells were stained with methylene blue (0.17% methylene blue in methanol) for 5 minutes. After incubation, the wells were rinsed with PBS until colonies were easily seen.

In Vitro Transduction

HUVECs (Clonetics) and the high titer PAI-1 and vitronectin producer cell lines (PA317/PAI-1 35 and PA317/VN 35, respectively) were grown to 70-80% confluent. The virus-containing medium from the producer cell lines was spun at 3000 rpm for 5 minutes to remove any cells. The cleared medium was added to the HUVECs with 8 μg/ml polybrene. After 4 to 12 hours, the medium was removed from the HUVECs and EGM medium was added. The HUVECs were grown for an additional 24 hours then G418 was added to a final concentration of 500 μg/ml. Once the HUVECs reached 90 to

121

100% confluent, the cells were split 1:10 and grown for 7 to 10 days under G418

selection.

DNA Isolation

DNA isolations were performed as described by Morgan *et al* (ref). Briefly, 1 x

10^6 cells were transferred to a microfuge tube and washed once with 1 ml of PBS. Cells

were resuspended in 100 µl of DNA isolation buffer (100 mM Tris pH 8.0, 100 mM

NaCl, 25 mM EDTA, 1% SDS, 250 µg/ml proteinase K). Samples were vortexed until a

clear lysate was produced and subsequently incubated at 60°C for 4-16 hours. The

samples were extracted with an equal volume of phenol/chloroform/isopentyl alcohol

then reextracted and ethanol precipitated. Samples were resuspended in 60 µl of water

and stored at –20°C until use.

PCR

PCR reactions were performed to confirm the insertion of vitronectin, PAI-1, the

neomycin gene and for the presence of envelope sequences. The following primers were

used in PCR reactions:

NEO 1	5' CAAGATGGATTGCACGCAGG 3'
NEO 5	5' CCCGCTCAGAAGAACTCGTC 3'
ENV 1	5' ACCTGGAGAGTCACCAACC 3'
ENV 3	5' TACTTTGGAGAGGTCGTAGC 3'
ssVN	5' ATGGCACCCCTGAGACCC 3'
seq #5	5' GGCTCTGACTCCTA 3'

seq #19   5' GATCAGCACCACAGACGC 3'

PAI-1 a.s.   5' TCAGGGTTCCATCATCTGG 3'

Reactions using the NEO primers, the ENV primers, the vitronectin primers or the PAI-1 primers generate a fragment of 790, 375, 1447 or 870 base pairs, respectively.

Direct Cell Lysis PCR

Direct cell lysis PCR was performed as described by Morgan *et al.* (*166*). Briefly, cells were trypsinized and washed once with PBS. For lysis and PCR, 20,000 cells were aliquoted into a tube containing 100 µl of the PCR mix (PCR buffer with varying concentrations of $MgCl_2$ (Idaho Technology), dNTPs (Idaho Technology), 0.5% Tween-20, 0.5% NP-40, 100 pmol of each primer, and 4.3 µg/ml proteinase K. The cells were incubated for 60 minutes at 56°C. The samples were heated at 95°C for 15 minutes to denature the proteinase K. The reactions were transferred to thin-walled PCR tubes with 0.5 units of *Taq* polymerase.

Cell Lysate Preparation

Lysates were prepared using a modified RIPA lysis buffer (150 mM sodium chloride, 50 mM Tris, pH7.4, 1 mM EDTA, 50 mM sodium fluoride, 10 mM sodium pyrophosphate, 1% Nonidet 40, 1% Triton X-100, 0.01% sodium dodecyl sulfate) with the addition of the protease inhibitors leupeptin (10 µg/ml, Sigma) and aprotinin (10 µg/ml, Sigma). Lysed cells were scraped from the culture flask and centrifuged at 15,000 rpm for 15 minutes at 4°C. The supernatant was collected and total protein quantitated using the BCA kit (Pierce).

Immunoblotting

Cell lysates were boiled in 2X SDS sample buffer for 5 minutes. The samples were separated by SDS-PAGE and transferred to nitrocellulose using a Semi-Dry Blotter (BioRad). Nitrocellulose and filter paper were equilibrated in transfer buffer (0.35 M glycine, 25 mM Tris, 20% methanol) before transfer. A current of 15 volts was applied for 30 minutes. The nitrocellulose membrane was incubated in 10% non-fat dry milk in PBS at room temperature for 60 minutes. The membrane was washed three times with PBS/Tween (0.05%). Primary antibody against vitronectin, PAI-1 and the integrins were diluted in PBS containing 2% non-fat dry milk for 60 minutes at room temperature. The following antibodies were used:

Bunny #12 (polyclonal anti-vitronectin)	1:2000
Anti-human PAI-1 (polyclonal, Tom Podor)	1:2500
Integrin α_2 subunit (polyclonal, Chemicon)	1:100
Integrin α_V subunit (monoclonal, Biogenesis)	1:1000
Integrin α_5 subunit (polyclonal, Chemicon)	1:100
Integrin β_1 subunit (monoclonal, Transduction Laboratories)	1:2500
Integrin β_3 subunit (monoclonal, Transduction Laboratories)	1:250

The membrane was washed and incubated in PBS containing 2% non-fat dried milk and 20 µl of the appropriate secondary antibody for 60 minutes at room temperature. After washing the membrane, any protein bands were visualized using developing solution (30 ml PBS, 50 mg/ml 4-chloro-napthol, 12 µl 30% H_2O_2).

Shear Stress Analysis

All apparatus used in the flow studies was generously loaned from Dr. Judy Cezeaux (Department of Mechanical and Aerospace Engineering and Engineering Science, University of Tennessee). The apparatus consists of two main parts, the flow chamber and the flow circuit. The flow chamber used is based on the well-defined parallel plate assembly. The top plate was constructed of circular polycarbonate with a rectangular flow channel engraved in the middle. The bottom plate was a circular glass slide. The plates were held together with a threaded aluminum collar. The shear stress (τ) on the glass slide is related to the flow rate (Q) through the flow chamber by the following equation:

$$\tau = 6\mu Q/bd^2$$

where μ is the viscosity, Q is the volumetric flow rate in ml/sec, b is the width of the flow channel (5.65 cm) and d is the height of the flow channel. The viscosity of the buffer (PBS with added dextran) was determined to be 0.033 g·cm/s using a viscometer (Brookfield DV-II$^+$, Sloughton, MA). The height of the flow channel was determined experimentally before each experiment by measuring the pressure drop across the flow channel.

Before assembly of the flow chamber, the glass slide was coated with human plasma fibronectin (Gibco BRL) to a final concentration of 10µg/cm^2. Glass slides were incubated with fibronectin for 2 hours at 37° C before they were rinsed with distilled water and stored at 4° C until use. After the flow chamber was assembled, the chamber was placed in a circulating flow circuit on the stage of an inverted phase contrast microscope (Axiovert 35, Carl Zeiss Inc.). The flow circuit consisted of an upper and

lower reservoir. The buffer was kept constantly moving between the reservoirs through the flow chamber by a peristaltic pump (Masterflex Model 7553-50, Cole-Parmer). The flow chamber could be monitored using the CCD camera attached to the microscope (Model CCD72S, Dage-MTI) and a monitor (Model VM-1220U, Hitachi). Images were captured over a two hour timecourse using a time-lapse video recorder (Model TL1800, Gyyr).

Cells to be analyzed were trypsinized and added to the flow chamber through a port. The cells were allowed to adhere to the glass slide for one hour. After one hour, flow was initiated and lasted for 2 hours. All cells were analyzed at a shear stress of 90 dynes/cm^2. Each cell line was evaluated three times.

Results

Generation of Transduced Endothelial Cells

Retroviral vectors can be used to generate transduced human umbilical vein endothelial cells. PAI-1 and vitronectin full-length cDNA containing their native signal sequences were subcloned into the retroviral vector pLXSN (Figures 3-4 and 3-5). The resulting constructs were named pLXSN/ssPAI-1 and pLXSN/ssVN. Both constructs were sequenced to ensure that the inserted DNA sequence was correct. The plasmids were transfected into the GP&E cell line, which contains the gag, polymerase and envelope genes. Once the plasmid is introduced into the GP&E cells, the cells are now able to make competent retrovirus (Figure 3-6). The retrovirus made in the GP&E cells contain either PAI-1 or vitronectin and were used to infect a producer cell line, PA317.
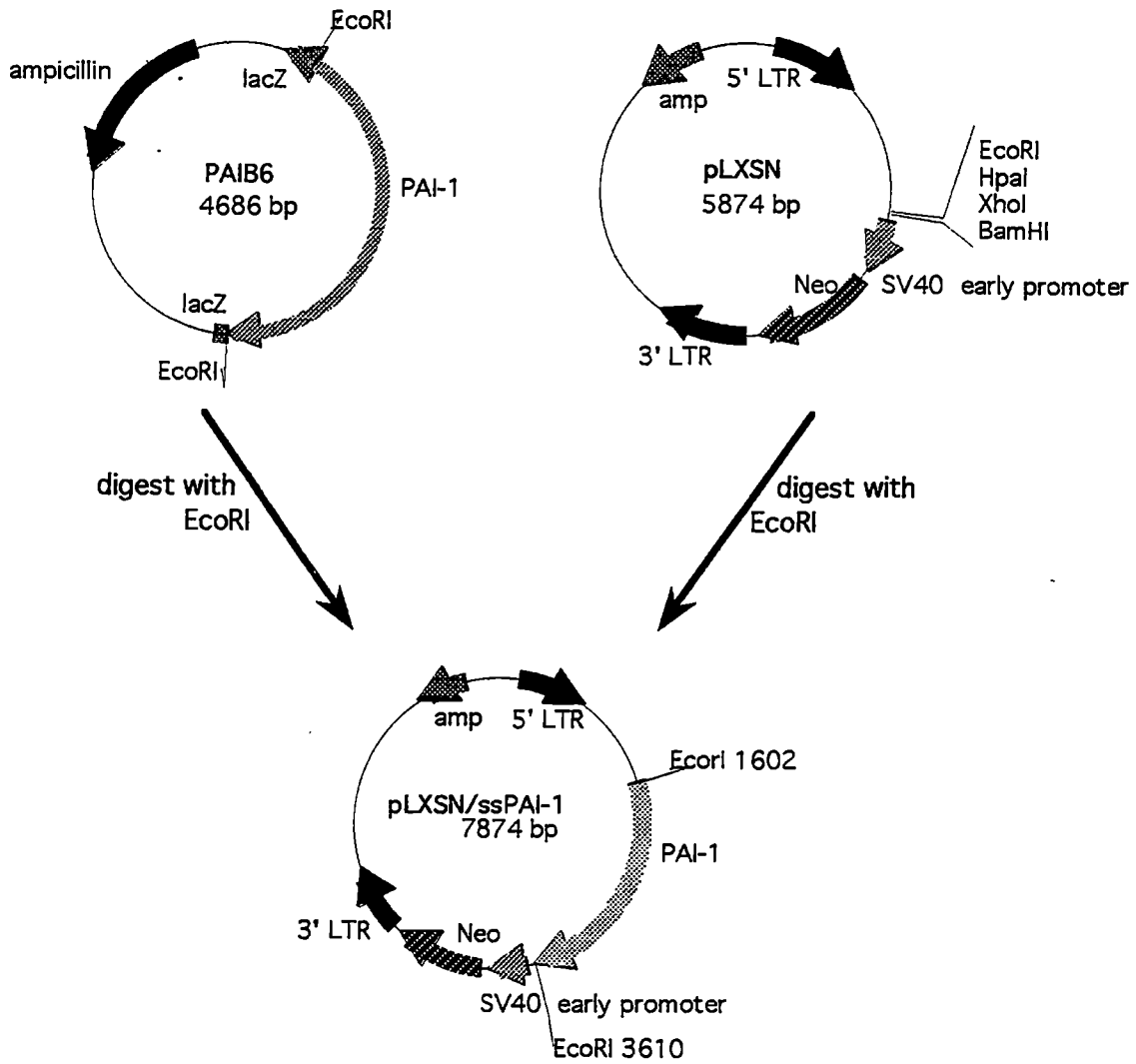
Figure 3-4: Construction of the Retroviral Vector pLXSN/ssPAI-1. The retroviral vector pLXSN was digested with EcorI and dephosphorylated. A plasmid, PAIB6, containing the full-length coding sequence for PAI-1 including the signal sequence was digested with EcoRI. The fragment was gel purified and ligated into the dephosphorylated pLXSN vector. The resulting plasmid was named pLXSN/ssPAI-1
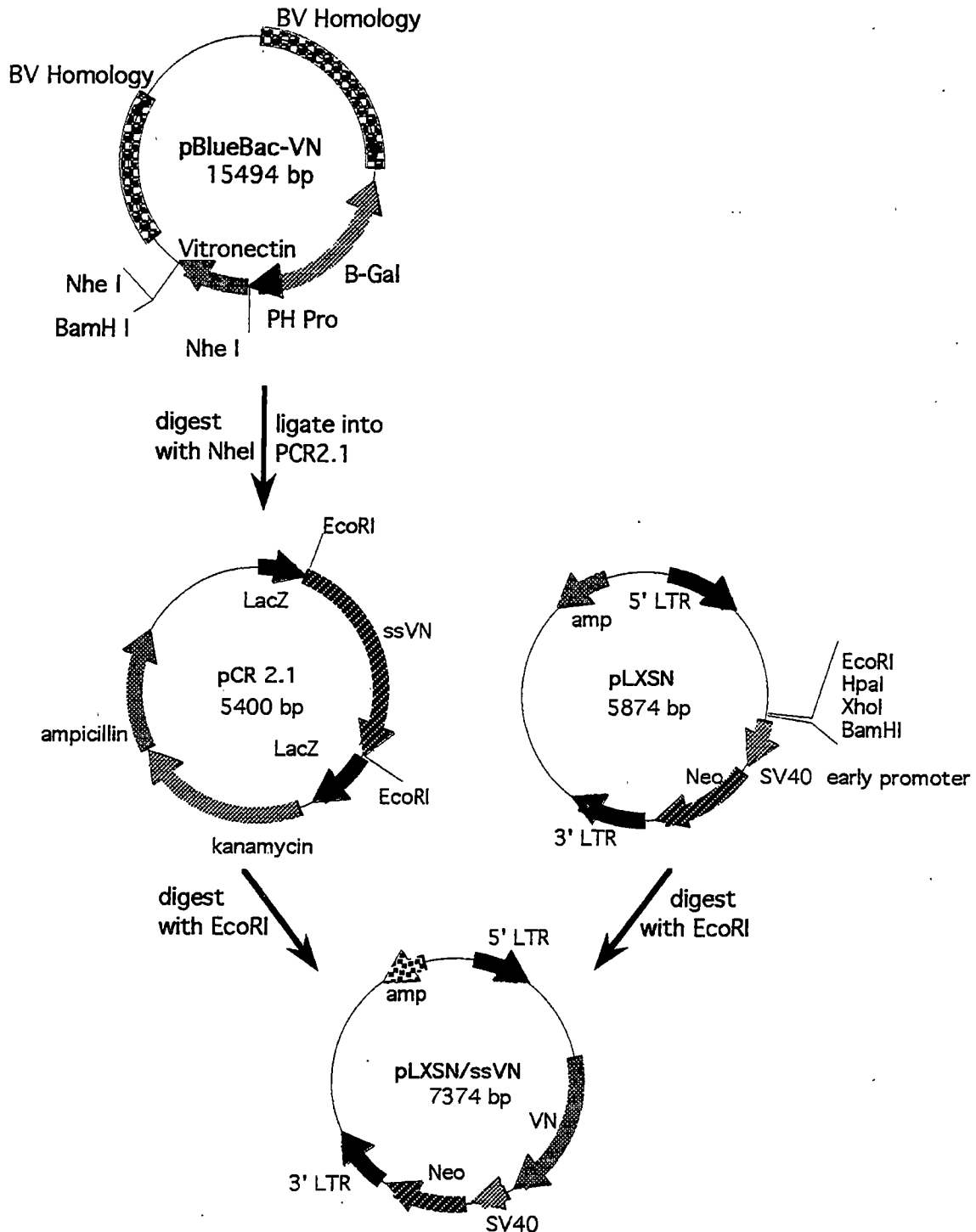
Figure 3-5: Construction of the Retroviral Vector pLXSN/ssVN. The plasmid pBlueBac/VN contains the entire vitronectin coding sequence, including the signal sequence for secretion. The full-length vitronectin coding sequence was excised with NheI. The fragment was gel purified, the ends were blunted and the fragment ligated into the PCR2.1 vector. Vitronectin was excised from PCR2.1/ssVN with EcoRI and ligated into the pLXSN vector digested with EcoRI. The resulting plasmid was named pLXSN/ssVN.
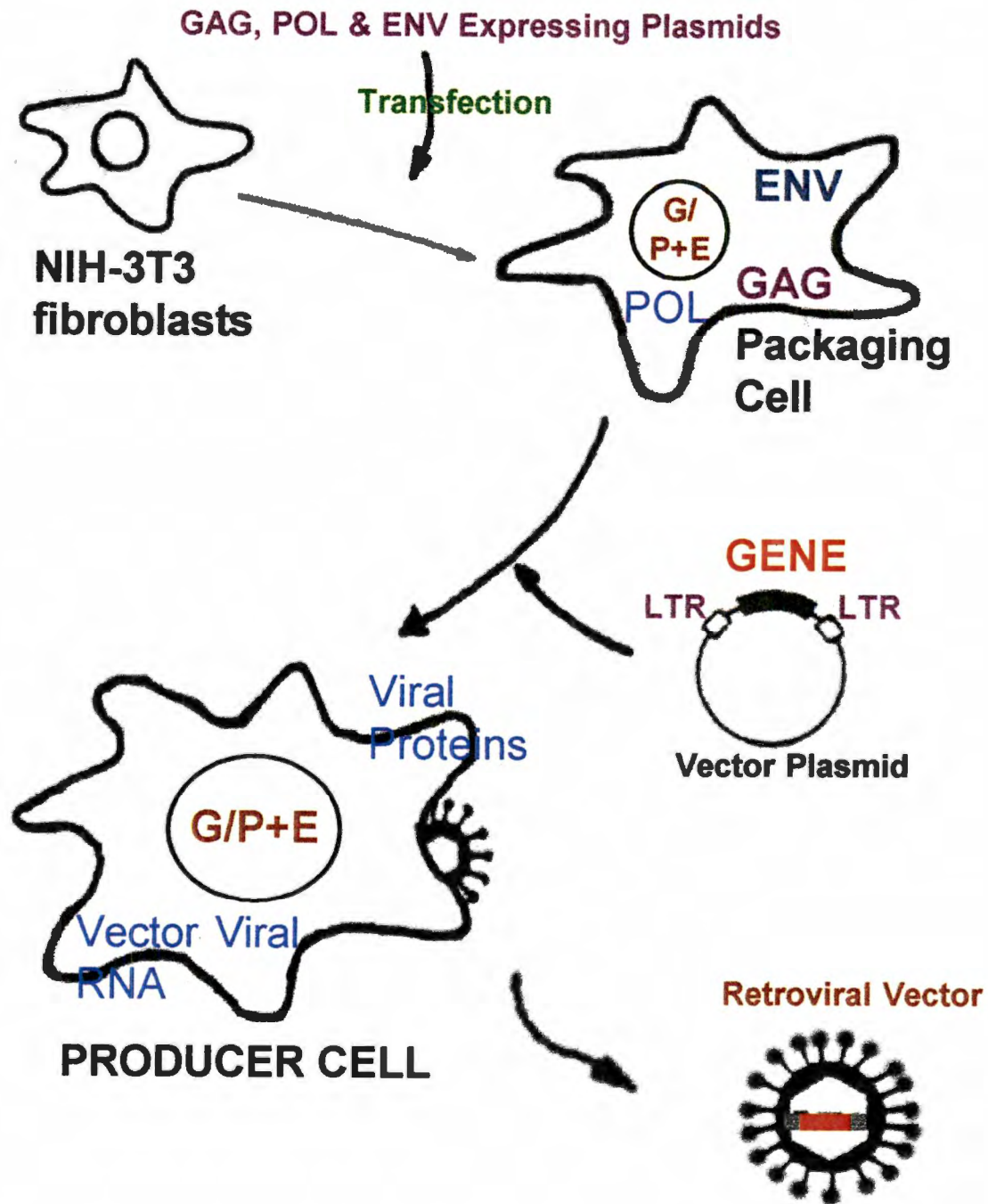
Figure 3-6: Generation of Competent Retroviral Vectors. NIH 3T3 cells were transfected with a plasmid containing gag, pol and env genes to create the GP&E cell line. The GP&E cells can be transfected with a gene on a plasmid containing all the additional information needed to produce competent vectors. The transfected GP&E cells are now called the producer cells. The retroviral vectors produced by the cells are competent to infect murine cells.

The PA317 cells produce a retrovirus that is amphotropic, or able to infect primate and human cells. The PA317 cell line contains deletions of the packaging signal, the 3' LTR and a portion of the 5' LTR. In order to create wild-type virus from this cell line, two recombination events would need to occur between the helper and the vector genomes (167). The likelihood of two recombination events taking place is low, but it is possible.

Individual PA317 colonies were screened for high titer viral production. One high titer colony was found for both PAI-1 and vitronectin. Both had titers that were approximately 10^6 virions per milliliter. These cells, PA317/PAI-1 and PA317/VN, were used to transduce HUVEC. For transduction, the cleared medium from the PA317/PAI-1 or PA317/VN was applied to HUVEC and infection was allowed to occur for 4 to 12 hours. A mock transduction was also performed in which medium from the PA317 cells was applied to HUVECs. As the final control, the plasmid pLXSN alone was transduced into the HUVEC.

Screening Transduced Endothelial Cells by PCR

The polymerase chain reaction (PCR) was used to confirm the insertion of the PAI-1 and vitronectin genes into the HUVECs. The primers used for vitronectin start at the beginning of the signal sequence and end with the final residues at the stop codon, resulting in the generation of a fragment of 1447 base pairs (Figure 3-7a). For these PCR reactions, DNA was isolated from cells and subsequently used in the PCR. As shown in Figure 3-7, bands corresponding to the anticipated size of vitronectin are seen with pLXSN/VN, PA317, PA317/VN and HUVEC/VN. The presence of vitronectin in the PA317 genome is not surprising. PA317 cells are derived from NIH3T3 fibroblast cells, which contain within them the coding sequence for vitronectin. A vitronectin band is not

130
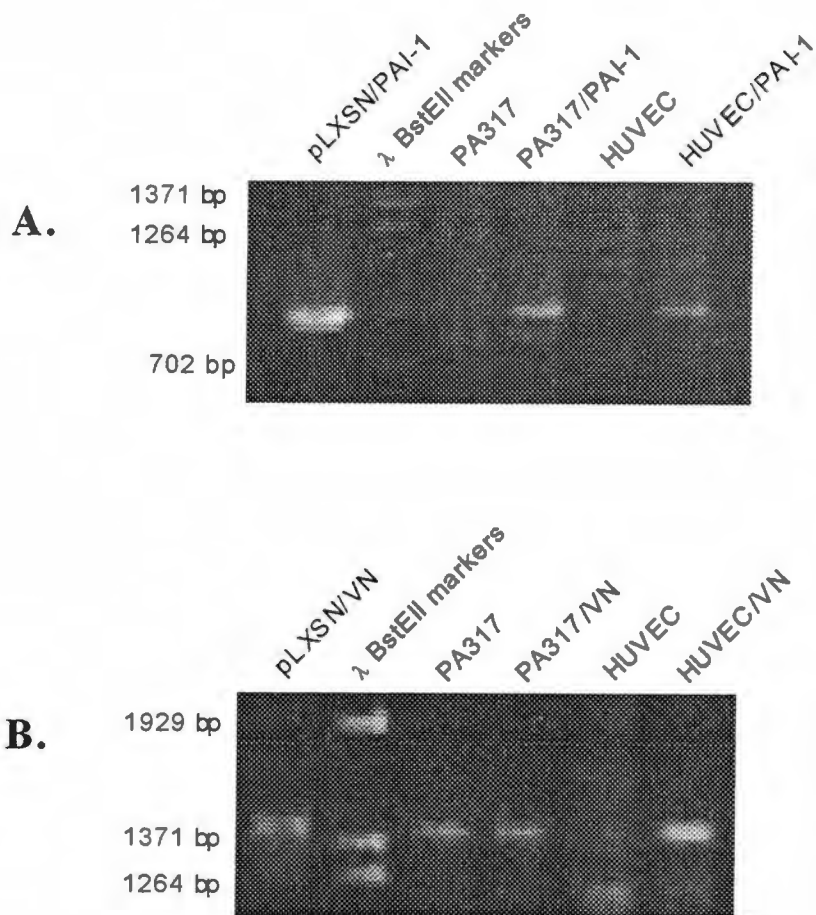
Figure 3-7: PCR Analysis of Transduced Endothelial Cells. The presence of either PAI-1 or vitronectin in the producer and transduced cells was examined by PCR. The pLXSN/PAI-1 and pLXSN/VN plasmids were included as controls for the PCR reaction. The results of the PAI-1 direct cell lysis PCR are shown in panel A. A band corresponding to the 870 base pair PAI-1 is visible in the pLXSN/PAI-1, PA317/PAI-1 and HUVEC/PAI-1 lanes. The gel in panel B shows the results of the vitronectin PCR. The 1447 base pair vitronectin band appears in the pLXSN/VN, PA317, PA317/VN and HUVEC/VN lanes.

seen in the naïve HUVEC, however. Since this PCR was performed on isolated DNA, the amount of DNA added to the PCR reaction was approximately quantitated using an agarose gel with varying concentrations of standards. This method is not very accurate, so the results of the PCR are not qunatitative. An 870 base pair piece of PAI-1 was generated using an internal PAI-1 primer with the other ending with the stop codon (Figure 3-7b). Direct cell lysis PCR was used with the PAI-1 primers. The 870 base pair PAI-1 band appears when using pLXSN/PAI-1, PA317/PAI-1 and HUVEC/PAI-1. Thus, it appears as if the HUVECs have been successfully transduced with either vitronectin or PAI-1.

When the integration event takes place with the gene of interest, the selectable marker, the neomycin-resistance gene (neo), also becomes integrated. The presence of the neo selectable marker was also confirmed in the cells transduced with PAI-1 or vitronectin. Direct cell lysis was used on the HUVEC, HUVEC/PAI-1 and HUVEC/VN cells (Figure 3-8a). The 790 base pair band corresponds to the neo gene. The gene is seen in the plasmid pLXSN/PAI-1 and in the cell lines HUVEC/PAI-1 and HUVEC/VN. There is no band present in the naïve HUVEC cells or in the culture medium. Therefore, the neo gene is from the genome of the HUVECs. The presence of the neo gene and of either vitronectin or PAI-1 means the HUVECs have been successfully transduced.

PCR was also employed to find if there were envelope sequences within the transduced endothelial cells. The presence of envelope sequences would indicate that recombination events had taken place and wild-type virus could be produced. This is an important consideration for clinical applications. Direct cell lysis was employed to investigate the presence of any envelope sequence (Figure 3-8b). As is shown in figure
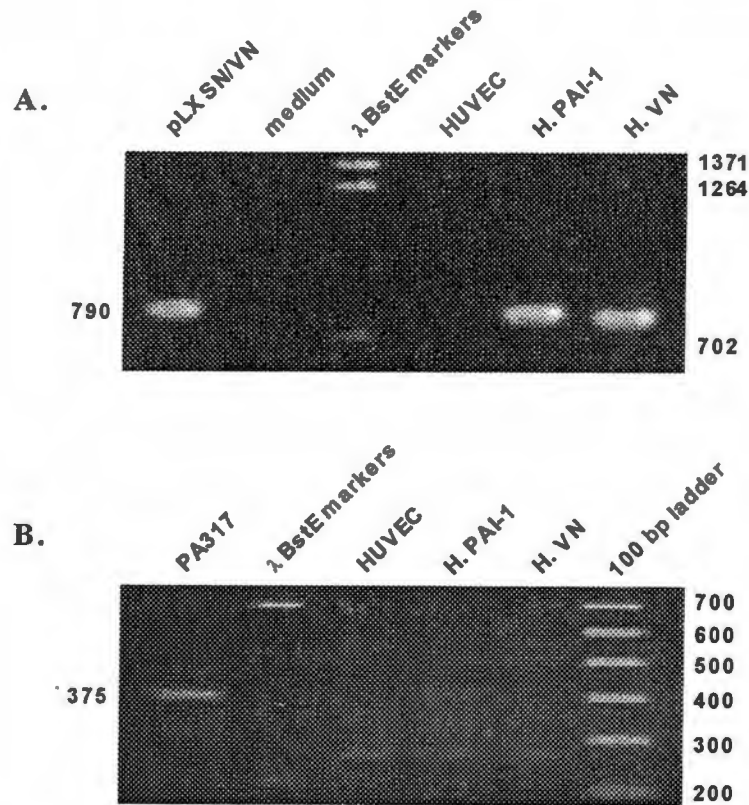
Figure 3-8: Direct Cell Lysis PCR for Neomycin and Envelope Sequences on Naïve and Transduced Cells. The presence of the neomycin gene further indicates that HUVEC have been successfully transduced with the retrovirus, as seen in panel A. A 790 base pair band has been amplified in transduced HUVEC cells and in the initial plasmid pLXSN. No band corresponding to neomycin is seen in naïve HUVEC or in the growth medium. Panel B represents the PCR using envelope primers to determine whether any envelope sequences have been inserted into the HUVEC genome. The envelope sequences are contained in the PA317 cell line, which serves as the positive control. A 375 base pair envelope band is seen in the PA317 cells and a faint band is also seen in the transduced HUVEC/PAI-1 cells. There is no band in either the naïve HUVEC or HUVEC/VN cells.

3-8b, there are no envelope sequences present in the HUVEC/VN cells or the naïve

HUVEC cells. The PA317 cell line serves as the positive control, since it packages

virions and therefore contains the envelope sequence. There is, however, a faint band

seen in the HUVEC/PAI-1 cells. It is possible, therefore, that the HUVEC/PAI-1 cells

are producing wild-type virus.

Transduced Endothelial Cells Secrete and Over-express Either Vitronectin or PAI-1

Transduced endothelial cells produce either vitronectin or PAI-1 at a higher level

than naïve endothelial cells. PCR analysis of the two transduced isolates indicates that

the transduction was successful. The ability of the transduced cells to produce protein

constituatively and at a higher level than naïve cells was investigated. Western blots

were performed to confirm the expression of either PAI-1 or vitronectin from transduced

cells (Figure 3-9). Western blotting confirms that the HUVEC/PAI-1 cells express PAI-1

while none is visible in the naïve HUVEC. The same is true with vitronectin. A

quantitative Western was performed to determine the amount of either vitronectin or PAI-

1 secreted by the transduced HUVECs. Standard curves for both PAI-1 and vitronectin

were made with purified proteins. It was determined from the quantitative Westerns that

neither PAI-1 nor vitronectin was expressed at a detectable level in naïve HUVECs. The

transduced cells did express either PAI-1 or vitronectin at a detectable level, that being 10

and 12 μg/ml, respectively.

Expression of Integrins in Transduced Endothelial Cells

The integrins of the transduced endothelial cells are intact. Three alpha and two

beta subunit antibodies were used in Westerns to determine whether or not the integrin

subunits were intact. Total protein was quantified from whole cell lysates of HUVEC,
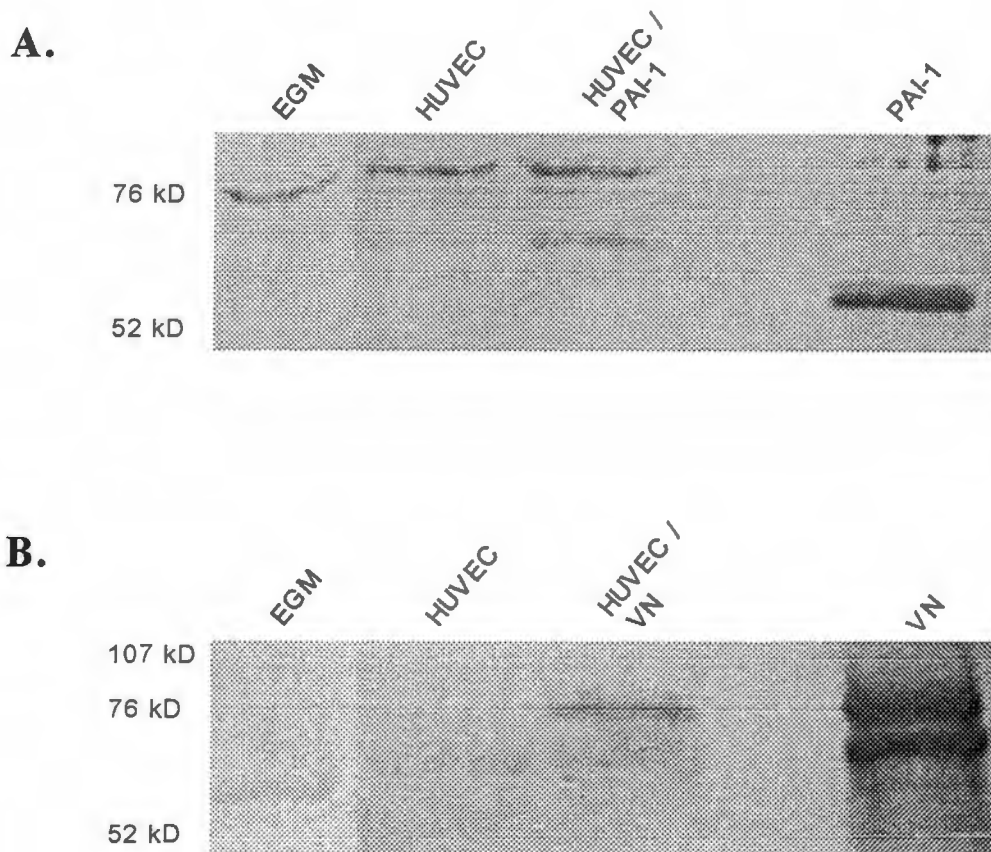
Figure 3-9: Immunoblots for Vitronectin and PAI-1 Production in Transduced Endothelial Cells. Medium from naïve and transduced HUVEC cell lines was removed for analysis of the presence of secreted PAI-1 or vitronectin. Medium from the bottle (EGM) was used as control to test for any background vitronectin or PAI-1 contributed from the added serum. Panel A shows the PAI-1 western probed with a polyclonal antibody. A faint band is present in the HUVEC medium, with a more prominent PAI-1 band in the HUVEC/PAI-1 lane. The PAI-1 used as a positive control is made in bacteria, therefore it is non-glycosylated and has a lower molecular weight than the PAI-1 secreted from the endothelial cells. The vitronectin western is shown in panel B. The characteristic 72 kDa band of vitronectin is absent in the medium and in the HUVEC cells. The vitronectin band appears in the transduced endothelial cells. Plasma vitronectin is the control.

HUVEC/PAI-1 and HUVEC/VN cell lines. Immunoblots show the 165 kDA band of the α_2 integrin subunit in all cell lines (Figure 3-10a). The 135 kDA band of the α_5 integrin subunit was also present in all cell lines (Figure 3-10b). Finally, the 125 kDA band associated with the α_v integrin subunit is clearly seen in all samples (Figure 3-10c). The three alpha integrin subunits were all intact.

Immunoblots for the beta integrin subunits β_1 and β_3 were also performed (Figure 3-11). The 130 kDA band of the β_1 subunit was visible in the HUVEC, HUVEC/PAI-1 and HUVEC/VN cells. The transduced cells all expressed an intact β_1 subunit. A single band for the β_3 integrin subunit of 115 kDa is also present in all cell lines probed, including the transduced cells.

It has been proposed that continuous selection of the transduced endothelial cells with G418 can lead to the lack of intact β integrin subunits. Transduced cell where either maintained in growth medium lacking or containing G418 for 10 days. Whole cell lysates were then made from the cells. Immunoblotting was performed to determine whether constant selection caused changes in the β_1 or β_3 integrin subunits. The results, shown in Figure 3-12, reveal that continuous selection of the cells does not affect the β integrin subunit. The 130 and 115 kDa bands of the β_1 and β_3 subunits, respectively, are clearly still present in the selected cells.

Transduction of Endothelial Cells with an Empty Retroviral Vector

Human umbilical vein endothelial cells were transduced with the retroviral vector, pLXSN, lacking the addition of any exogenous gene. A similar cell line had been

136
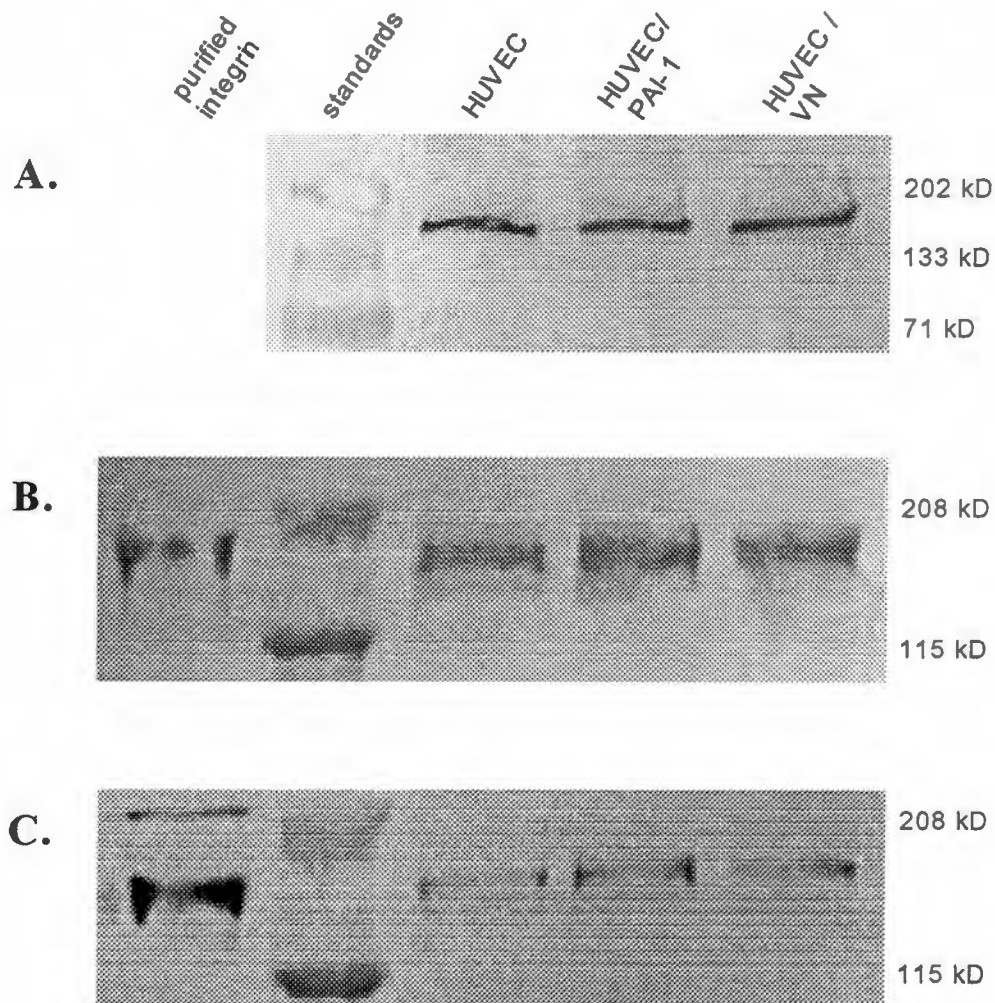
Figure 3-10: Immunoblot Analysis of Endothelial Cell Lysates for the Detection of Alpha Integrin Subunits. Monoclonal antibodies to α_5 and α_v and polyclonal antibodies to α_2 were used for detection of the 135, 125 and 165 kDa integrin subunits, respectively. Panel A shows the α_2 integrin subunits are intact. The α_5 subunits are shown in panel B. The integrin subunits are present in all samples. Panel C is the Western for the α_v subunit. The integrin standard is commercially available (Chemicon) purified integrin.

A.

purified integrin | standards | HUVEC | HUVEC/ PAI-1 | HUVEC / VN

208 kD
115 kD
79 kD

B.

208 kD
15 kD
79 kD
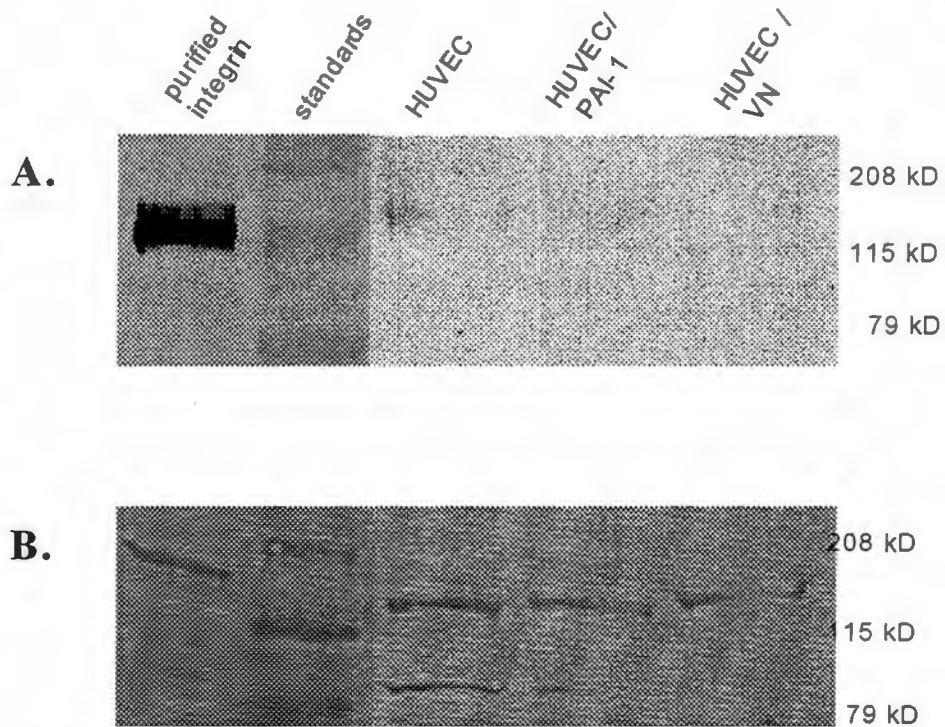
Figure 3-11: Immunoblot Analysis of the Beta Integrins. Endothelial cell lysates were examined for the presence of the β_1 or the β_3 integrin subunits. All cell lines examined showed the two β integrin subunits were intact. Panel A is the immunoblot with the β_1 monoclonal antibody while panel B is the β_3 monoclonal antibody. Purified integrin used as the positive control was from a commercial supplier (Chemicon).
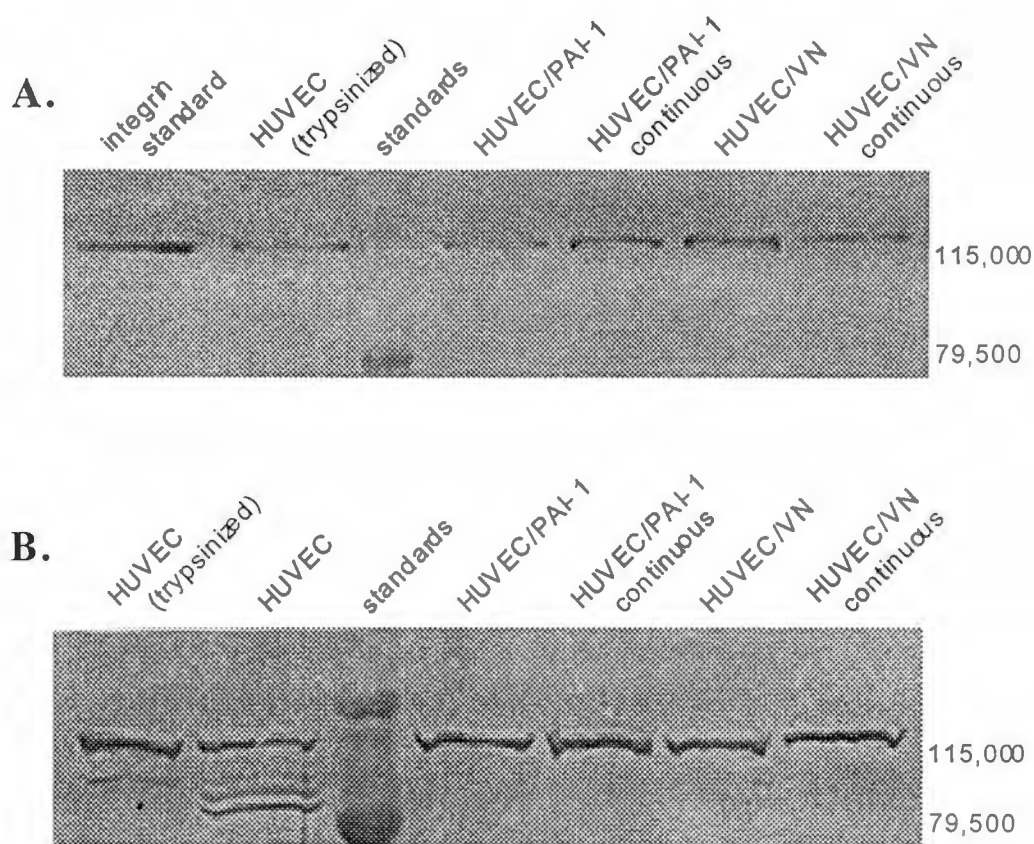
Figure 3-12: Expression of Beta Integrin Subunits in Continuous versus Non-continuous Selection. Cells were grown either continuously with the antibiotic G418 or under no selection for 10 days before the cells were lysed and scraped from the flask. The whole cell lysates were used for western blotting. A total of 15 ug total protein was loaded on the gel. Panel A depicts the effects of selection on the β_1 integrin subunit. Trypsinized cells were included to deduce the effects of trypsin on the epitope for the monoclonal antibody. Panel B shows the β_3 integrin subunit integrity with non-selected and continuously selected cells. Once again, the trypsinized cells were included to determine if the monoclonal antibody's epitope was present after trypsinization of the cells from the tissue culture flask.

generated by Sackman and degradation of the β-integrins had been observed in these cells (*152*). Therefore, this cell line was generated to act as a control.

Direct cell lysis PCR was performed on the cells transduced with the retroviral vector alone. The presence of the neomycin phosphotransferase gene was assessed in the HUVEC/pLXSN cells (Figure 3-13). A 790 base pair fragment can be seen in both the positive control, plasmid pLXSN/PAI-1, and the HUVEC/pLXSN cells. The presence of the neo gene in the HUVEC/pLXSN cells confirms these cells have been successfully transduced. The HUVEC/pLXSN cells were also tested for the presence of any envelope sequences. As shown in Figure 3-13, envelope sequences can easily be seen in the control PA317 DNA, however, no corresponding envelope sequences are seen in the cells transduced with vector alone. This suggests that the HUVEC/pLXSN cells are not producing any competent helper viruses.

Expression of Integrins in Endothelial Cells Transduced with an Empty Retroviral Vector

HUVEC/pLXSN cells were grown to approximately 70% confluence. This was more challanging than it seems. The endothelial cells transduced with the vector alone grew much more slowly than those transduced with either PAI-1 or vitronectin. Another way these cells differed was in their growth pattern. As the cells approached 80 to 90% confluent, a large number of them would die. Therefore, these cells were harvested to make lysate at a lower density than the other cell lines, which were harvested at approximately 90% confluent. Since these cells were so much more difficult to grow, these integrin western blots were done independently of the other transduced cells.
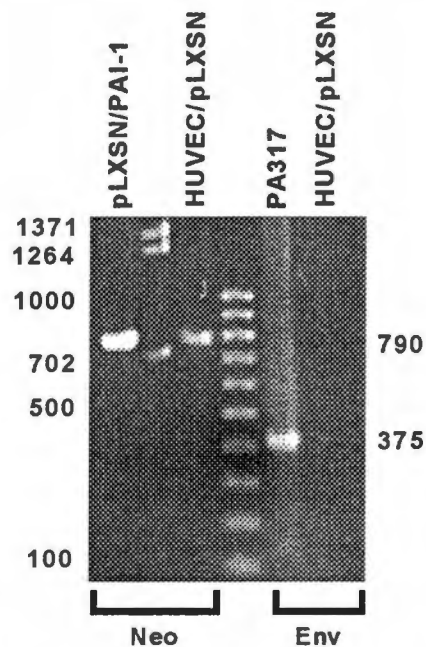
Figure 3-13: PCR Analysis of Endothelial Cells Transduced with Vector. Direct cell lysis PCR was performed on the HUVEC cells transduced with the vector alone, pLXSN. The presence of the neomycin phosphotransferase and envelope sequences was determined by PCR (see Materials and Methods for PCR primer sequence). The PCR reactions carried out in lanes 1 and 3 used the neo primers. Lane 1 is the plasmid pLXSN/PAI-1, which was used as a positive control for the neomycin phosphotransferase gene. Lane 2 contains the λ BstE III markers. Lane 3 is the HUVEC/pLXSN cells. Lanes 5 and 6 are the results of a PCR reaction using envelope sequences for primers. Lane 4 is 100 kB ladder markers. Lane 5 contains PA317 DNA, which contains the envelope sequence within its genome. Lane 6 is the HUVEC/pLXSN cells.

141

After the HUVEC/pLXSN cells were lysed, the total protein was quantitated.

Equal concentrations of cell lysates were run on SDS-PAGE gels for Western blotting

with the five integrin antibodies. As shown in Figure 3-14a, the HUVEC cells transduced

with vector alone still express intact α_2, α_5 and α_v integrins. The expression of the β_1 and

β_3 integrins was also tested using the appropriate integrin antibodies (Figure 3-14b). The

HUVEC/pLXSN cells expressed intact β_1 and β_3 integrins, just as the endothelial cells

transduced with PAI-1 or vitronectin.

Shear Stress Analysis of Transduced and Non-transduced Endothelial Cells

Endothelial cells genetically modified using retroviral vectors appear impaired in

their ability to adhere to and spread on synthetic vascular grafts when placed *in vivo*

under physiological shear stress. In order to evaluate the adhesive ability of both the

transduced and non-transduced endothelial cells, the cells were tested for their ability to

withstand shear stress. A shear stress of 90 dynes/cm^2 was chosen as it closely

approximates peak aortic shear stress (*168, 169*). Naïve HUVEC, "mock" transduced

HUVEC, and HUVEC transduced with PAI-1, vitronectin and the empty vector pLXSN

were all analyzed for the ability to adhere to fibronectin at a shear stress of 90 dynes/cm^2.

The data is expressed as the percent of cells detached at various time points (Figure 3-

15). The data was analyzed to determine if there was any significant difference between

the cell lines. After analysis it was determined there was no statistically significant

difference between any of the cell lines.
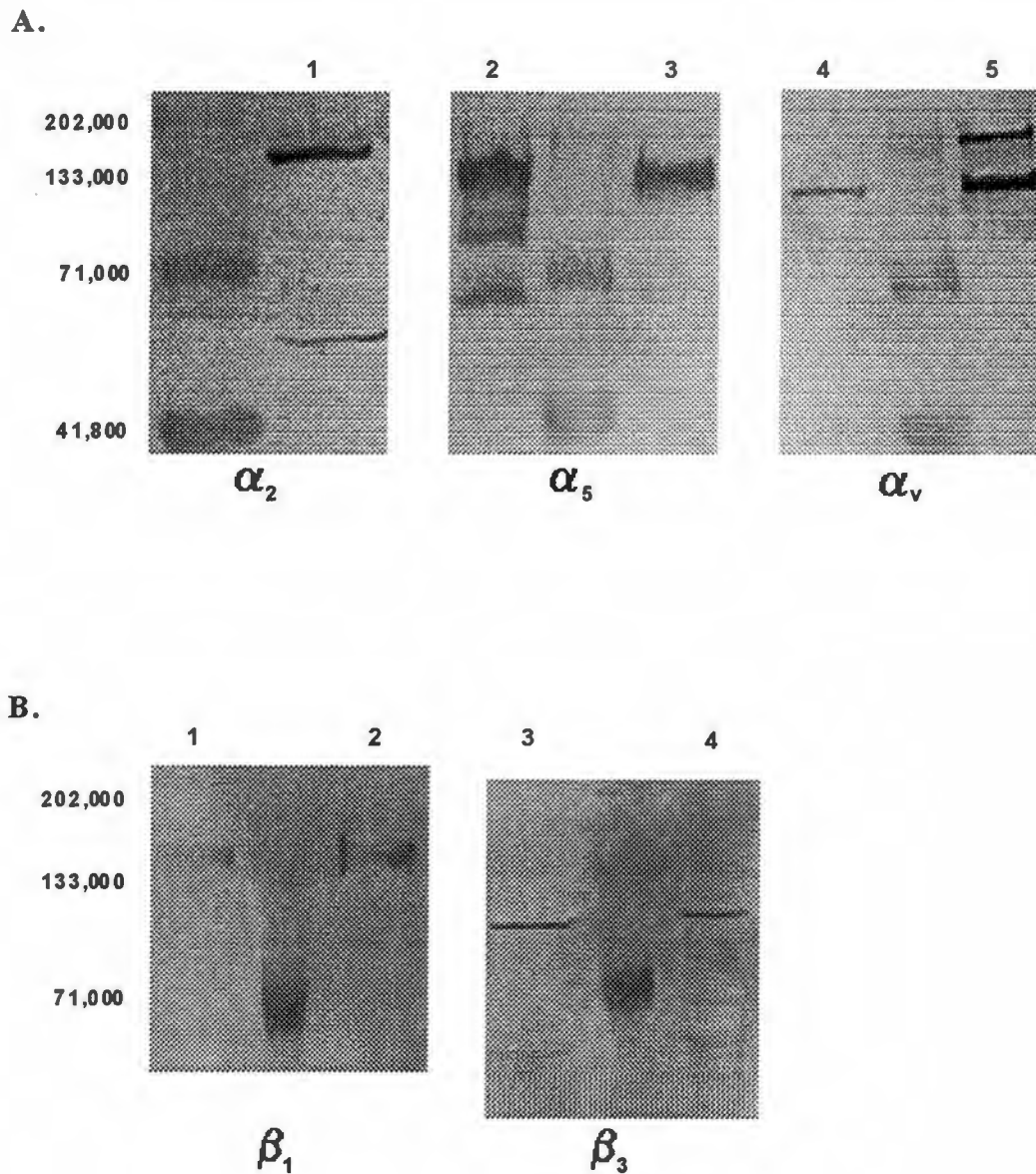
Figure 3-14: Immunoblot Analysis of Integrin Expression in HUVEC/pLXSN Cells.
The amount of total protein was loaded was 10 µg and 15 µg for the alpha integrins and
the beta integrins. Panel A shows the expression of the alpha integrins. Lane 1 contains
the HUVEC/pLXSN lysate. Lane 2 is a positive control, the integrin $\alpha_5\beta_1$. Lanes 3 and
4 are the HUVEC/pLXSN lysate. Lane 5 is a positive control, the integrin $\alpha_v\beta_3$. Panel B
respresents the expression of the β–integrins. Lanes 1 and 3 are the HUVEC/pLXSN
lysate. Lane 2 is an integrin positive control, $\alpha_5\beta_1$. Lane 4 is a commercial cell lysate
control for β_3 expression.
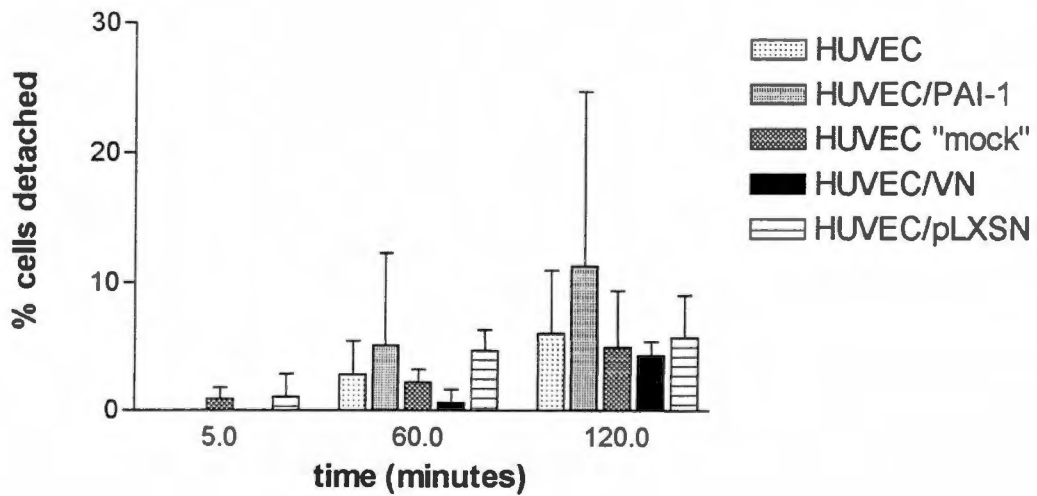
Figure 3-15: Ability of Transduced Cells to Withstand Shear Stress. Each of the five different cell lines was examined for their ability to withstand a shear stress of 90 dynes/cm^2. Cells were allowed to incubate for one hour before flow was started. The number of cells present at the start of flow was recorded, as well as the number at 5, 60 and 120 minutes after the initiation of flow. The percent of cells detached at the various times could then be calculated. The error bars represent standard deviation.

Discussion

Gene therapy, the introduction of nucleic acids as therapeutic molecules, has many potential applications (*170, 171*). Endothelial cells are a popular target for gene therapy applications. The vascular endothelium is thought to play a major role in the regulation of intravascular coagulation and fibrinolysis (*172*). Endothelial cells synthesize a variety of pro-coagulant and anti-coagulant molecules, including tissue plasminogen activator (tPA), PAI-1 and heparin sulfates. Endothelial cells also express surface binding sites for proteins involved in coagulation and fibrinolysis. Therefore, endothelial cells play a role in both coagulation and fibrinolysis. This is why endothelial cells are an attractive target for gene therapy.

The retroviral-mediated gene transfer of proteins involved in cellular adhesion and migration, namely PAI-1 and vitronectin, was undertaken in this dissertation project in an effort to determine if these proteins could be useful target for gene therapy. Vitronectin and PAI-1 have both been implicated in regulating cellular contacts with the extracellular matrix. These cellular contacts maintain the cell in an adhesive state or, with the loss of these contacts, allow for migration. The goal of this research was to successfully introduce PAI-1 and vitronectin genes into human endothelial cells in order to assess the adhesive phenotype of the cells.

Can PAI-1 and Vitronectin be Successfully Introduced into Endothelial Cells by Retroviral-Mediated Gene Transfer?

Retroviruses are extremely competent at infecting cells that are actively dividing (*145, 173*). Since the DNA introduced into the cell by the retrovirus becomes integrated into the host cell's DNA, the introduced sequences can theoretically be maintained over

145

the lifespan of the cell. Polymerase chain reaction was used to screen endothelial cells for integration of the gene of interest. HUVEC transduced with PAI-1, vitronectin or the empty retroviral vector were tested for the incorporation of the neomycin phosphotransferase gene, the envelope gene and either PAI-1 or vitronectin. Results of the PCR experiments indicated the three different cell lines had been successfully transduced.

Do Transduced Endothelial Cells Over-express the Introduced Gene?

Successful introduction of PAI-1 and vitronectin has been demonstrated by PCR. It remained to be seen whether the endothelial cells would actually express the proteins into the culture medium. The HUVEC cells were grown in medium containing only 1% fetal bovine serum. This reduced the amount of exogenous PAI-1 and vitronectin. The spent medium from the HUVEC/VN an HUVEC/PAI-1 cells was assayed by Western blotting for the presence of either vitronectin or PAI-1. A medium only control from naïve cells was also included to determine if there was any vitronectin or PAI-1 contribution from the serum in the medium. The results of the Western blot indicated that vitronectin and PAI-1 were being secreted into the medium by the HUVEC/VN and HUVEC/PAI-1 cells, respectively. There were no bands corresponding to either vitronectin or PAI-1 in the naïve cell medium.

In order to quantify the amount of vitronectin and PAI-1 secreted into the medium, a quantitative Western was performed. Any amount of vitronectin or PAI-1 in the medium of naïve endothelial cells was not detectable. Vitronectin was secreted into the medium at a concentration of 12 µg/ml. The PAI-1 transduced cells secreted PAI-1 into the medium at a concentration of 10 µg/ml. The demonstration of secretion of

vitronectin and PAI-1 at levels significantly greater than naïve cells clearly indicates that the endothelial cells have been successfully transduced.

Integrin Expression in Transduced Cells

One proposed explanation for the decreased adherence of retrovirally transduced endothelial cells is that integrin subunit expression is altered. In order to test this theory and determine if vitronectin or PAI-1 may modify the expression of integrin subunits, the expression of several integrin subunits in the transduced and naïve endothelial cells was investigated. The expression of the α_2, α_5 and α_v subunits in the endothelial cells transduced with PAI-1, vitronectin or the vector pLXSN was not altered. The same was true of the β_1 and β_3 integrin subunits. This result is in marked disagreement with a previous report. Sackman *et al.* transduced human umbilical vein endothelial cells and canine vascular endothelial cells with two different empty retroviral vectors and one retroviral vector containing tPA (*152*). The expression of the α_2, α_5 and α_v integrin subunits was not altered, however, the expression of the beta subunits was altered. Both canine and human endothelial cells transduced with empty viral vectors and one containing tPA no longer expressed a β_1 subunit. The β_3 integrin subunit in the same cells was shown to be degraded.

The observation that HUVEC cells transduced with an empty retroviral vector did not alter the expression of the integrin subunits tested was surprising. The HUVEC/pLXSN cells had to be generated more than once. During the selection process, the cells were slower to recover than the cells transduced with PAI-1 or vitronectin. The HUVEC/pLXSN cells also had an altered appearance. The cells transduced with PAI-1 or vitronectin were not as well defined as non-transduced cells. In other words, they

were generally more spherically shaped than non-transduced cells. The cells transduced with pLXSN were even more altered. Rather than spreading out on the surface of the tissue culture flask, the cells often appeared to be curling around the edges, as if they were not adhering to the flask well. Another interesting observation with the HUVEC/pLXSN cells was as they approached 70 to 80% confluent, number of attached cells would drop and cells could be seen floating in the medium. These observations seemed to indicate that there was a difference in the adhesive ability of the endothelial cells transduced with the empty retroviral vector pLXSN.

What could be the cause of this discrepancy? The HUVEC cells used in these experiments were not the same. Sackman received cells from the ATCC whereas cells for the work in this dissertation were purchased from Clonetics. More importantly, the cells received from Clonetics were primary cultures from a single donor. The ATCC endothelial cells come with no such information. It may be possible that certain genotypes of cells are more susceptible to disruption by the introduction of genes by retroviral vectors than others. Finally, perhaps other integrin subunits are disrupted, at least in the HUVEC/pLXSN cells, which seemed to exhibit a decreased ability to adhere to tissue culture flasks.

Adhesive Ability of Transduced and Naïve Endothelial Cells as Determined by Shear Stress Analysis

The goal of this study was to compare the ability of non-transduced and retrovirally transduced HUVEC cells to adhere to the matrix protein fibronectin at a shear stress that approximates the peak aortic value. The matrix protein fibronectin and a shear stress of 90 dynes/cm^2 were chosen for the experiment as the greatest differences in

adhesion were seen using these conditions previously (*151*). Five different cell lines were examined using this technique: naïve HUVEC, "mock" transduced HUVEC, HUVEC/pLXSN, HUVEC/PAI-1 and HUVEC/VN. Cells were allowed to incubate on the fibronectin-coated glass slides for one hour before start of flow. The number of cells that remained attached was counted over a two hour period. Over time, the number of cells attached decreased. There were no statistically significant differences in adhesion between any of the cell types. Therefore, the adhesive character of the transduced cells was comparable to that of naïve and "mock" transduced cells.

A similar study was performed with dramatically different results. Previous work by Sackman (*151*) indicated that canine vascular endothelial cells transduced with an empty retroviral vector exhibited decreased adherence to fibronectin at a shear stress of 90 dynes/cm^2. These were the same cells described above as having altered integrin expression.

Other studies have used gene transfer and over-expression of molecules involved in fibrinolysis in an effort to enhance the antithrombotic activity of endothelial cells (*174-176*). Plasminogen activators have been proposed as candidates for expression in endothelial cells to enhance fibrinolytic activity. These cells might enhance the fibrinolytic system and thereby decrease local thrombosis. Retroviral-mediated gene transfer of plasminogen activators has been performed in sheep, bovine, canine and baboon endothelial cells (*175-177*). Although these transduced endothelial cells have not been examined for integrin integrity, the adhesive ability of several of these transduced cell types has been explored. Sheep endothelial cells transduced with tPA or β-galactosidase were seeded on a small diameter Dacron graft and cell retention monitored

for 2 hours after placement in an *in vitro* flow system (*178*). The results show that tPA transduced endothelial cells detached at a significantly higher rate (33%) than those transduced with β-galactosidase (20%) or naïve cells (19%). Results from graft implanted after seeding retained only 6% of the tPA transduced cells and 32% of the β-galactosidase cells. This reduction could be caused by the action of tPA, since the cells transduced with β-galactosidase exhibited an almost identical adhesive phenotype as the naïve cells. The results of this study implicate that the choice of gene transduced into the cell is responsible for a decrease in adhesion, not the retroviral vector.

Further investigation using retrovirally transduced canine vascular endothelial cells suggest that the graft surface itself and the length of time transduced cells are allowed to recover after G418 selection are responsible for lack of endothelial cell coverage (*179*). Grafts that were subjected to fibronectin forced through the graft interstices then seeded with cells that were allowed to recover for 5 days post G418 selection and incubated for 4 days before implantation significantly improved the adherence of the transduced endothelial cells after 30 days *in vivo*. The retroviral vector was of the LXSN-type and carried the gene for pro-urokinase. The canine jugular vein endothelial cells were of the same type and transduced with the same retroviral vector as those used in the study showing altered integrin expression by Sackman (*152*). Integrin integrity of these cells was not examined nor was the ability of the transduced cells to produce pro-urokinase. Therefore, the basis of the transduced cells improved adherence is not known. It may be due to the effects of pro-urokinase or an improved surface for the transduced cells to adhere to, or perhaps a combination of the two.

Interestingly, different results have been obtained when human endothelial cells are used in shear-type studies. Human microvascular endothelial cells transduced with a retrovirus containing the β-galactosidase gene were evaluated for both adhesion and pro-thrombotic/pro-inflammatory responses (*180*). Transduced and non-transduced cells were coated to coverslips and Dacron graft surfaces which were exposed to either static or shear conditions. After six hours, transduced cells and non-transduced cells exposed to shear forces demonstrated similar retention on the graft surface. Adhesion of the cells on the coverslips was not performed. The cells on the coverslips were used to determine platelet and neutrophil adhesion to transduced and non-transduced cells. Of note, the transduced cells did not illicit a pro-thrombotic or pro-inflammatory response.

It is worth noting that most retroviral transductions are performed in cell types other than human. The results described above by Jankowski in human microvascular endothelial cells suggest that transduced human endothelial cells are just as adhesive as naïve cells. Other data suggest this is so, as well. Human endothelial cells transduced with tPA in an LXSN vector were also subjected to shear stress analysis. No significant difference in cellular adhesion was found between the transduced and non-transduced human endothelial cells (J. Cezeaux, unpublished results). The results presented in this dissertation confirm the results noted by Dr. Cezeaux and question the correlation between animal and human cells with respect to investigating the cellular adhesion of transduced endothelial cells.

Will Cells that Over-express PAI-1 Cause a Decrease in Cellular Adhesion?

PAI-1 has been implicated in decreasing cellular adhesion. It can do so potentially by binding to vitronectin that anchors the cell in the extracellular matrix and

151

displacing uPAR binding (*68-70*) or by blocking integrin binding to vitronectin (*10, 116*). An alternate theory is that high concentrations of PAI-1 inhibit the formation of proteolytic enzymes, thereby increasing cellular adhesion (*113, 115*). The HUVEC cells transduced with PAI-1 in this dissertation project exhibited no changes in cellular adhesion compared to naïve HUVEC cells. The HUVEC/PAI-1 cells remained attached and spread in the tissue culture flask. These same cells also retained an adhesive character under flow conditions.

Does this mean that PAI-1 does not effect cellular adhesion and migration? The amount of PAI-1 these transduced endothelial cells secrete is approximately 10 μg/ml, or 230 nM. In experiments designed to block cell migration, the concentration of PAI-1 needed to block cell migration was reported as 1 μM (*10*) to 2 μM (*116*), concentrations approximately four to eight times higher than the amount secreted by the HUVEC/PAI-1 cells. For the uPAR blocking experiments, concentrations of PAI-1 up to 10 μM were necessary to disrupt the interaction between vitronectin and uPAR. This concentration is approximately 40 times higher than that secreted by the HUVEC/PAI-1 cells. This makes it unlikely that any changes in adhesion due to PAI-1 would be seen with the HUVEC/PAI-1 cells.

Concluding Remarks and Future Directions

Vascular endothelium, due to its intimate contacts with the bloodstream and underlying cells of the arterial wall, is certainly an attractive target for genetic manipulation. Genetically modified endothelial cells expressing recombinant proteins

could control inflammation or reduce the cellular proliferation associated with such problems as atherosclerosis and synthetic graft failure. Currently, researchers are exploring the use of expressing recombinant proteins from transduced endothelial cells to treat intravascular thrombosis.

Vitronectin and PAI-1 are attractive proteins to use for gene therapy. Whereas there are no other reports in the literature about using vitronectin as a target for gene therapy, there are several cases describing the use of PAI-1. Adenovirus-mediated PAI-1 gene transfer has been used in nude mice to study its effects on inhibition of tumor metastasis (*181*). *In vivo* infection of the mice with PAI-1 adenovirus already harboring tumors show an antimetaststic effect. More relevant to the work presented in this chapter, PAI-1 replaced in PAI-1 deficient mice by adenoviral mediated gene transfer reduced neointima formation in the mice after arterial injury and inhibited vascular wound healing (*121*). The presence of PAI-1 appears to slow the healing of the vascular wound, which reduced neointima formation. A current paper out in 1999 describes the use of adenoviral vectors to increase expression of rat PAI-1 in rat carotid arteries (*182*). This work describes the optimization of adenoviral mediated gene transfer of PAI-1 in order to help elucidate the role of PAI-1 in the artery wall, and to begin to clarify whether manipulation of vascular PAI-1 expression might be a target for gene therapy. Clearly, PAI-1 may have an important role in gene therapy to control vascular thrombosis.

The transduced cell lines generated in this project have several potential uses. The endothelial cells expressing PAI-1 and vitronectin could be used to explore cellular migration and adhesion. Although the transduced cells exhibited no differences in their adhesive ability based on the shear stress studies, these studies were conducted on glass

slides coated with fibronectin. It would be interesting to determine how adhesive the

cells would be on synthetic graft material. Would differences in adhesion become

evident on the hydrophobic surface of the graft material? Another potential use for the

transduced cells is for protein production. The medium used to grow the cells contains

very little serum. The expression levels of PAI-1 and vitronectin are both approximately

10 μg/ml, or 10 mg/L. Since the retrovirus incorporates the gene its carrying into the

host cell's genome, the transduced cells should express PAI-1 or vitronectin until death.

It would certainly be worthwhile to determine the oligomeric state of the vitronectin

produced from the HUVEC/VN cells.

Chapter 4

Advancing Vitronectin Research

Introduction

Vitronectin has been implicated as participating in a wide variety of roles to
maintain hemostasis, promote cellular adhesion, inhibit the membrane attack complex,
clear serpin complexes from the circulation and even provide a surface for bacteria and
fungus to attach to cells. The ability of vitronectin to binds so many diverse ligands and
display different functions is likely based on the domain organization of the protein. The
domain structure of vitronectin allows for multiple ligand binding sites. Despite all that
is known regarding the ligand binding ability of vitronectin, the relationship between
structure and function is still in doubt. This is in part due to difficulties inherent with
vitronectin. There is no crystal structure or NMR data available for the study of
vitronectin. Its large size, glycosylated nature and propensity to oligomerize make full-
length vitronectin unsuitable for crystallography or NMR. Therefore, the majority of
work done on vitronectin to determine structural information has relied on the use of
conformation-specific antibodies, loss or gain of ligand binding abilities and the
monitoring of multimerization by native gel electrophoresis.

The ability to express recombinant vitronectin in eukaryotic cells that effectively
mimics plasma vitronectin can contribute to the elucidation of determinants required for

ligand binding as well structure. However, very little has been done in the field of vitronectin research with expression of full-length or mutant vitronectin. The domains of vitronectin have been expressed in bacteria (*45, 107, 122*). Two other expression systems have been used to generate full-length and mutant vitronectin: the baculovirus system and transfection of baby hamster kidney cells. Expression of RGD mutants of vitronectin were performed in the baby hamster kidney cells in 1993 (*22*). Also in 1993, there were two reports of expressing vitronectin using the baculovirus system (*123, 124*). Full-length, deletion mutant and site directed mutants of vitronectin were expressed in this system. The goal of both these studies using recombinant vitronectin was to determine the sequences necessary for cell adhesion. No further characterization or use of vitronectin expressed in eukaryotic cells was performed by anyone until 1998, when Gibson presented results which characterized a full-length and a carboxy-terminal deletion mutant of vitronectin. Clearly, most vitronectin researchers have shunned the use of recombinant vitronectin expressed in eukaryotic cells.

The work described in this dissertation has two basic goals. The first is to express a somatomedin B deletion mutant of vitronectin and characterize its similarity to plasma vitronectin, with particular attention being focused on the PAI-1 binding ability of this recombinant protein. The second goal of this project is focused on the expression of vitronectin and PAI-1 in retrovirally transduced human endothelial cells in order to study the adhesive ability of these transduced cells.

Research Summary

Can a Somatomedin B Deletion Mutant be Expressed Using the Baculovirus System as a Functional Recombinant Protein?

The somatomedin B deletion mutant was successfully expressed using the baculovirus system. This deletion mutant lacks the first 40 amino acids of vitronectin, yet retains the integrin binding consensus sequence, RGD. A histidine tag at the carboxyl-terminus of the protein allowed for one step purification of the recombinant protein over a metal chelating column. This process was effective at purifying milligram quantities of protein from a liter of spent medium.

The ability of the somatomedin B deletion mutant to mimic the function of plasma vitronectin was investigated. The protein, ssΔsBVN-his, was capable of binding heparin, the integrin GPIIb/IIIa and supported cell binding. The recombinant protein exhibited a cell binding ability nearly identical to plasma and multimeric vitronectin. The ssΔsBVN-his protein also was able to bind the platelet integrin GPIIb/IIIa. This deletion mutant as well as recombinant full-length vitronectin bound significantly better to the integrin. This could be due to the oligomeric nature of the proteins. As determined by gel filtration, the ssΔsBVN-his protein is large, greater than 669 kDa. This may effectively cluster the RGD sequences in the recombinant proteins, increasing their ability to bind the integrin GPIIb/IIIa. Finally, the ability of the recombinant protein to neutralize heparin activity in a kinetic assay demonstrated the ssΔsBVN-his protein behaves in a similar manner to multimeric vitronectin with respect to heparin binding. The midpoint for heparin neutralization was 0.14 μM compared to 0.18 μM for multimeric vitronectin generated by denaturation and denaturation. Based on these

results, the somatomedin B deletion mutant did not exhibit functional differences with respect to cell binding, integrin binding and heparin binding.

Does Deletion of the Somatomedin B Domain Result in Any Loss of PAI-1 Binding Ability?

The PAI-1 binding ability of the somatomedin B deletion mutant is significantly different than that of plasma vitronectin. PAI-1 far-Western analysis indicates that the ssΔsBVN-his protein retains PAI-1 binding activity. A direct PAI-1 binding immunoassay confirmed PAI-1 binding to the deletion mutant, however, due to the nature of the direct assay, little information could be ascertained about relative binding affinities. A solution based competitive PAI-1 binding assay was performed to compare the PAI-1 binding ability of the recombinant deletion mutant, multimeric vitronectin and native vitronectin. Both native and multimeric vitronectin in solution could effectively compete for PAI-1 binding. The deletion mutant, on the other hand, could still bind PAI-1 in solution, but to a lesser extent than native or multimeric vitronectin. Whereas native and multimeric vitronectin inhibited PAI-1 binding to immobilized vitronectin on a microtiter plate by 95%, the somatomedin B deletion mutant only inhibited PAI-1 binding by 35%. These results indicate there is another PAI-1 binding site outside of the somatomedin B domain. This site, however, is not solely responsible for PAI-1 binding, as 100% PAI-1 binding inhibition was not observed.

The results obtained from the PAI-1 binding studies are consistent with a more complex model for PAI-1 binding rather than the one binding site model. The results of this dissertation research support a PAI-1 binding model that has recently been proposed. Research from our laboratory as well as research conducted by a collaborator support a

more complex model for PAI-1 binding (see figure 2-25). The binding of active PAI-1 to vitronectin at either one or both PAI-1 binding sites induces multimerization of vitronectin, resulting in the formation of vitronectin:PAI-1 complexes with a stoichiometry of 2:4. Once formed, the vitronectin multimers are not able to revert to monomeric form. After active PAI-1 becomes latent and dissociates from vitronectin, the oligomeric form of vitronectin persists. This may be one mechanism for the conversion of monomeric vitronectin in the bloodstream into the oligomeric form believed to be deposited in the extracellular matrix.

Does Expression of PAI-1 or Vitronectin from Retrovirally Transduced Human Endothelial Cells Alter the Adhesive State of the Cells?

Human umbilical vein endothelial cells transduced with either PAI-1 or vitronectin did not adversely affect the adhesive ability of the cells. The transduced cells were examined for gene incorporation and protein production. The amount of protein secreted into the medium from the PAI-1 or vitronectin transduced cells was 10 and 12 µg/ml, respectively. The amount of PAI-1 or vitronectin secreted by naïve cells or present in the medium was not detectable in the quantitative Western that was performed. Further analysis of these PAI-1 and vitronectin transduced cells was performed, testing their ability to withstand a shear stress similar to that found in arteries. At a flow rate of 90 dynes/cm^2, the transduced cells exhibited no difference in adhesive ability compared to naïve cells. Cells transduced with an empty retroviral vector, previously shown to exhibit decreased adherence in canine endothelial cells, showed no appreciable difference in adhesive character as naïve cells.

The growth pattern and cell shape of the transduced cells also argues against any alteration of adhesive phenotype. The PAI-1 and vitronectin transduced cells grew at similar rates, reaching a near confluent state in approximately the same number of days. The cell shape was somewhat altered from naïve cells. The naïve cells had well defined shapes and borders whereas the transduced cells were more circular in shape. The cells transduced with the empty retroviral vector, on the other hand, often appeared to be curling around the edges.

The amount of vitronectin or PAI-1 secreted by the trasnduced cells may not be at a high enough concentration to affect cellular adhesion. Therefore, one must be cautious about making conclusions about the adhesive nature of the cells. However, under the conditions of these experiments, the adhesive state of HUVEC cells was not affected by the secretion of PAI-1 or vitronectin into the growth medium.

Concluding Remarks

Two projects were undertaken in this dissertation research. The first project focused on the nature of PAI-1 binding by generating a mutant lacking one of the putative PAI-1 binding sites. The second project involved efforts to probe the role of vitronectin and PAI-1 in cellular adhesion.

The first project utilized the baculovirus system for production of a somatomedin B deletion mutant. This project evolved from research done by Angelia Gibson as a major focus of her dissertation research, which demonstrated the feasibility of using such a system. This expression system can be utilized further to express other vitronectin

domains, truncation mutants or even point mutants. Further mutagenesis of vitronectin in this manner can be valuable in testing function and evaluating structure.

Inducing retrovirally transduced cells to over-express either PAI-1 or vitronectin did not alter adhesive function. Although this result needs to be viewed with caution, this system could be beneficial in studying the adhesive nature of endothelial cells. These cells may also be important for gene therapy and controlling vascular thrombotic events. Since the adhesion of the transduced cells was not altered by transduction with PAI-1 or vitronectin, these vectors could potentially be used to transduce endothelial cells to control coagulation and fibrinolysis or render a synthetic graft non-thrombogenic.

The work described in this dissertation has the potential to further define ligand binding sites, provide insight into the mechanism of PAI-1:vitronectin interaction and adhesion as well as determine the plausibility of using PAI-1 or vitronectin in gene therapy applications.

References

1. Holmes, R. (1967) *J. Cell Biol. 32*, 297-308.

2. Jenne, D., and Stanley, K. (1985) *EMBO Journal 4*, 3153-3157.

3. Preissner, K. T., Heimburger, N., Anders, E., and Muller-Berghaus, G. (1986) *Biochem Biophys Res Commun 134*, 951-6.

4. Tomasini, B. R., and Mosher, D. F. (1986) *Blood 68*, 737-42.

5. Zhuang, P., Chen, A. I., and Peterson, C. B. (1997) *J Biol Chem 272*, 6858-67.

6. de Boer, H. C., Preissner, K. T., Bouma, B. N., and de Groot, P. G. (1992) *J Biol Chem 267*, 2264-8.

7. Dano, K., Andreasen, P. A., Grondahl-Hansen, J., Kristensen, P., Nielsen, L. S., and Skriver, L. (1985) *Adv Cancer Res 44*, 139-266.

8. Liotta, L. A., Steeg, P. S., and Stetler-Stevenson, W. G. (1991) *Cell 64*, 327-36.

9. Brooks, P. C., Clark, R. A., and Cheresh, D. A. (1994) *Science 264*, 569-71.

10. Stefansson, S., and Lawrence, D. A. (1996) *Nature 383*, 441-3.

11. Liang, O. D., Flock, J. I., and Wadstrom, T. (1994) *J Biochem (Tokyo) 116*, 457-63.

12. Liang, O. D., Preissner, K. T., and Chhatwal, G. S. (1997) *Biochem Biophys Res Commun 234*, 445-9.

13. Limper, A. H., Standing, J. E., Hoffman, O. A., Castro, M., and Neese, L. W. (1993) *Infect Immun 61*, 4302-9.

14. Limper, A. H., and Standing, J. E. (1994) *Immunol Lett 42*, 139-44.

15. Tollefsen, D. M., Weigel, C. J., and Kabeer, M. H. (1990) *J Biol Chem 265*, 9778-81.

16. Conlan, M. G., Tomasini, B. R., Schultz, R. L., and Mosher, D. F. (1988) *Blood 72*, 185-90.

17. Sigurdardottir, O., and Wiman, B. (1994) *Biochim Biophys Acta 1208*, 104-10.

18. Chain, D., Kreizman, T., Shapira, H., and Shaltiel, S. (1991) *FEBS Lett 285*, 251-6.

19. Gechtman, Z., Belleli, A., Lechpammer, S., and Shaltiel, S. (1997) *Biochem J 325*, 339-49.

20. Merberg, D. M., Fitz, L. J., Temple, P., Giannotti, J., Murtha, P., Fitzgerald, M., Scaltreto, J., Kelleher, K., Preissner, K., Kriz, R., Jacobs, K., and Turner, K. (1993) in *First International Vitronectin Workshop* (Preissner, K. T., Rosenblatt, S., Kost, C., Wegerhoff, J., and Mosher, D. F., Eds.) pp 45-55, Elsevier Science Publishers, Marburg, Germany.

21. Deissler, H., Lottspeich, F., and Rajewsky, M. F. (1995) *J Biol Chem 270*, 9849-55.

22. Cherny, R. C., Honan, M. A., and Thiagarajan, P. (1993) *J Biol Chem 268*, 9725-9.

23. Hynes, R. O. (1992) *Cell 69*, 11-25.

24. Jenne, D., Hille, A., Stanley, K. K., and Huttner, W. B. (1989) *Eur J Biochem 185*, 391-5.

25. Sane, D. C., Moser, T. L., Pippen, A. M., Parker, C. J., Achyuthan, K. E., and Greenberg, C. S. (1988) *Biochem Biophys Res Commun 157*, 115-20.

26. Skorstengaard, K., Halkier, T., Hojrup, P., and Mosher, D. (1990) *FEBS Lett 262*, 269-74.

27. Seger, D., Gechtman, Z., and Shaltiel, S. (1998) *J Biol Chem 273*, 24805-13.

28. Jenne, D., and Stanley, K. (1987) *Biochemistry 26*, 6735-6742.

29. Korc-Grodzicki, B., Tauber-Finkelstein, M., and Shaltiel, S. (1988) *Proc Natl Acad Sci U S A 85*, 7541-5.

30. Chain, D., Korc-Grodzicki, B., Kreizman, T., and Shaltiel, S. (1991) *Biochem J 274*, 387-94.

31. McGuire, E. A., Peacock, M. E., Inhorn, R. C., Siegel, N. R., and Tollefsen, D. M. (1988) *J Biol Chem 263*, 1942-5.

32. Gechtman, Z., and Shaltiel, S. (1997) *Eur J Biochem 243*, 493-501.

33. Morgan, W. T., and Smith, A. (1984) *J Biol Chem 259*, 12001-6.

34. Takahashi, N., Takahashi, Y., and Putnam, F. W. (1985) *Proc Natl Acad Sci U S A 82*, 73-7.

35. Altruda, F., Poli, V., Restagno, G., Argos, P., Cortese, R., and Silengo, L. (1985) *Nucleic Acids Res 13*, 3841-59.

36. Faber, H. R., Groom, C. R., Baker, H. M., Morgan, W. T., Smith, A., and Baker, E. N. (1995) *Structure 3*, 551-9.

37. Gohlke, U., Gomis-Ruth, F. X., Crabbe, T., Murphy, G., Docherty, A. J., and Bode, W. (1996) *FEBS Lett 378*, 126-30.

38. Gomis-Ruth, F. X., Gohlke, U., Betz, M., Knauper, V., Murphy, G., Lopez-Otin, C., and Bode, W. (1996) *J Mol Biol 264*, 556-66.

39. Paoli, M., Anderson, B. F., Baker, H. M., Morgan, W. T., Smith, A., and Baker, E. N. (1999) *Nat Struct Biol 6*, 926-31.

40. Morgan, W. T., Muster, P., Tatum, F. M., McConnell, J., Conway, T. P., Hensley, P., and Smith, A. (1988) *J Biol Chem 263*, 8220-5.

41. Smith, A., Tatum, F. M., Muster, P., Burch, M. K., and Morgan, W. T. (1988) *J Biol Chem 263*, 5224-9.

42. Fulop, V., and Jones, D. T. (1999) *Curr Opin Struct Biol 9*, 715-21.

43. Gibson, A. (1998) in *A New Approach to Vitronectin Research: Using Molecular Biology and Biophysical Chemistry to Elucidate the Contributions of the C-Terminal Domain of Vitronectin to Heparin Binding, PAI-1 Binding and Vitronectin Self-Association*, University of Tennessee, Knoxville.

44. Suzuki, S., Pierschbacher, M. D., Hayman, E. G., Nguyen, K., Ohgren, Y., and Ruoslahti, E. (1984) *J Biol Chem 259*, 15307-14.

45. Gibson, A. D., Lamerdin, J. A., Zhuang, P., Baburaj, K., Serpersu, E. H., and Peterson, C. B. (1999) *J Biol Chem 274*, 6432-42.

46. Tomasini, B. R., and Mosher, D. F. (1988) *Blood 72*, 903-12.

47. Zhuang, P., Li, H., Williams, J. G., Wagner, N. V., Seiffert, D., and Peterson, C. B. (1996) *J Biol Chem 271*, 14333-43.

48. Preissner, K. T., and Muller-Berghaus, G. (1987) *J Biol Chem 262*, 12247-53.

49. Tomasini, B. R., Owen, M. C., Fenton, J. W. d., and Mosher, D. F. (1989) *Biochemistry 28*, 7617-23.

50. Stockmann, A., Hess, S., Declerck, P., Timpl, R., and Preissner, K. T. (1993) *J Biol Chem 268*, 22874-82.

51. Zhuang, P., Blackburn, M. N., and Peterson, C. B. (1996) *J Biol Chem 271*, 14323-32.

52. Behrendt, N., Ploug, M., Patthy, L., Houen, G., Blasi, F., and Dano, K. (1991) *J Biol Chem 266*, 7842-7.

53. Roldan, A. L., Cubellis, M. V., Masucci, M. T., Behrendt, N., Lund, L. R., Dano, K., Appella, E., and Blasi, F. (1990) *Embo J 9*, 467-74.

54. Ploug, M., Behrendt, N., Lober, D., and Dano, K. (1991) *Semin Thromb Hemost 17*, 183-93.

55. Moller, L. B., Ploug, M., and Blasi, F. (1992) *Eur J Biochem 208*, 493-500.

56. Cubellis, M. V., Nolli, M. L., Cassani, G., and Blasi, F. (1986) *J Biol Chem 261*, 15819-22.

57. Petersen, L. C., Lund, L. R., Nielsen, L. S., Dano, K., and Skriver, L. (1988) *J Biol Chem 263*, 11189-95.

58. Ellis, V., Scully, M. F., and Kakkar, V. V. (1987) *J Biol Chem 262*, 14998-5003.

59. Stephens, R. W., Pollanen, J., Tapiovaara, H., Leung, K. C., Sim, P. S., Salonen, E. M., Ronne, E., Behrendt, N., Dano, K., and Vaheri, A. (1989) *J Cell Biol 108*, 1987-95.

60. Ellis, V., Scully, M. F., and Kakkar, V. V. (1989) *J Biol Chem 264*, 2185-8.

61. Cubellis, M. V., Andreasen, P., Ragno, P., Mayer, M., Dano, K., and Blasi, F. (1989) *Proc Natl Acad Sci U S A 86*, 4828-32.

62. Ellis, V., Wun, T. C., Behrendt, N., Ronne, E., and Dano, K. (1990) *J Biol Chem 265*, 9904-8.

63. Bergman, B. L., Scott, R. W., Bajpai, A., Watts, S., and Baker, J. B. (1986) *Proc Natl Acad Sci U S A 83*, 996-1000.

64. Cubellis, M. V., Wun, T. C., and Blasi, F. (1990) *Embo J 9*, 1079-85.

65.   Conese, M., Olson, D., and Blasi, F. (1994) *J Biol Chem 269*, 17886-92.

66.   Herz, J., Clouthier, D. E., and Hammer, R. E. (1992) *Cell 71*, 411-21.

67.   Nykjaer, A., Petersen, C. M., Moller, B., Jensen, P. H., Moestrup, S. K., Holtet, T. L., Etzerodt, M., Thogersen, H. C., Munch, M., Andreasen, P. A., and et al. (1992) *J Biol Chem 267*, 14543-6.

68.   Simon, D. I., Rao, N. K., Xu, H., Wei, Y., Majdic, O., Ronne, E., Kobzik, L., and Chapman, H. A. (1996) *Blood 88*, 3185-94.

69.   Kanse, S. M., Kost, C., Wilhelm, O. G., Andreasen, P. A., and Preissner, K. T. (1996) *Exp Cell Res 224*, 344-53.

70.   Deng, G., Curriden, S. A., Wang, S., Rosenberg, S., and Loskutoff, D. J. (1996) *J Cell Biol 134*, 1563-71.

71.   Ishikawa-Sakurai, M., and Hayashi, M. (1993) *Cell Struct Funct 18*, 253-9.

72.   Izumi, M., Shimo-Oka, T., Morishita, N., Ii, I., and Hayashi, M. (1988) *Cell Struct Funct 13*, 217-25.

73.   Mimuro, J., Muramatsu, S., Kurano, Y., Uchida, Y., Ikadai, H., Watanabe, S., and Sakata, Y. (1993) *Biochemistry 32*, 2314-20.

74.   Liang, O. D., Rosenblatt, S., Chhatwal, G. S., and Preissner, K. T. (1997) *FEBS Lett 407*, 169-72.

75.   Kost, C., Stuber, W., Ehrlich, H. J., Pannekoek, H., and Preissner, K. T. (1992) *J Biol Chem 267*, 12098-105.

76.   Gechtman, Z., Sharma, R., Kreizman, T., Fridkin, M., and Shaltiel, S. (1993) *FEBS Lett 315*, 293-7.

77. Waltz, D. A., Natkin, L. R., Fujita, R. M., Wei, Y., and Chapman, H. A. (1997) *J Clin Invest 100*, 58-67.

78. Ishikawa, M., and Hayashi, M. (1992) *Biochim Biophys Acta 1121*, 173-7.

79. Tschopp, J., Masson, D., Schafer, S., Peitsch, M., and Preissner, K. T. (1988) *Biochemistry 27*, 4103-9.

80. Bosma, P. J., van den Berg, E. A., Kooistra, T., Siemieniak, D. R., and Slightom, J. L. (1988) *J Biol Chem 263*, 9129-41.

81. Lawrence, D., Strandberg, L., Grundstrom, T., and Ny, T. (1989) *Eur J Biochem 186*, 523-33.

82. Declerck, P. J., Alessi, M. C., Verstreken, M., Kruithof, E. K., Juhan-Vague, I., and Collen, D. (1988) *Blood 71*, 220-5.

83. Loskutoff, D. J., and Edgington, T. S. (1981) *J Biol Chem 256*, 4142-5.

84. Loskutoff, D. J., van Mourik, J. A., Erickson, L. A., and Lawrence, D. (1983) *Proc Natl Acad Sci U S A 80*, 2956-60.

85. Kruithof, E. K., Tran-Thang, C., Ransijn, A., and Bachmann, F. (1984) *Blood 64*, 907-13.

86. Huber, R., and Carrell, R. W. (1989) *Biochemistry 28*, 8951-66.

87. Stein, P. E., Leslie, A. G., Finch, J. T., Turnell, W. G., McLaughlin, P. J., and Carrell, R. W. (1990) *Nature 347*, 99-102.

88. Carrell, R. W., Evans, D. L., and Stein, P. E. (1991) *Nature 353*, 576-8.

89. Carrell, R. W., and Evans, L. I. (1992) *Current Opinion in Structural Biology 2*, 438-446.

90. Wilczynska, M., Fa, M., Ohlsson, P. I., and Ny, T. (1995) *J Biol Chem 270*, 29652-5.

91. Kraut, J. (1997) *Ann Rev Biochem 46*, 331-358.

92. Shore, J. D., Day, D. E., Francis-Chmura, A. M., Verhamme, I., Kvassman, J., Lawrence, D. A., and Ginsburg, D. (1995) *J Biol Chem 270*, 5395-8.

93. Lawrence, D. A. (1997) *Nat Struct Biol 4*, 339-41.

94. Franke, A. E., Danley, D. E., Kaczmarek, F. S., Hawrylik, S. J., Gerard, R. D., Lee, S. E., and Geoghegan, K. F. (1990) *Biochim Biophys Acta 1037*, 16-23.

95. Hekman, C. M., and Loskutoff, D. J. (1985) *J Biol Chem 260*, 11581-7.

96. Mottonen, J., Strand, A., Symersky, J., Sweet, R. M., Danley, D. E., Geoghegan, K. F., Gerard, R. D., and Goldsmith, E. J. (1992) *Nature 355*, 270-3.

97. Egelund, R., Schousboe, S. L., Sottrup-Jensen, L., Rodenburg, K. W., and Andreasen, P. A. (1997) *Eur J Biochem 248*, 775-85.

98. Lawrence, D. A., Olson, S. T., Palaniappan, S., and Ginsburg, D. (1994) *Biochemistry 33*, 3643-8.

99. Sharp, A. M., Stein, P. E., Pannu, N. S., Carrell, R. W., Berkenpas, M. B., Ginsburg, D., Lawrence, D. A., and Read, R. J. (1999) *Structure Fold Des 7*, 111-8.

100. Gibson, A., Baburaj, K., Day, D. E., Verhamme, I., Shore, J. D., and Peterson, C. B. (1997) *J Biol Chem 272*, 5112-21.

101. Declerck, P. J., De Mol, M., Alessi, M. C., Baudner, S., Paques, E. P., Preissner, K. T., Muller-Berghaus, G., and Collen, D. (1988) *J Biol Chem 263*, 15454-61.

102. Seiffert, D., and Loskutoff, D. J. (1991) *Biochim Biophys Acta 1078*, 23-30.

103. Lawrence, D. A., Berkenpas, M. B., Palaniappan, S., and Ginsburg, D. (1994) *J Biol Chem 269*, 15223-8.

104. van Meijer, M., Gebbink, R. K., Preissner, K. T., and Pannekoek, H. (1994) *FEBS Lett 352*, 342-6.

105. Padmanabhan, J., and Sane, D. C. (1995) *Thromb Haemost 73*, 829-34.

106. Seiffert, D., and Loskutoff, D. J. (1991) *J Biol Chem 266*, 2824-30.

107. Seiffert, D., Ciambrone, G., Wagner, N. V., Binder, B. R., and Loskutoff, D. J. (1994) *J Biol Chem 269*, 2659-66.

108. Preissner, K. T., Grulich-Henn, J., Ehrlich, H. J., Declerck, P., Justus, C., Collen, D., Pannekoek, H., and Muller-Berghaus, G. (1990) *J Biol Chem 265*, 18490-8.

109. Naski, M. C., Lawrence, D. A., Mosher, D. F., Podor, T. J., and Ginsburg, D. (1993) *J Biol Chem 268*, 12367-72.

110. Ehrlich, H. J., Gebbink, R. K., Keijer, J., Linders, M., Preissner, K. T., and Pannekoek, H. (1990) *J Biol Chem 265*, 13029-35.

111. Stefansson, S., Lawrence, D. A., and Argraves, W. S. (1996) *J Biol Chem 271*, 8215-20.

112. Pepper, M. S., Sappino, A. P., Stocklin, R., Montesano, R., Orci, L., and Vassalli, J. D. (1993) *J Cell Biol 122*, 673-84.

113. Morimoto, K., Mishima, H., Nishida, T., and Otori, T. (1993) *Thromb Haemost 69*, 387-91.

114. Estreicher, A., Muhlhauser, J., Carpentier, J. L., Orci, L., and Vassalli, J. D. (1990) *J Cell Biol 111*, 783-92.

115. Reinartz, J., Schafer, B., Batrla, R., Klein, C. E., and Kramer, M. D. (1995) *Exp Cell Res 220*, 274-82.

116. Kjoller, L., Kanse, S. M., Kirkegaard, T., Rodenburg, K. W., Ronne, E., Goodman, S. L., Preissner, K. T., Ossowski, L., and Andreasen, P. A. (1997) *Exp Cell Res 232*, 420-9.

117. Carmeliet, P., Stassen, J. M., Schoonjans, L., Ream, B., van den Oord, J. J., De Mol, M., Mulligan, R. C., and Collen, D. (1993) *J Clin Invest 92*, 2756-60.

118. Zheng, X., Saunders, T. L., Camper, S. A., Samuelson, L. C., and Ginsburg, D. (1995) *Proc Natl Acad Sci U S A 92*, 12426-30.

119. Fay, W. P., Parker, A. C., Ansari, M. N., Zheng, X., and Ginsburg, D. (1999) *Blood 93*, 1825-30.

120. Carmeliet, P., Moons, L., Ploplis, V., Plow, E., and Collen, D. (1997) *J Clin Invest 99*, 200-8.

121. Carmeliet, P., Moons, L., Lijnen, R., Janssens, S., Lupu, F., Collen, D., and Gerard, R. D. (1997) *Circulation 96*, 3180-91.

122. Yoneda, A., Ogawa, H., Kojima, K., and Matsumoto, I. (1998) *Biochemistry 37*, 6351-60.

123. Zhao, Y., and Sane, D. C. (1993) *Arch Biochem Biophys 304*, 434-42.

124. Zhao, Y., and Sane, D. C. (1993) *Biochem Biophys Res Commun 192*, 575-82.

125. Daughaday, W. H., Hall, K., Raben, M. S., Salmon, W. D., Jr., Brande, J. L. v. d., and Wyk, J. J. v. (1972) *Nature 235*, 107.

126. Fryklund, L., and Sievertsson, H. (1978) *FEBS Lett 87*, 55-60.

127. Standker, L., Enger, A., Schulz-Knappe, P., Wohn, K. D., Germer, M., Raida, M., Forssmann, W. G., and Preissner, K. T. (1996) *Eur J Biochem 241*, 557-63.

128. Deng, G., Royle, G., Wang, S., Crain, K., and Loskutoff, D. J. (1996) *J Biol Chem 271*, 12716-23.

129. Seiffert, D., and Smith, J. W. (1997) *J Biol Chem 272*, 13705-10.

130. Thiagarajan, P., and Kelly, K. L. (1988) *J Biol Chem 263*, 3035-8.

131. Seiffert, D. (1995) *FEBS Lett 368*, 155-9.

132. Seiffert, D., and Loskutoff, D. J. (1996) *J Biol Chem 271*, 29644-51.

133. Voorhees, A. B., Jr., Jaretski, A., III, and Blakemore, A. H. (1952) *Annals of Surgery 135*, 332-336.

134. Sauvage, L. R., Berger, K. E., Wood, S. J., Yates, S. G. d., Smith, J. C., and Mansfield, P. B. (1974) *Arch Surg 109*, 698-705.

135. Yates, S. G., Barros D'Sa, A. A., Berger, K., Fernandez, L. G., Wood, S. J., Rittenhouse, E. A., Davis, C. C., Mansfield, P. B., and Sauvage, L. R. (1978) *Ann Surg 188*, 611-22.

136. Bergan, J. J., Veith, F. J., Bernhard, V. M., Yao, J. S., Flinn, W. R., Gupta, S. K., Scher, L. A., Samson, R. H., and Towne, J. B. (1982) *Surgery 92*, 921-30.

137. Weatherford, D. A., MD, Ombrellaro, M. P., MD, Schaeffer, D. O., DVM, MS, Stevens, S. L., MD, Sackman, J. E., DVM, PhD, Freeman, M. B., MD, and Goldman, M. H., MD. (1997) *Annals of Vascular Surgery 11*, 54-61.

138. van Oene, G. H., Yue, X., van der Lei, B., Schakenraad, J. M., Kuit, J. H., Feijen, J., and Wildevuur, C. R. H. (1987) in *1st European Workshop on Advanced*

Technologies in Vascular Surgery (Zilla, P. P., Fasol, M., and Deutsch, M., Eds.) pp 258, Karger, Vienna.

139. Bull, D. A., Hunter, G. C., Holubec, H., and al., e. (1995) *Journal of Surgical Research 58*, 58-68.

140. Clowes, A. W., Kirkman, T. R., and Reidy, M. A. (1986) *American journal of pathology 123*, 220-230.

141. Stanley, J. C., Burkel, W. E., Ford, J. W., Vinter, D. W., Kahn, R. H., Whitehouse, W. M., Jr., and Graham, L. M. (1982) *Surgery 92*, 994-1005.

142. Golden, M. A., Au, Y. P. T., Kirkman, T. R., and al., e. (1991) *Journal of Clinical Investigation 87*, 406-414.

143. Lynch, C. M., Clowes, M. M., Osborne, W. R., Clowes, A. W., and Miller, A. D. (1992) *Proc Natl Acad Sci U S A 89*, 1138-42.

144. Geary, R. L., Clowes, A. W., Lau, S., Vergel, S., Dale, D. C., and Osborne, W. R. (1994) *Hum Gene Ther 5*, 1211-6.

145. Clowes, M. M., Lynch, C. M., Miller, A. D., Miller, D. G., Osborne, W. R., and Clowes, A. W. (1994) *J Clin Invest 93*, 644-51.

146. Miller, A. D., and Rosman, G. J. (1989) *BioTechniques 7*, 980-990.

147. Lemarchand, P., Jones, M., Yamada, I., and Crystal, R. G. (1993) *Circ Res 72*, 1132-8.

148. Kessler, P. D., Podsakoff, G. M., Chen, X., McQuiston, S. A., Colosi, P. C., Matelis, L. A., Kurtzman, G. J., and Byrne, B. J. (1996) *Proc Natl Acad Sci U S A 93*, 14082-7.

149. Kaplitt, M. G., Leone, P., Samulski, R. J., Xiao, X., Pfaff, D. W., O'Malley, K. L., and During, M. J. (1994) *Nat Genet 8*, 148-54.

150. Podsakoff, G., Wong, K. K., Jr., and Chatterjee, S. (1994) *J Virol 68*, 5656-66.

151. Sackman, J. E., D.V.M., Ph.D, Cezeaux, J. L., Ph.D., Teddick, T. T., M.S., Freeman, M. B., M.D., Stevens, S. L., M.D., and Goldman, M. H., M.D. (1996) *Tissue Engineering 2*, 223-234.

152. Sackman, J. E., Wymore, A. M., Reddick, T. T., Freeman, M. B., Stevens, S. L., and Goldman, M. H. (1997) *J Surg Res 69*, 45-50.

153. Ruoslahti, E. (1997) *Kidney Int 51*, 1413-7.

154. Gumbiner, B. M. (1996) *Cell 84*, 345-57.

155. Calvete, J. J. (1999) *Proc Soc Exp Biol Med 222*, 29-38.

156. Nolte, M., Pepinsky, R. B., Venyaminov, S., Koteliansky, V., Gotwals, P. J., and Karpusas, M. (1999) *FEBS Lett 452*, 379-85.

157. Rich, R. L., Deivanayagam, C. C., Owens, R. T., Carson, M., Hook, A., Moore, D., Symersky, J., Yang, V. W., Narayana, S. V., and Hook, M. (1999) *J Biol Chem 274*, 24906-13.

158. Tuckwell, D. S., and Humphries, M. J. (1997) *FEBS Lett 400*, 297-303.

159. Springer, T. A. (1997) *Proc Natl Acad Sci U S A 94*, 65-72.

160. Valera, A., Perales, J. C., Hatzoglou, M., and Bosch, F. (1994) *Human Gene Therapy 5*, 449-456.

161. Tapley, P., Horwitz, A. F., Buck, C. A., Burridge, K., Duggan, K., Hirst, R., and Rohrshneider, L. (1989) *Oncogene 4*, 325-333.

162. Hess, S., Kanse, S. M., Kost, C., and Preissner, K. T. (1995) *Thromb Haemost 74*, 258-65.

163. Hanahan, D., and Folkman, J. (1996) *Cell 86*, 353-64.

164. Cheresh, D. A., Berliner, S. A., Vicente, V., and Ruggeri, Z. M. (1989) *Cell 58*, 945-53.

165. Ploug, M., Ellis, V., and Dano, K. (1994) *Biochemistry 33*, 8991-7.

166. Morgan, R. A., Cornetta, K., and Anderson, W. F. (1990) *Hum Gene Ther 1*, 135-49.

167. Miller, A. D., Law, M. F., and Verma, I. M. (1985) *Mol Cell Biol 5*, 431-7.

168. Cezeaux, J. L. (1989) in *Department of Biomedical Engineering*, Rensselaer Polytechnic Institute.

169. Cezeaux, J. L., and van Grondelle, A. (1997) *Anals of Biomedical Engineering 25*, 536-546.

170. Smith, A. E. (1999) *Lancet 354 Suppl 1*, SI1-4.

171. Anderson, W. F. (1998) *Nature 392*, 25-30.

172. Nachman, R. L., and Hajjar, K. A. (1991) *Ann N Y Acad Sci 614*, 240-9.

173. Miller, D. G., Adam, M. A., and Miller, A. D. (1990) *Mol Cell Biol 10*, 4239-42.

174. Dichek, D. A., Neville, R. F., Zwiebel, J. A., Freeman, S. M., Leon, M. B., and Anderson, W. F. (1989) *Circulation 80*, 1347-53.

175. Dichek, D. A., Nussbaum, O., Degen, S. J., and Anderson, W. F. (1991) *Blood 77*, 533-41.

176. Dichek, D. A., Lee, S. W., and Nguyen, N. H. (1994) *Blood 84*, 504-16.

177. Podrazik, R. M., Whitehill, T. A., Ekhterae, D., Williams, W. D., Messina, L. M., and Stanley, J. C. (1992) *Ann Surg 216*, 446-52; discussion 453.

178. Dunn, P. F., Newman, K. D., Jones, M., Yamada, I., Shayani, V., Virmani, R., and Dichek, D. A. (1996) *Circulation 93*, 1439-46.

179. Falk, J., Townsend, L. E., Vogel, L. M., Boyer, M., Olt, S., Wease, G. L., Trevor, K. T., Seymour, M., Glover, J. L., and Bendick, P. J. (1998) *J Vasc Surg 27*, 902-8; discussion 908-9.

180. Jankowski, R. J., Severyn, D. A., Vorp, D. A., and Wagner, W. R. (1997) *J Vasc Surg 26*, 676-84.

181. Ma, D., Gerard, R. D., Li, X. Y., Alizadeh, H., and Niederkorn, J. Y. (1997) *Blood 90*, 2738-46.

182. DeYoung, M. B., Zamarron, C., Lin, A. P., Qiu, C., Driscoll, R. M., and Dichek, D. A. (1999) *Hum Gene Ther 10*, 1469-78.

VITA

November 14, 1969 was not just another beautiful fall day. It was the day Christine Rene' Schar was born to her pleased parents, Ron and Marilyn Schar, in Long Beach, California. Christine had the pleasure of moving quite often across the country, never attending a school for more than four years in her academic career. In June of 1988, she graduated from Adolfo Camarillo High School, in the sleepy town of Camarillo, California. Quick to make her escape, she attended the University of California, San Diego in the fall of 1988. Christine received her Bachelor's of Science degree in June of 1992, with a major in Molecular Biology and a minor in Roman Art History. While attending UCSD and for several years following her graduation, Christine worked for Dr. Katherine A. Jones at the Salk Institute for Biological Sciences, located on a bluff overlooking the Pacific Ocean. In August of 1994, Christine left southern California behind her and made the move to Tennessee to attend graduate school at the University of Tennessee, Knoxville. She joined Dr. Cynthia Peterson's lab in the summer of 1995 and most of time enjoyed doing the research presented in this dissertation on vitronectin. She received the Doctor of Philosophy Degree in Biochemistry in May 2000.

Christine is presently engaged in hiking the Appalachain Trail, from Georgia to Maine, after which she plans on finding employment.